The Role of LATS1 in DNA Damage Signalling

By

Robert Latusek

A thesis submitted for the degree of Doctor of Philosophy

Gray Institute for Radiation Oncology and Biology,

University of Oxford

Balliol College

Trinity Term 2012





Abstract

Genomic DNA is constantly exposed to assaults, which if not dealt with, can lead to genomic instability and carcinogenesis. In response to stress including either Ionising Radiation (IR) or replication stress, ATM and ATR promote the activation of cell cycle checkpoints and initiate repair of DNA damage. Recent studies have revealed that ATM signalling can activate LATS1 via a cascade through RASSF1A and MST2. LATS1 is a tumour suppressor, which forms a barrier to carcinogenesis restricting cell proliferation and promoting apoptosis by stabilising a YAP/p73 transcriptional complex, hence upregulating p73 responsive genes. LATS1 is inactivated through promoter hypermethylation in a number of cancer types including breast cancer and soft tissue sarcoma. This research project seeks to define the mechanism through which LATS1 is involved in IR-induced DNA damage signalling. The data presented in this thesis shows that LATS1 controls CDK2 and regulates phosphorylation of S3291 on BRCA2. Cells lacking LATS1 exhibited enhanced accumulation of damage-induced Rad51 foci leading to cell cycle arrest at the G_2/M checkpoint. Furthermore, the data presented here suggests that LATS1 may not be required for homologous recombination. This work supports the hypothesis that LATS1 inhibits CDK2-dependent phosphorylation of BRCA2 at S3291, hence protecting stalled replication forks from nucleolytic degradation.

Acknowledgments

This D.Phil. thesis is a product of 4 years of research undertaken with the support and guidance of many individuals, without whom it could not have been completed.

I am in dept to my supervisor, Dr. Eric O'Neill for continuous guidance and insightful discussion on both practical and theoretical aspects of my thesis. I would like to thank Prof. Thomas Helleday for his support and encouragement.

I would like to acknowledge Vertex Pharmaceuticals Incorporated for generous financial patronage without which this achievement would not be possible.

Finally, thank you to everyone at University of Oxford, who I have worked with, all of you have made this an exceptional experience.

TABLE OF CONTENTS

I – ABSTRACT
II – ACKNOWLEDGMENTS
III – TABLE OF CONTENTS
VI – LIST OF FIGURES
VIII – ABREVIATTIONS

CHAPTER 1: INTRODUCTION 1

1.1 CANCER 2
1.1.1 CANCER 2
1.1.2 CANCER FORMATION 2
1.1.3 ONCOGENES 3
1.1.3.1 Introduction 3
1.1.3.2 Growth Factors 4
1.1.3.3 Receptors 4
1.1.3.4 Effectors 5
1.1.4 TUMOUR SUPPRESSORS 9
1.1.4.1 Introduction 9
1.1.4.2 Inhibition of Cell Cycle Progression 9
1.1.4.3 Induction of Apoptosis 12
1.1.4.4 DNA Damage Repair 15
1.2 CELL CYCLE 16
1.2.1 INTRODUCTION 16
1.2.2 REGULATION OF CDKS' ACTIVITY 17
1.2.3 THE MECHANISM OF CELL CYCLE REGULATION 19
1.2.4 DNA REPLICATION 21
1.2.4.1 Introduction 21
1.2.4.2 Pre-Initiation of the Replication 21
1.2.4.3 Initiation of the Replication 22
1.2.5 CELL CYCLE CHECKPOINTS 24
1.3 DNA DAMAGE RESPONSE 25
1.3.1 INTRODUCTION 25
1.3.2 RECOGNITION OF DNA DAMAGE 26
1.3.3 CELL CYCLE CHECKPOINTS 27
1.3.3.1 G_1/S Checkpoint 27
1.3.3.2 G_2/M Checkpoint 28
1.3.3.3 S-Phase Checkpoint 29
1.3.4 NON-HOMOLOGOUS END JOINING 33
1.3.5 HOMOLOGOUS RECOMBINATION 36
1.3.6 DNA DAMAGE REPAIR DURING S-PHASE 41
1.3.6.1 Introduction 41
1.3.6.2 HR-Dependent Models of DNA Damage Repair During S-Phase 41
1.3.6.3 Regressed Fork Protection 45
1.4. LARGE TUMOUR SUPPRESSOR 47
1.4.1 INTRODUCTION 47
1.4.2 HOMOLOGUES AND MOLECULAR STRUCTURE 48
1.4.3 DEVELOPMENTAL REGULATION 52
1.4.4 APOPTOSIS 58

1.4.5 Involvement of LATS1 in Cell Cycle 60
1.5 Aim of the Thesis 63

CHAPTER 2: MATERIALS AND METHODS 64

2.1 Buffer Compositions 65
2.2 Tissue Culture 66
2.3 Cells Freezing 67
2.4 Cells Thawing 68
2.5 siRNA Transfection 68
2.6 DNA Transfection 70
2.6.1 DNA Transfection Protocol 70
2.6.2 Plasmids Used in the Thesis 70
2.7 Drug Treatments 73
2.7.1 Hydroxyurea 73
2.7.2 Nocodazole 73
2.7.3 Colcemid 74
2.8 Cell Irradiation 74
2.9 Propidium Iodide (PI) Staining 74
2.10 BrdU Staining 75
2.11 Cell Lysis 76
2.12 Immunoprecipitation 77
2.13 Electrophoresis 77
2.14 Western Blotting 78
2.15 Metaphase Spread 80
2.16 Recombination Assay 80
2.17 Immunofluorescent Assay 82
2.18 Comet Assay 83
2.19 Statistical Analysis 84
2.20 List of Antibodies Used 86

CHAPTER 3: LATS1 IN CELL CYCLE REGULATION 87

3.1 Introduction 88
3.2 LATS1 Interaction with CDK1 and CDK2 in Response to IR 89
3.3 Optimisation of Transfection of siRNA 93
3.4 The Accumulation of LATS1-Deficient Cells in the G_2 Phase after IR 95
3.5 The Accumulation of LATS1-Deficient Cells in the S-Phase after IR 101
3.6 Discussion 106

CHAPTER 4: LATS1 IN DNA DAMAGE 109

4.1 Introduction 110
4.2 Retardation of the DNA Repair in the Absence of LATS1 111
4.3 The Persistence of Phosphorylation of H2AX after IR in the Absence of LATS1 113
4.4 The Persistence of the γH2AX Foci Post IR in the Absence of LATS1 118
4.5 RAD51 Foci Formation Defects in the Absence of LATS1 122
4.6 The Lack of Effect on HR in the Absence of LATS1 128
4.7 Discussion 130

CHAPTER 5: THE LATS1 REGULATION OF BRCA2 PHOSPHORYLATION 132

5.1 Introduction 133
5.2 The LATS1 Requirement for the RAD51 Foci Formation in Response to Fork Stalling 134
5.3 The LATS1 Regulation of the CDK2 and BRCA2 Interaction 136
5.4 The BRCA2 Phosphorylation Increase in the Absence of LATS1 139
5.5 The LATS1 Regulation of the DNA Damage-Induced Phosphorylation of BRCA2 140
5.6 Discussion 143

CHAPTER 6: GENERAL DISCUSSION 146

APPENDICES 155

Appendix 1: Metaphase Spread 156
Appendix 2: Identification of Novel LATS1 Binding Partners 157

REFERENCES 161

LIST OF FIGURES

CHAPTER 1 **1**

FIGURE 1.1 MAPK/ERK SIGNALLING PATHWAY 8
FIGURE 1.2 THE TUMOUR SUPPRESSOR-DEPENDENT REGULATION OF THE CELL CYCLE 11
FIGURE 1.3 THE MECHANISM OF THE APOPTOSIS 14
FIGURE 1.4 THE REGULATION OF CDK'S ACTIVITY 18
FIGURE 1.5 THE CELL CYCLE REGULATION 20
FIGURE 1.6 THE REGULATION OF CELL CYCLE CHECKPOINTS 32
FIGURE 1.7 NON-HOMOLOGOUS END JOINING 35
FIGURE 1.8 HOMOLOGOUS RECOMBINATION 40
FIGURE 1.9 THE DNA DAMAGE DURING S-PHASE 44
FIGURE 1.10 LATS HOMOLOGUES 50
FIGURE 1.11 STRUCTURES OF LATS1 AND LATS2 51
FIGURE 1.12 THE HIPPO PATHWAY 57
FIGURE 1.13 THE INVOLVEMENT OF LATS1 IN THE G2/M TRANSITION 62

CHAPTER 2 **64**

FIGURE 2.1 PLASMID MAP OF pRc/CMV PLASMID 71
FIGURE 2.2 PLASMID MAP OF pCAGEN PLASMID 72
FIGURE 2.3 WESTERN BLOT STACK 79
TABLE 2.1 THE LIST OF siRNAs USED IN THE PROJECT 69
TABLE 2.2 THE LIST OF PRIMARY ANTIBODIES USED IN THE PROJECT 86

CHAPTER 3 **87**

FIGURE 3.1 LATS1 ASSOCIATES WITH CDK1 AND CDK2 IN RESPONSE TO IR IN U2OS CELLS 90
FIGURE 3.2 ASSOCIATION OF LATS1 WITH CDK1 AND CDK2 IN CONFLUENT U20S CULTURES IS REGULATED IN AN IR-DEPENDENT MANNER 92
FIGURE 3.3 SIRNA TRANSFECTION OPTIMISATION 94
FIGURE 3.4 DEFECTS IN THE CELL CYCLE DISTRIBUTION IN THE ABSENCE OF LATS1 POST IR IN U2OS CELLS 96
FIGURE 3.5 DEFECTS IN THE CELL CYCLE DISTRIBUTION IN THE ABSENCE OF LATS1 POST IR IN HELA CELLS 98
FIGURE 3.6 DEFECTS IN THE CELL CYCLE DISTRIBUTION IN THE ABSENCE OF LATS1 POST IR IN MEFs 100
FIGURE 3.7 DEFECTS IN THE S-PHASE DISTRIBUTION IN THE ABSENCE OF LATS1 IN U2OS CELLS 102
FIGURE 3.8 DEFECTS IN THE S-PHASE DISTRIBUTION IN THE ABSENCE OF LATS1 IN HELA CELLS 103
FIGURE 3.9 DEFECTS IN THE S-PHASE DISTRIBUTION IN THE ABSENCE OF LATS1 IN MEFs 105

CHAPTER 4 **109**

FIGURE 4.1 DNA REPAIR IS RETARDED IN THE ABSENCE OF LATS1 112
FIGURE 4.2 THE ABSENCE OF LATS1 CAUSES PERSISTENCE OF PHOSPHORYLATION OF H2AX POST IR IN MEFs 115
FIGURE 4.3 THE ABSENCE OF LATS1 CAUSES PERSISTENCE OF PHOSPHORYLATION OF H2AX POST IR IN U2OS CELLS 117
FIGURE 4.4 γH2AX FOCI PERSIST IN THE ABSENCE OF LATS1 POST IR IN U2OS CELLS 120
FIGURE 4.5 DIFFERENCE IN γH2AX FOCI RESOLUTION 4 hrs POST IR IN U2OS CELLS 121
FIGURE 4.6 RAD51 FOCI FORMATION DEFECTS IN THE ABSENCE OF LATS1 POST IR IN MEFs 124
FIGURE 4.7 RAD51 FOCI FORMATION DEFECTS IN THE ABSENCE OF LATS1 POST IR IN U2OS CELLS 125
FIGURE 4.8 RAD51 FOCI FORMATION DEFECTS IN THE ABSENCE OF LATS1 POST IR IN U2OS CELLS CULTURED IN STARVING MEDIUM 127
FIGURE 4.9 HR IS NOT AFFECTED IN THE ABSENCE OF LATS1 IN U2OS CELLS 129

CHAPTER 5 **132**

FIGURE 5.1 RAD51 FOCI FORMATION DEFECTS IN THE ABSENCE OF LATS1 IN U2OS CELLS TREATED WITH HYDROXYUREA 135
FIGURE 5.2 THE ASSOCIATION BETWEEN BRCA2 AND CDK2 IS REGULATED IN AN IR-DEPENDENT MANNER AND DEPENDS ON LATS1 IN U2OS CELLS 137
FIGURE 5.3 THE ASSOCIATION BETWEEN BRCA2 AND CDK2 IS REGULATED IN AN IR-DEPENDENT MANNER AND DEPENDS ON LATS1 IN MEFs 138
FIGURE 5.4 BRCA2 INCREASES THE PHOSPHORYLATION ON S3291 IN THE ABSENCE OF LATS1 IN HT1080 CELLS 140
FIGURE 5.5 BRCA2 MAINTAINS THE PHOSPHORYLATION ON S3291 IN THE ABSENCE OF LATS1 POST IR IN HT1080 CELLS 142

CHAPTER 6 **146**

FIGURE 6.1 THE ROLE OF LATS1 IN DNA DAMAGE SIGNALLING 154

APPENDICES **155**

FIGURE S1 METAPHASE SPREAD 156
FIGURE S2 PROTEOMIC SCREEN FOR LATS1 BINDING PARTNERS 159
FIGURE S3 LATS1 ASSOCIATES WITH P54(NRB) IN IR-DEPENDENT MANNER 160

Abbreviations

53BP1 – P53 Binding Protein 1

9-1-1 – Rad9/Rad1/Hus1

AGC – A, G and C Protein Kinase Families (PKA, PKC, PKG)

Apaf-1 – Apoptotic Protease-Activating Factor-1

APC – Adenomatous Polyposis Coli

ARF – Alternate Reading Frame

ARS – Autonomously Replicating Sequences

ATM – Ataxia Telengeictasia Mutaded

ATR – ATM and Rad3 Related

BAX – Bcl2-Associated X Protein

BCL-2 – B-Cell Lymphoma 2

BLM – Bloom Syndrom, RecQ Helicase-Like

BRCA2 – Breast Cancer 2 Susceptibility Protein

BRCT – BRCA1 C-Terminus Domain

BRDU – 5-Bromo-2-Deoxyuridine

BSA – Bovine Serum Albumin

CAK – CDK Activating Kinase

CDC – Cell Division Cycle

CDK – Cyclin Dependent Kinase

CHK – Checkpoint Kinase

Cip – CDK Interacting Protein

CKI – CDK Inhibitor

CPT – Camptothecin

Crb – Crumbs

DAPI – 4,6-Diamidino-2-Phenylindole

Dco – Discs Overgrown

DDR – DNA Damage Response

DIAP1 – Drosophila Inhibitor of Apoptosis 1

DMEM – Dulbecco's Modified Eagle's Medium

DNA – Deoxyribonucleic Acid

DNA-PK – DNA Dependent Protein Kinase

DNA-PKcs – DNA Dependent Protein Kinase Catalytic Subunit

dNTP – Deoxyribonucleotide Triphosphate

Ds – Dachsous

DSB – Double Strand Break

DTT – Dithiothreitol

EDTA – Ethylenediaminetetraacetic Acid

EGF – Epidermal Growth Factor

EGFR – Epidermal Growth Factor Receptor

Ex – Expanded

EXO1 – Exonuclease 1

FACS – Fluorescence-Activated Cell Sorting

FBS – Fetal Bovine Serum

G_1 – Gap 1 Phase

G_2 –Gap 2 Phase

GADD45 – Growth Arrest and DNA-Damage-Inducible

GDP – Guanosine Diphosphate

GFP – Green Fluorescent Protein

GRB2 – Growth Factor Receptor-Bound Protein 2

GSK-3β – Glycogen Synthase Kinase-3β

GTP – Guanosine Triphosphate

H2AX – Histone 2A Variant X

HEPES – 4-(2-hydroxyethyl)-1-piperazineethanesulfonic Acid

HJ – Holliday Junction

Hpo – Hippo

HR – Homologous Recombination

HU – Hydroxyurea

IAP – Inhibitor of Apoptosis

IGF – Insulin-Like Growth Factor

Ink4a – Inhibitor of Kinase 4

IP – Immunoprecipitation

IR – Ionising Radiation

IκB – Inhibitor of Kappa-Light-Chain-Enhancer of Activated B Cells

KD – Kinase Dead

Kip – Kinase Inhibitory Protein

LATS1 – Large Tumour Suppressor 1

LIMK1 – LIM Domain Kinase 1

LOH – Loss of Heterozygosity

M – Mitosis

MAPK – Mitogen Activated Protein Kinase

MATR3 – Matrin 3

Mats – MOB as Tumour Suppressor 1

Mcm2-7 – Minichromosome Maintenance Complex Component 2-7

MDC1 – Mediator of DNA-Damage Checkpoint 1

MDM2 – Murine Double Minute 2

MEF – Mouse Embryonic Fibroblasts

Mer – Merlin

MMS – Methyl Methanesulfonate

Mre11 – Meiotic Recombination 11

MRN – Mre11, Rad50 and Nbs1 Complex

MST2 – Mammalian STE20-Like Protein Kinase 2

MYT1 – Myelin Transcription Factor 1

NBS1 aka NBN– Nibrin

NDR – Nuclear Dbf2-Related

NHEJ – Non-Homologous End Joining

ORC – Origin Recognition Complex

P54(NRB) – 54 kDa Nuclear RNA-and DNA- Binding Protein

PBD – Protein Binding Domain

PBS – Phosphate Buffered Saline

PCNA – Proliferating Cell Nuclear Antigen

PDGF – Platelet-Derived Growth Factor

PDK1 – 3-Phosphoinositide-Dependent Protein Kinase 1

PI – Propidium Iodide

PI3K – Phosphatidyinositol-3-Kinase

PI(4,5)P2 – Phosphatidylinositol(4,5)bis-Phosphate

PNK – Polynucleotide Kinase

Pre-RC – Pre-Replication Complex

PTEN – Phosphatase and Tensin Homologue Deleted on Chromosome 10

PUMA – P53 Upregulated Modulator of Apoptosis

RASSF – RAS Association Domain Family Member 1

Rb – Retinoblastoma

RDS – Radioresistant DNA Synthesis

RFC – Replication Factor C

RNA – Ribonucleic Acid

RPA – Replication Protein A

RT – Room Temperature

S – Synthesis Phase

Sav – Salvador

Sd – Scalloped

SDS-PAGE – Sodium Dodecyl Sulphate Poly-Acrylamide Gel Electrophoresis

siNT – siRNA Non Targeting

siRNA – Small Interfering RNA

SMC1 – Structural Maintenance of Chromosomes

SOS – Son of Sevenless

SSB – Single Strand Break

ssDNA – Single Stranded DNA

TAZ – Tafazzin

TDP1 – Tyrosyl-DNA Phosphodiesterase

TdT – Terminal Deoxynucleotidyl Transferase

TEAD – TEA Domain Family Member

Tim – Timeless

Tipin – Tim Interacting Protein

TLS – Translesion Synthesis

TNF α – Tumour Necrosis Factor α

TRAIL – TNF-Related Apoptosis-Inducing Ligand

Tris – Tris(hydroxymethyl)aminomethane

UV – Ultra Violet

WNT – Wingless-type MMTV Integration Site Family

WRN – Werner Syndrome

Wt – Wild Type

Wts – Warts

XLF – XRCC4-Like Factor

XRCC4 – X-ray Complementing Defective Repair in Chinese Hamster Cells 4

YAP – Yes-Associated Protein

Yki – Yorkie

Chapter 1:
Introduction

1.1 Cancer

1.1.1 Cancer

Cancer is a neoplastic disease characterised by autonomous deregulated proliferation and surivival of individual cells that progress to form a tumour mass. To develop further the neoplasm requires the formation of a tumour microenvironment through the promotion of additonal events such as angiogenesis, and can lead to tumour cell invasion and metastasis to distant sites. Excessivelly proliferating cells can form both solid and non-solid tumours like leukemia or lymphoma. Solid tumours can be either benign, which can be removed surgically together with preventative chemotheraphy/radiotherapy, or malignant. Malignant refers to more extensive, invasive and quickly growing tumours that can often be difficult to treat and frequently manifest metastatic characteristics. Metastasis is a spread of tumour from one site of the body to another site, which is not immediately adjacent to the original tumour. Metastasis and invasion are features, which differentiate cancer as a disease from a single site tumour. Metastasis limits the utilisation of surgery and radiotherapy as treatment options and relies more on chemotherapy due to the dissemination of tumour sites throughout the body (Hanahan and Weinberg 2000).

1.1.2 Cancer Formation

The initation of tumorigenesis requires a series of specific events that perturb normal cellular regulation. These are best described as steps in the progression of a developing tumour cell and include proliferation

independently of growth signals, circumvention of programmed cell death, the ability to replicate indefinitely, the induction of a vascular supply, and the ability to invade tissues. In the initial stages of cancer, these events occur due to cellular mutations that alter the expression or function of genes responsible for the regulation of cell division, differentiation or cell death. The initiation of tumorigenesis is multi-step process where the cancerogenesis depends on both inactivation of tumour suppressors and the conversion of proto-oncogenes into oncogenes (Nordling 1953; Knudson 1971; Hanahan and Weinberg 2000).

1.1.3 Oncogenes

1.1.3.1 Introduction

Oncogenes are a group of genes, which when they mutate or express at high levels, progressively convert a normal cell into a cancer cell (Hanahan and Weinberg 2000). Oncogenes are activated through mutations, chromatin re-arrangements or gene amplification, which lead to deregulation of its expression or result in a change in the structure of an oncogene leading for instance to its consecutive activation (see Section 1.1.3.4). Oncogenes stimulate extensive cell proliferation and inhibit apoptosis. They can be divided into three subgroups: growth factors, tyrosine kinase receptors and effectors (Bishop 1991; Hanahan and Weinberg 2000).

1.1.3.2 Growth Factors

Normal cell requires growth factor stimulation to withdraw from the quiescent state and move to active proliferation. Growth factors bind to trans-membrane receptors and send signals to the nucleus where specific genes are transcribed. Oncogenes mimic growth signalling to gain autonomy from mitogenic stimulation, which subsequently contributes to malignant transformation of the cell through promoting unrestricted growth (Hanahan and Weinberg 2000). Cancer cell synthesises growth factors such as platelet-derived growth factor (PDGF) in glioblastoma, tumour growth factor α (TGF-α) in sarcomas, epidermal growth factor (EGF) or insulin growth factor I (IGF-I) (Kolibaba and Druker 1997; Heldin and Westermark 1999). These factors bind to their receptors and create a positive feedback loop called autocrine loop. Through this mechanism, the cell becomes independent of signalling from other cells in the tissue. Extensive production and secretion of growth factors leads to abnormal stimulation of growth receptors, which translates ultimately into gene transcription and tumour growth (Hanahan and Weinberg 2000).

1.1.3.3 Receptors

Receptors are trans-membrane proteins that function as tyrosine kinases. Following ligand binding, the kinase receptor dimerises and becomes active. In a cancerous cell, the receptors are extensively stimulated due to the abundance of growth factors or alternatively, acquire mutations, which activate them irrespectively of ligand binding or dimerisation (Tsatsanis and Spandidos 2000). Activated receptor trans-phosphorylates tyrosine residues in the intracellular domain. This creates an interaction site for cytoplasmic

proteins called effectors, which contain binding domains like SRC homology 2 domain (SH-2) (Cooper and Howell 1993; Rodrigues and Park 1994).

1.1.3.4 Effectors

Receptors activate the protein cascades downstream leading to extensive cell proliferation and inhibition of apoptosis. A classic example of such pathway is MAPK kinase pathway, which has implications in promoting cell division and downregulation of apoptosis (Figure 1.1) and (Aplin, Howe et al. 1998; Giancotti and Ruoslahti 1999). The MAPK pathway is induced in response to the activation of epidermal growth factor receptor (EGFR). Phosphorylated EGFR interacts with the growth factor receptor-bound protein 2 (GRB2) through phosphorylated tyrosine residues and promotes its binding to guanine nucleotide exchange factor SOS (Schulze, Deng et al. 2005; Zarich, Oliva et al. 2006). Next, SOS stimulates Ras, which then releases GDP and exchanges it for GTP gaining activity. Ras, in association with GTP, recruits Raf kinase from cytosol and leads to subsequent phosphorylation and activation of MEK1/2 and then (Mitogen Activated Protein Kinase) MAPK kinases ERK1/2 (Avruch, Khokhlatchev et al. 2001). ERK1/2 phosphorylate cytosolic signalling proteins including p90 ribosomal S6 kinase (p90RSK) and MAPK-interacting serine/threonine kinase (MNK). In addition, ERK1/2 phosphorylate transcription factors including E26 (ETS)-like transcription factor 1 (Elk-1), c-Myc, c-Fos, Cdc25 and MSK1/2 (Figure 1.1) and (Pearson, Robinson et al. 2001). c-Myc increases expression of Cyclin A and Cyclin E and modulates levels of Cyclin D1. High levels of c-Myc prevent inhibitory association of $p27^{kip}$ with CDK2/Cyclin E, lead to $p27^{kip}$ degradation and

therefore facilitate G_1/S transition (Leone, DeGregori et al. 1997; Kerkhoff, Rapp 1998). Furthermore, c-Myc activates expression of Cyclin A via its effects on CDK2/Cyclin E complex. Inhibition of CDK2 kinase activity or mutations in c-Myc that fail to induce cyclin E-dependent kinase activity fail to promote cyclin A expression (Rudolph, Saffrich et al. 1996). The c-Myc-dependent regulation of Cyclin D1 is unclear with reports showing conflicting data (Jansen-Durr, Meichle et al. 1993; Daksis, Lu et al. 1994; Hanson, Shichiri et al. 1994; Hoang, Cohen et al. 1994; Philipp, Schneider et al. 1994). The overexpression of Cyclin D1 or Cyclin E facilitates release of E2F transcription factor from inhibitory complex formed with pRb enhancing cell proliferation and contributing towards carcinogenesis (Figure 1.2) and (see Section 1.2.3) and (Donnellan and Chetty 1998; Moroy and Geisen 2004). Additionally, c-Myc down-regulates p21 transcription through repression of the p21 promoter inducing cell proliferation. Alternatively, c-Myc cooperates with Ras to activate the promoter of CDK1 (Born, Frost et al. 1994; Gartel, Ye et al. 2001). c-Fos dimerises with c-Jun to form AP-1 transcription factor, which upregulates transcription of genes involved in proliferation and differentiation. Moreover, Erk1/2 can phosphorylate Cdc25 and increase its phosphatase activity leading to mitotic induction (Wang, He et al. 2007). Activated p90RSK kinase phosphorylates pro-apoptotic Bad and inhibits Bad-mediated cell death. Furthermore p90RSK phosphorylates and inactivates Glycogen Synthase Kinase 3 beta (GSK3β) (Tan, Ruan, et al. 1999). Additionally, p90RSK activates the transcription factor cAMP response element binding protein (CREB) and Estrogen Receptor alpha (ER α). CREB upregulates antiapoptotic Bcl-2, Bcl-xl and Bcl-1 therby promoting cell survival (Bonni,

Brunet et al. 1999; Ballif and Blenis 2001). Moreover, Ras oncogene contributes to the growth enhancement and inhibition of apoptosis through PI3K signaling. PI3K kinase is activated by binding to Ras-GTP and then phposphorylates PIP2 to PIP3. Finally, PIP3 activates AKT and anti-apoptotic signalling downstream of AKT (Figure 1.1) and (see Section 1.1.4.3). When Ras signalling is no longer required, GTP is hydrolysed to GDP, which leads to inactivation of Ras. In 20% of all human tumours and in 90% of pancreatic cancer, Ras is permanently activated by a point mutation in codons 12, 13 or 61 due to which GTPase reaction can no longer be stimulated by GAP. In mutated Ras, GAP is no longer able to provide a domain that is crucial for the activation of the Ras GTPase. GTP is not hydrolysed to GDP, consequently mutated Ras-GTP stays active and continously transduces signals downstream (Aplin, Howe et al. 1998; Downward 2003). Finally, Raf-1 inhibits apoptosis by binding to MST2 and blocking the subsequent phosphorylation of LATS1 kinase and the stabilisation of p73 (Figure 1.12 b) and (see Section 1.4.4) and (O'Neill, Rushworth et al. 2004; O'Neill and Kolch 2005; Matallanas, Romano et al. 2007).

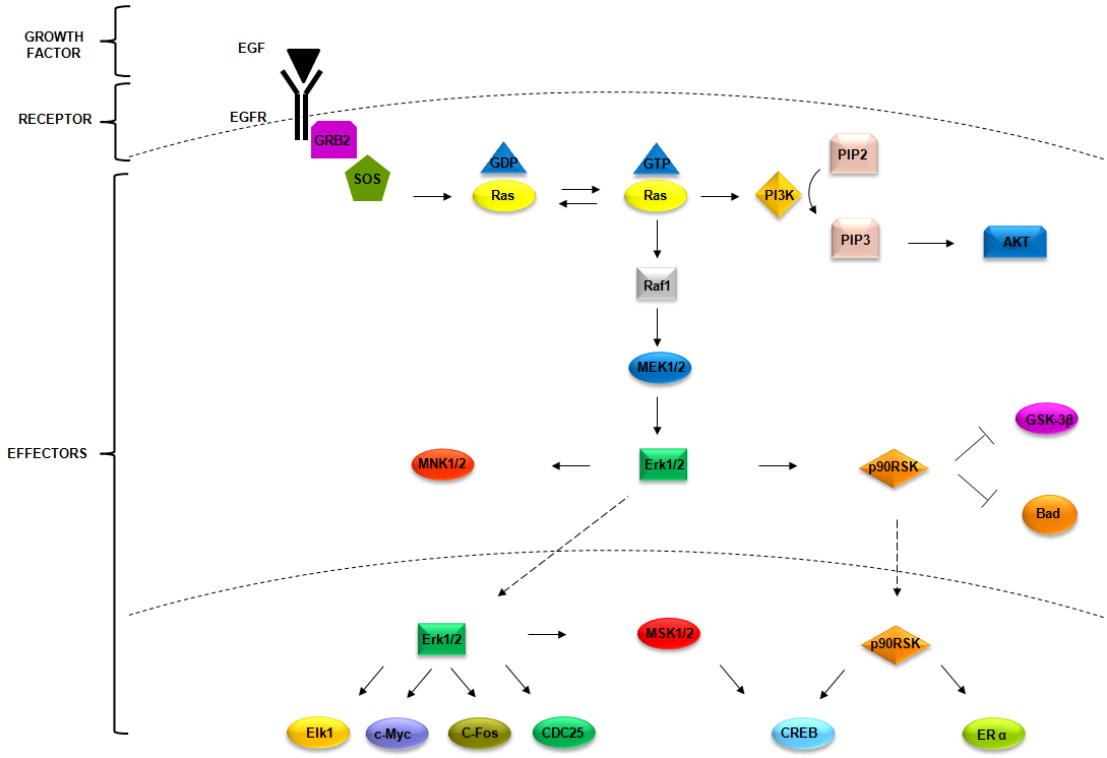


Figure 1.1 MAPK/ERK Signalling Pathway. The figure represents simplified MAPK/ERK signalling cascade showing division of the pathway onto growth factor, receptor and effectors. Epidermal Growth Factor (EGF) binds to EGF receptor (EGFR) in the cell membrane and promotes the signalling cascade. This leads to a subsequent activation of Erk1/2 kinases, which regulate activity of cytosolic signalling protein and many transcription factors. Moreover, the signalling pathway controls activity of AKT kinase.

1.1.4 Tumour Suppressors

1.1.4.1 Introduction

Tumour suppressors are growth-controlling genes, which constrain cell proliferation, suppress metastasis, promote apoptosis and are involved in DNA damage response. Inactivating or losing these functions free the cell from the process of controlled division and leads to tumour formation. Tumour suppressor genes are recessive and require two alleles mutation for full inactivation (Knudson 1971; Comings 1973). The exceptions to this rule are tumour suppressors whose function can be abolished by mutation of a single allele. Tumour suppressors demonstrating haploinsufficiency include p27, Adenomatous Polyposis Coli (APC), and cyclin D binding protein DMP1 (Fero, Randel et al. 1998; Inoue, Zindy et al. 2001; Yan, Dobbie et al. 2002).

1.1.4.2 Inhibition of Cell Cycle Progression

The main function of the tumour suppressor is inhibition of cell division. The group of genes responsible for the suppression of proliferation includes retinoblastoma (Rb), adenomatous polyposis coli (APC), Alternate Reading Frame (ARF), CDK inhibitors and p53. Rb restricts the progression of the cell to the S-phase through the control of the restriction point gate (R point) during G_1. Rb binds to E2F transcription factor, restricts its activity and inhibits the expression of genes that are indispensible for the S-phase entry including Cyclin A, Cyclin E, polymerase α or genes involved in DNA replication. Additionally, Rb recruits histone deacetylases and chromatin remodeling factors to further repress the expression of S-phase promoting factors (Magnaghi-Jaulin, Groisman et al. 1998; Harbour and Dean 2000). The

CDK4/6/Cyclin D and the CDK2/Cyclin E phosphorylate Rb and cancel the repression of E2F enabling the cell cycle to progress (see Section 1.2.3) and (Weinberg 1995; Vandel, Nicolas et al. 2001). Further, inhibition of the cell cycle may be provided by CDK inhibitors (CKI), $p16^{INK4a}$ and $p14^{ARF}$. $P16^{INK4a}$ blocks the ability of CDK4/6 to phosphorylate Rb, whereas $p14^{ARF}$ activates the p53 tumour suppressor by binding to the p53 negative regulator MDM2 and subsequently preventing p53 degradation (Figure 1.2) and (see Section 1.2.2) and (Sharpless and DePinho 1999; Sherr 2001). The active p53 targets transcription of $p21^{Cip1}$, which then inhibits the CDK2/Cyclin E-mediated phosphorylation of Rb (Figure 1.2) and (el-Deiry, Tokino et al. 1993; Sherr 1996). Further regulation is provided by APC, which restricts the expression of genes promoting proliferation, including c-Myc and Cyclin D1. APC forms a complex with axin and glycogen synthase kinase-3β (GSK-3β) and associates with β-catenin. GSK-3β phosphorylates β-catenin, which is then recognised by E3 ubiquiting ligase and marked for degradation (Rubinfeld, Souza et al. 1993).

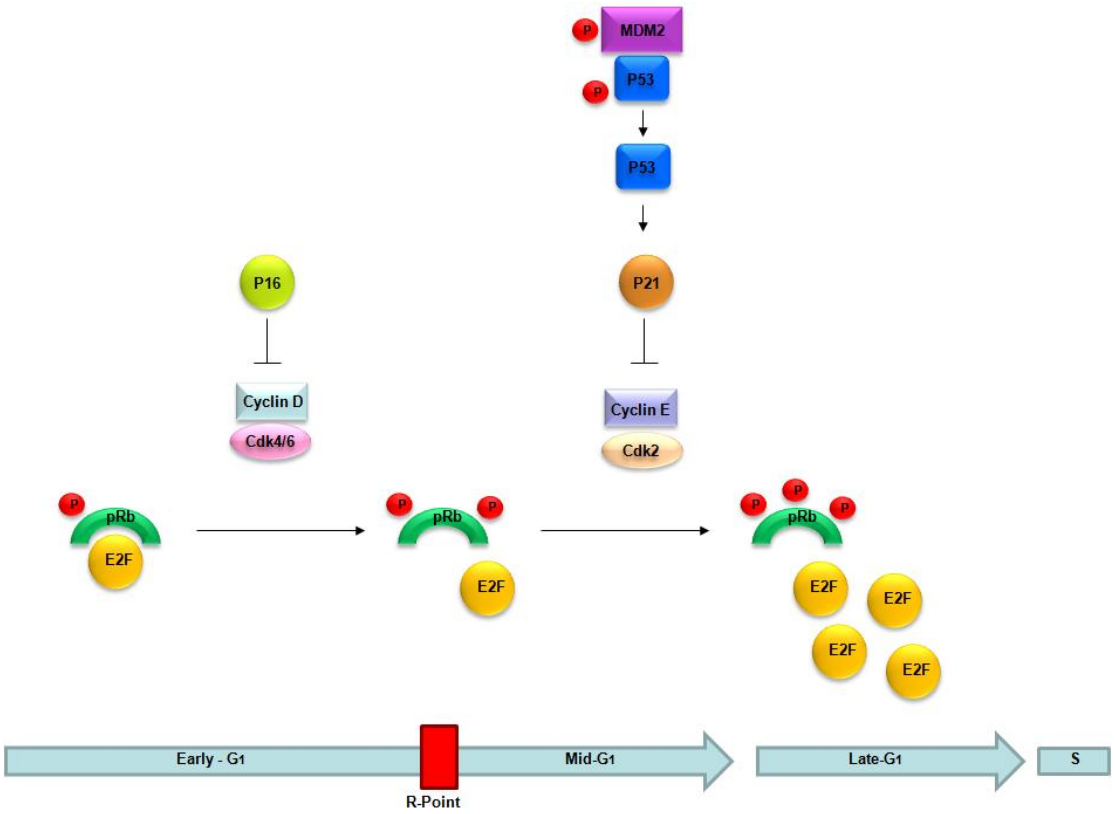


Figure 1.2 The Tumour Suppressor-Dependent Regulation of the Cell Cycle. The E2F transcription factor is inactive while in a complex with pRb tumour suppressor. In response to the mitogenic stimulation Cdk4/6/Cyclin D phosphorylate pRb resulting in the initial release of E2F. Further release of E2F is promoted by Cdk2/Cyclin E. The activity of Cdk4/6/Cyclin D is restricted by p16 and Cdk2/Cyclin E by p21 cyclin-dependent inhibitors. The figure adapted from (Deckbar, Jeggo et al. 2011).

1.1.4.3 Induction of Apoptosis

Tumour suppressors, including p53, APC and PTEN, promote programmed cell death called apoptosis to restrain carcinogenesis (Shen and White 2001; Simpson and Parsons 2001; Steigerwald, Behbehani et al. 2005). P53 promotes apoptosis through the transcription of PUMA and Bax. PUMA activates Bax/Bak by relieving the inhibition imposed by the antiapoptotic members of the Bcl-2 family. Bax is a mitochondrial pore protein that is able to elicit a change in the permeability of the mitochondrial outer membrane and subsequently release cytochrome C (Yu and Zhang 2008). Cytochrome C associates with the cytosolic protein Apaf-1 to form the heptameric holoenzyme complex called apoptosome. The apoptosome helps to initiate apoptosis through conversion of pro-caspase 9 into active caspase 9 (Zou, Li et al. 1999; Yuan, Yu 2011). This activates the other procaspases 3, 6, 7 and leads to the cleavage of death substrates, proteins which degradation facilitates cell death (Figure 1.3) and (Shen and White 2001). Death substrates cleaved by caspases include factors involved in DNA repair (PARP, DNA-PK), homeostasis (Rb) and cell structure maintenance (Actin) (Denner 1999). The process of apoptosis can be additionally stimulated by APC, which activates cell death through caspase 8 or by negative regulation of Akt imposed by PTEN (Figure 1.3) and (Steigerwald, Behbehani et al. 2005). First, PI3K catalyses the conversion of phosphatidylinositol(4,5)bis-phosphate [PI(4,5)P2] to PI(3,4,5)P3. Then, PI(3,4,5)P3 recruits Akt to the membrane where it is phosphorylated and activated by PDK1. Akt inhibits pro-apoptotic Bad and caspase 9 and activates anti-apoptotic IκB. Akt enhances cell cycle progression through inhibition of anti-proliferative GSK-β, p53 or p27

and p21. PTEN negatively regulates the conversion of [PI(4, 5)P2] to PI(3,4,5)P3 and as a result, restricts the activation of Akt, which facilitates apoptosis and restricts cell proliferation (Simpson and Parsons 2001). Moreover, tumour suppressors such as RASSF1A abolish the inhibitory effect of oncogenes on pro-apoptotic signalling. In response to irradiation, RASSF1A removes the inhibitory association of Raf-1 with MST2 and promotes signalling downstream leading to the activation of LATS1 and the subsequent stabilisation of p73 (see Section 1.4.4) and (O'Neill, Rushworth et al. 2004; O'Neill and Kolch 2005; Matallanas, Romano et al. 2007).

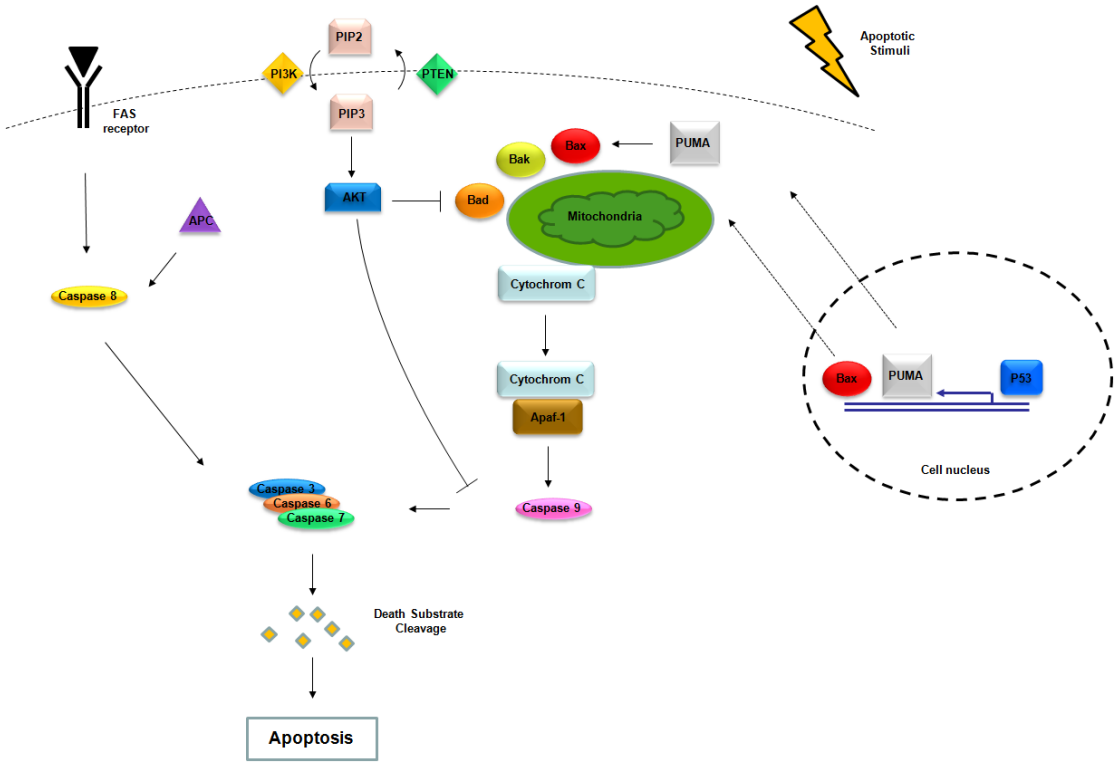


Figure 1.3 The Mechanism of the Apoptosis. The apoptosis can be initiated by two alternative pathways: either through mitochondria (intrinsic pathway) or through death receptors on the cell surface (extrinsic pathway). In intrinsic pathway apoptotic stimuli activate p53-dependent transcription of Bax and PUMA proteins which in turn lead to release of Cytochrom C from mitochondria. Cytochrom C together with Apaf-1 form apoptosome and activate caspase cascade leading to cleavage of death substrates and subsequent apoptosis. Alternatively, death receptor Fas activates Caspase 8 and promotes caspase cascade. This pathway may require APC tumour suppressor.

1.1.4.4 DNA Damage Repair

Tumour suppressors are involved in DNA damage repair. Individuals carrying mutations in ATM, ATR, BRCA1, BRCA2, NBS1 and CHK1/2 are prone to many tumours. Ataxia-telangiectasia-mutated (ATM) and Ataxia-telangiectasia and Rad3 mutated (ATR) are activated in response to a DNA double-strand breaks (DSB) or single-stranded DNA (ssDNA) respectively, and phosphorylate a number of proteins responsible for checkpoint activation and DNA damage repair. In response to irradiation, ATM/ATR restricts cell cycle progression by activating Chk1/2 and takes active role in both non-homologous end joining (NHEJ) and homologous recombination (HR). Recent reports indicate that ATM-dependent activation of LATS1 in response to IR may have implications in DNA damage repair (Matsuoka, Ballif et al. 2007; Hamilton, Yee et al. 2009).

1.2 Cell Cycle

1.2.1 Introduction

Cell cycle is a complex process of cell growth and duplication. It can be divided into a quiescent state referred as G_0 phase and active cell cycle. The latter is divided into two main phases: interphase during which cell prepares for division, and the cell division. The interphase consists of three stages: G_1, S and G_2. During G_1 the cell grows, synthesises proteins, develops organelles, and increases the volume of cytoplasm. Then, the cell replicates DNA in the S-phase and resumes growth in preparation for mitosis in the G_2 phase. After interphase, the cell initiates a process of division, which consists of mitosis and cytokinesis. During mitosis, the cell separates chromosomes to form two nuclei with exactly the same DNA content. The process of mitosis is divided into five stages. First, chromatin condenses into chromosomes and forms centrosomes in the prophase. Then, in the prometaphase microtubules attach to kinetochores and the nuclear membrane disintegrates. Subsequently, chromosomes align in the metaphase and are pulled apart to opposite centrosomes in the anaphase. Finally, the chromatin decondenses and the nuclear membrane surrounds two newly formed nuclei in the telophase. The mitosis is followed by cytokinesis, which separates the cytoplasm, the nuclei and the cell membrane to form two independent cells containing a similar set of cellular components. The eukaryotic cells have developed a regulatory network of protein interactions, which controls the main events of the cell cycle and ensures the error-free progression of the cell cycle. The regulatory network consists of two major groups of proteins:

Cyclin Dependent Kinases (CDK) and cyclins (Pines and Hunter 1991; Sherr 1996; Schafer 1998).

1.2.2 Regulation of CDKs' Activity

The process of transition from one cell cycle phase to another is regulated by the cyclin dependent kinases (CDK). CDKs belong to the serine/threonine kinases and are activated at specific time points during the cell cycle. The level of CDK is constant during the cell cycle in contrast to the variability of their activating partners, the cyclins. The level of cyclins oscillates with the cell cycle and in this way they periodically bind and activate the catalytic activity of the CDKs (Figure 1.5) and (Evans, Rosenthal et al. 1983; Pines 1991; Pines and Hunter 1991) . The active site of non-induced CDK is blocked by a T-loop formation restricting ATP binding. The cyclin association translocates the T-loop from the active site, which partially activates CDK. Full activation is gained when the CDK activating kinase (CAK) phosphorylates threonine or tyrosine residue in the vicinity of the active site of CDK. The phosphorylation promotes conformational changes and enhances the cyclin binding (Jeffrey, Russo et al. 1995). In addition to the cyclin-dependent regulation, CDK1 is phosphorylated and inactivated by Wee1 and Myt1 kinases. The inhibitory phosphorylation is removed by Cdc25 and is indispensible for the activation of CDK1 and further progression of the cell cycle (Figure 1.4) and (Lew and Kornbluth 1996). When activity of a specific CDK is no longer desired, its partner cyclin is rapidly degraded. The cyclin is polyubiquitinated by the ubiquitin ligase and targeted for proteolytic breakdown in the proteasome (Figure 1.4). An additional level of regulation is provided by CDK inhibitors

(CKI), which are divided into two groups: the INK4 and Cip/Kip family (Sherr and Roberts 1995; Sherr 2001). The INK4 (p15, p16, p18 and p19) family antagonises the G_1 CDKs, CDK4 and CDK6 and have no effect on either CDK1 or CDK2. These proteins form a stable complex with CDKs and prevent the cyclin association (Carnero and Hannon 1998). The Cip/Kip group consisting of $p21^{Cip1}$, $p27^{Kip1}$ and $p57^{Kip1}$, targets the CDK/Cyclin E activity (Roberts, Koff et al. 1994; Harper, Elledge et al. 1995; Reynisdottir, Polyak et al. 1995). The LATS kinases utilise a mechanism similar to the CKI inhibition. LATS1 associates with CDK1 and prevents Cyclin A from binding, thereby arresting cells at G_2/M (Tao, Zhang et al. 1999; Xia, Qi et al. 2002). LATS2 modulates CDK2/Cyclin E activity through an unknown mechanism and affects the G_1/S transition (see Section 1.4.5) and (Li, Pei et al. 2003).

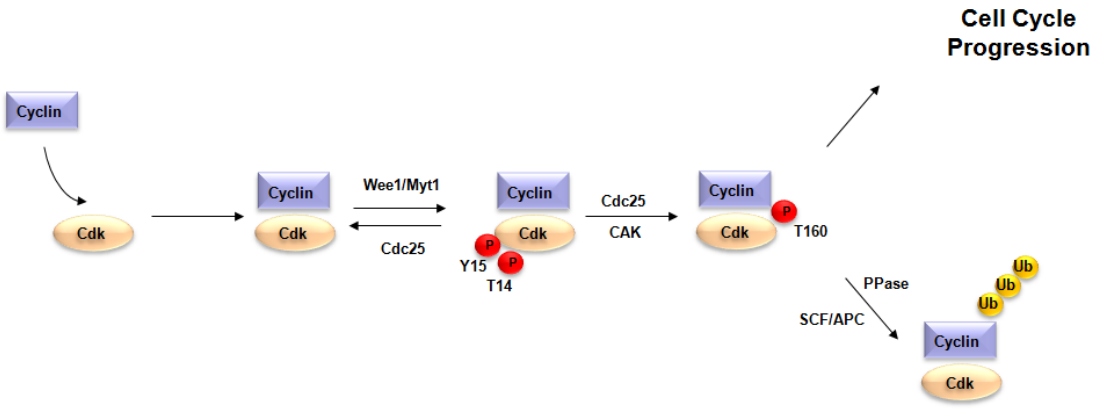


Figure 1.4 The Regulation of CDK's Activity. Depending on a cell cycle phase specific cyclins bind to partner Cdks and facilitate cell cycle progression. Further Cdk/Cyclin complex is regulated by inhibitory phosphorylation by Wee1/Myt1 and activating dephosphorylation mediated by Cdc25 phosphatases. Full activity is gained upon phosphorylation mediated by CAK. When Cdk/Cyclin complex activity is not required any longer, cyclin is ubiquitinated and subsequently degraded. The figure adapted from (Yata and Esashi 2009).

1.2.3 The Mechanism of Cell Cycle Regulation

The G_1 phase is controlled by the CDK4/6/Cyclin D complex (Sherr 1994). The Cdk4/6/Cyclin D complex phosphorylates Rb and leads to the initial release of the E2F transcription factor from Rb. E2F creates a positive feedback loop, which promotes cell cycle progression to the restriction point (R point), after which the cell progresses to the S-phase irrespectively of growth factors stimulation. After the R point, the feedback loop upregulates Cyclin E, which associates with CDK2 and further stimulates the liberation of the E2F transcription factor promoting transition from the G_1 to the S-phase (Figure 1.2) and (Sherr 1994; Ohtsubo, Theodoras et al. 1995; Harbour and Dean 2000). The G_1/S transition requires additionally CDK3, which contributes to the E2F activation (van den Heuvel and Harlow 1993; Hofmann and Livingston 1996; Braun, Holzl et al. 1998). When the cell enters the S-phase, the level of Cyclin A increases and it replaces Cyclin E as the binding partner of CDK2 and enables the S-phase to progress (Girard, Strausfeld et al. 1991). As the S-phase progresses, Cyclin A switches CDK2 for CDK1. At the same time, the transcription of another Cyclin, Cyclin B, commences and reaches a peak in the late G_2 phase (Fung and Poon 2005). Later in the G_2 or at the onset of mitosis, CDK1 partners with Cyclin B and triggers the G_2/M transition. At the end of M phase, the level of Cyclin B decreases due to degradation and the cyclin is almost non-detectable at the onset of a new cell cycle (Figure 1.5) and (Fung and Poon 2005).

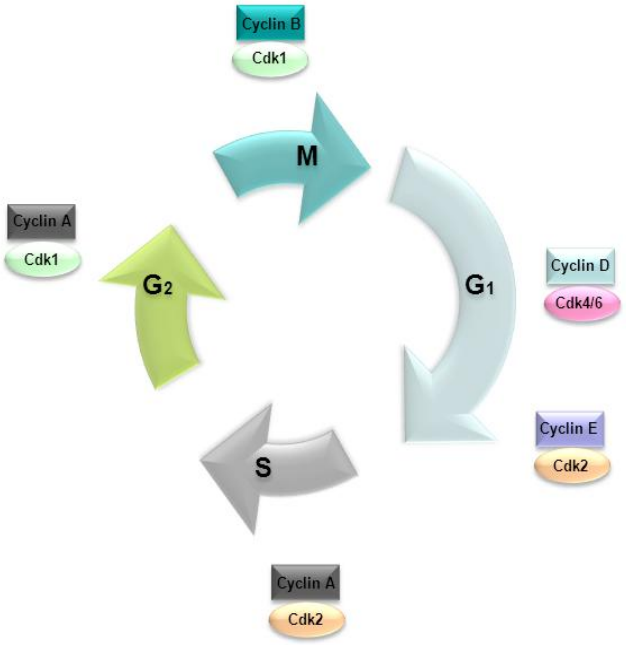


Figure 1.5 The Cell Cycle Regulation. Schematic representation of the cell cycle divided into four phases; G1, S, G2 and M. Progression through the cell cycle is regulated by CDK/Cyclin complexes.

1.2.4 DNA Replication

1.2.4.1 Introduction

Replication is a process of DNA duplication, which occurs in the S-phase. The eukaryotic genome is replicated at the rate of 500 nucleotides per minute and requires multiple initiation locations referred to as replication origins. The replication is a step-wise process, which starts with the establishment of the pre-replicative complex followed by DNA unwinding, and recruitment of polymerases. The progression through replication is protected by the S-phase checkpoint, which slows down replication in the event of DNA damage and protects stalled replication fork (see Section 1.3.6).

1.2.4.2 Pre-Initiation of the Replication

The process of replication starts in the early G_1 phase by assembling the pre-replicative complex (pre-RC) at the replication origins. The components of the pre-RC are recruited at the origin in a step-wise manner. First, a group of six proteins forms the origin recognition complex (ORC), which is located at the replication origins (Gilbert 2001). Although the ORC complex proteins are conserved in the eukaryotes, the mechanism of recruitment at the origin differs between species and is hard to define. In *S. cerevisiae* the ORC recognises the autonomously replicating sequences (ARS), which are a few hundred base pairs long. By contrast, in *S. pombe* the AT-rich elements are sufficient to recruit the complex and in humans the ORC can bind to any DNA sequence and therefore can commence replication at multiple locations (Bell and Stillman 1992; Segurado, de Luis et al. 2003; Vashee, Cvetic et al. 2003). Studies in *Drosophila* showed that ORC binding depends on the structure of

the chromatin with a preference towards negatively super-coiled DNA rather than one specific DNA sequence (Remus, Beall et al. 2004). Once established, the ORC attracts the initiation factors Cdc6 and Cdt1, which facilitate loading of the hetero-hexameric Mcm2-7 complex onto the chromatin. Mcm2-7 complex functions as the replication fork helicase and its ablation causes fork stalling. When Mcm2-7 complex is loaded onto the origin, the remaining components of the pre-RC are dispensable for initiation of the replication (Donovan, Harwood et al. 1997; Labib and Diffley 2001). The eukaryotic cell establishes more than necessary pre-RC complexes to ensure that the genome will replicate in full, even if some replication origins fail to fire. In case the neighbouring pre-RC fails to trigger replication, the dormant origins will be fired. Additionally, high concentration of replication origins limits the distance, which a fork needs to travel in order to complete the replication and therefore decreases the time of replication and the probability of stalling (Santocanale, Sharma et al. 1999; Vujcic, Miller et al. 1999).

1.2.4.3 Initiation of the Replication

First, Mcm10 is recruited to the pre-RC and associates with Mcm2-7 and stimulates origin binding of Cdc45 (Wohlschlegel, Dhar et al. 2002; Lee, Seo et al. 2003). The Mcm2-7 complex is phosphorylated by Cdc7-Dbf4, referred as DDK complex, which interacts with the chromatin at the G_1/S (Lei, Kawasaki et al. 1997). Then Cdc45 is recruited and phosphorylated in step-wise manner, first by Cdc7 and then by CDK2. Activated Cdc45 binds to Mcm2-7 and stimulates helicase activity of the latter. (Zou and Stillman 1998; Walter 2000; Van Hatten, Tutter et al. 2002; Masuda, Mimura et al. 2003).

Loading and activation of Cdc45 promotes the origin unwinding and the initiation of the DNA synthesis. The unwound ssDNA is immediately covered and stabilised by RPA proteins, which further facilitate the unwinding of the origin (Walter and Newport 2000). Next, Cdc45 links the components of pre-RC with polymerase α, leaves origin and travels with the Mcm2-7 complex and other components of the replication fork (Mimura and Takisawa 1998; Kukimoto, Igaki et al. 1999; Mimura, Masuda et al. 2000; Tercero, Labib et al. 2000). The Cdc45 is capable of loading polymerases onto both the origin and the elongating forks (Tercero, Labib et al. 2000). The activity of Mcm2-7 depends upon its interaction with Cdc45, which ensures that helicase-dependent DNA unwinding is coupled with the progression of polymerases (Kim, Dallmann et al. 1996; Tercero, Labib et al. 2000). Recruited to Cdc45, polymerase α synthesises primers for both the leading and the lagging strand synthesis and recruits proliferating cell nuclear antigen (PCNA). Once the RNA primer has been produced, polymerase α is replaced with polymerase δ and ε. Polymerases δ and ε associate with the ringed shaped PCNA, which links the polymerases with the DNA template (Mossi and Hubscher 1998; Mimura, Masuda et al. 2000; Hubscher, Maga et al. 2002). The DNA polymerases match complementary nucleotides to the template as they move forward and as a result, create the replication fork structure. The fork consists of two arms: leading strand 3'-5' and lagging strand 5'-3'. Both strands are synthesised by polymerases δ and ε. The leading strand synthesis is continuous, whereas the lagging strand progresses through Okazaki fragments and requires polymerase α for primer synthesis. The RNA primers are replaced with DNA nucleotides by polymerase δ. Next, Okazaki

fragments are ligated in a process catalysed by ligase I (Levin, Bai et al. 1997; Hubscher, Maga et al. 2002; Jin, Ayyagari et al. 2003).

1.2.5 Cell Cycle Checkpoints

To ensure fidelity of cell division, the cell engages checkpoint mechanisms. Four principle checkpoints control the cell cycle in eukaryotes. The G_1 checkpoint makes the key decision as to whether the cell should divide, delay division or enter a resting stage. The S-phase checkpoint controls replication of DNA and triggers inhibition when a replication fork stalls. The G_2 checkpoint assesses the completion of DNA replication and triggers the start of mitosis. The accuracy of mitosis is assessed at the spindle checkpoint, which detects a possible failure of the spindle fibers to attach to the kinetochores (Figure 1.6) and (see Section 1.3.3).

1.3 DNA Damage Response

1.3.1 Introduction

Genomic DNA is constantly exposed to damaging factors including ionising radiation (IR), chemicals and metabolic products such as reactive oxygen species. Those assaults introduce deleterious damages to the DNA and challenge the genetic stability leading to carcinogenesis. Ionising radiation is among the most serious threats to the DNA integrity. It is composed of particles, which have sufficient energy to remove an electron from an atom and produce free radicals. Free radicals are very active chemically and introduce both single-strand (SSB) and double-strand breaks (DSB) to the DNA. Unrepaired DSBs lead to cell death or genomic instability, and SSBs persisting into the S-phase stall or collapse replication forks into DSBs (Wyman and Kanaar 2006; Kastan 2008). The replication fork is additionally stalled in response to insufficient deoxyribonucleotides (dNTP) or DNA adducts, which inhibit fork progression and may lead to genomic instability if not repaired properly (see Sections 1.3.6). To maintain the integrity of the DNA, cells have developed a DNA damage response mechanism (DDR), which regulates the cell cycle progression and activates the DNA repair mechanism, or initiates apoptosis if the DNA damage is extensive. The DSBs are repaired by non-homologous end joining (see Section 1.3.4) or by homologous recombination (see Section 1.3.5). The defects in the replication fork are addressed using a recombination-dependent or a recombination-independent pathway (see Section 1.3.6) and (Kastan 2008).

1.3.2 Recognition of DNA Damage

Breaks in the DNA or replication stress activate a signalling response, which coordinates DNA damage repair and the cell cycle progression (Wyman and Kanaar 2006; Kastan 2008). In response to DSB stress, the Rad50/Mre11/Nbs1 (MRN) complex is recruited to the DSB site and forms a dimeric structure that binds to both ends of the DNA lesion (de Jager, van Noort et al. 2001; Hopfner, Craig et al. 2002; Lisby, Barlow et al. 2004). Next, the Nbs1 unit in the MRN complex recruits the ATM, which consists of inactive homodimers. ATM then autophosphorylates at S1981 and dissociates to form active monomers (Bakkenist and Kastan 2003; Berkovich, Monnat et al. 2007; Williams, Lees-Miller et al. 2010). The active ATM targets proteins responsible for the checkpoint activation and DNA damage repair (see Section 1.3.3) and (Lavin and Kozlov 2007). First, ATM phosphorylates histone H2AX proximal to DSB, which then recruits Mediator of DNA damage checkpoint 1 (MDC1), and additional MRN complexes to the site of the damage (Burma, Chen et al. 2001; Stucki, Clapperton et al. 2005). Increased concentration of MRN leads to further activation of ATMs and to a spread of H2AX phosphorylation resulting in a large focus formation. γH2AX is used as a docking site for BRCA1, 53BP1 and the MRN complex and is dephosphorylated by the protein phosphatase 2A (PP2A) after the DNA damage is repaired (Chowdhury, Keogh et al. 2005; Kim, Minter-Dykhouse et al. 2006). DSB is repaired by either non-homologous end joining (Figure 1.7) and (see Section 1.3.4) or homologous recombination (Figure 1.8) and (see Section 1.3.5). The balance between the repair pathways may depend on the cell cycle phase favouring NHEJ in G_1 and G_2 and HR in the S-phase. Similar to DSB, the stalled

replication fork promotes phosphorylation of the histone H2AX, labelling stretches of ssDNA and initiating checkpoint activation. Initially, ATR phosphorylates H2AX adjacent to the stalled fork, and this phosphorylation signal is spread further to the distant chromatin regions within 1 h from the fork stalling (Sirbu, Couch et al. 2011). Prolonged stalling of the fork triggers hyperphosphorylation of RPA, a further spread of γH2AX catalysed by ATM/DNA-PK and an accumulation of Mre11, KU70/80 and RAD51 to the site. The stalled replication fork is stabilised to allow the repair of the DNA damage and then restarts or collapses into DSB to be processed by HR (Lambert and Carr 2005; Petermann, Orta et al. 2010; Sirbu, Couch et al. 2011).

1.3.3 Cell Cycle Checkpoints

1.3.3.1 G_1/S Checkpoint

After the DNA damage or replication stress has been recognised, the cell cycle progression is restrained to limit the entry into mitosis or the S-phase in the presence of unrepaired DNA. This in turn provides time for the effective removal of the damage. The stress activates the checkpoint at the G_1/S or the G_2/M boundary and replication defects halt the cell cycle during the S-phase (Figure 1.6 and 1.9). The induction of DSB during G_1 phase leads to the G_1/S checkpoint activation, which acts through two parallel pathways targeting activity of CDK/Cyclin complexes. In the first pathway, ATM targets the p53 negative regulator MDM2 causing induction and stabilisation of p53. Activation of p53 leads to transcriptional upregulation of p21, which then binds

and inhibits the CDK2/Cyclin E and the CDK4/6/Cyclin D complexes. Additionally, the DSB stress promotes ATM-dependent phosphorylation of Chk2 followed by destruction of Cdc25 phosphatase. Cdc25 is ubiquitinated and targeted for degradation via the SCF ubiquitin ligase complex. This rapid inactivation of Cdc25 results in retention of the inhibitory phosphorylation on CDK2 (Figure 1.6). The negative regulation of the CDK/Cyclin complex inhibits phosphorylation of Rb. As a result, Rb does not dissociate from E2F transcription factor thus halting the downstream transcription events and preventing the transition to the S-phase (Harbour and Dean 2000; Falck, Mailand et al. 2001; Lukas, Lukas et al. 2004; Deckbar, Jeggo et al. 2011).

1.3.3.2 G_2/M Checkpoint

Similar to the G_1/S checkpoint, the G_2/M is coordinated through two parallel cascades, which serve to inactivate the CDK1/Cyclin B complex. ATM phosphorylates Chk2, which in turn phosphorylates Cdc25. The phosphorylation of Cdc25 leads to its cytoplasmic translocation and results in retention of the inhibitory phosphorylation on CDK1. In parallel, p53 dissociates from MDM2 and regulates transcription of genes downstream including: 14-3-3, GADD45 and p21. 14-3-3 binds to the phosphorylated CDK1/Cyclin B1 and promotes its translocation to the cytoplasm, GADD45 disrupts CDK1/Cyclin B1, and p21 binds and inhibits the activity of the CDK1/Cyclin B1 complex (Figure 1.6).

1.3.3.3 S-Phase Checkpoint

Cells, which experience DNA damage during the S-phase, initiate a signalling pathway to slow down replication and allow DNA repair. This enhances the chances for the proper duplication of DNA and reduces the genomic instability and cancer risk (Hartwell and Weinert 1989; Kastan and Bartek 2004). The cellular response in the S-phase depends on the magnitude and the identity of the insult and can be divided into intra-S checkpoint and replication checkpoint (Figure 1.6 and 1.9). The intra-S checkpoint is induced by DNA damage including DSB and inhibits the origin firing but does not alter the progression of the replication fork (Painter and Young 1980; Falck, Petrini et al. 2002; Merrick, Jackson et al. 2004). When the intra-S checkpoint is defective, cells do not reduce the rate of the DNA synthesis in response to IR and instead undergo Radioresistant DNA Synthesis (RDS) (Painter and Young 1980; Bartek, Lukas et al. 2004). In response to IR, ATM inhibits the new origin firing through two parallel pathways (Falck, Petrini et al. 2002; Bakkenist and Kastan 2003). The first pathway involves ATM-dependent phosphorylation of the Chk1/2 kinases, which mark the Cdc25 phosphatase for degradation and subsequently inactivate the CDK2/Cyclin E complex. This in turn prevents the loading of Cdc45, which is involved in the polymerase recruitment, onto replication origin and inhibits new origin initiation (see Section 1.2.4.3) and (Takisawa, Mimura et al. 2000; Walter and Newport 2000; Falck, Petrini et al. 2002; Busino, Donzelli et al. 2003; Jin, Shirogane et al. 2003). The second pathway acts through ATM by activating NBS1 and subsequently leading to the phosphorylation of the cohesion protein SMC1 (Figure 1.6). The reduction of the DNA synthesis through this pathway is still

elusive (Xu, Kim et al. 2001; Kim, Xu et al. 2002; Yazdi, Wang et al. 2002; Lou, Chini et al. 2003; Lukas, Melander et al. 2004). By contrast, the replication checkpoint is promoted by an insufficient pool of deoxyribonucleotides (dNTP) induced with HU, the chemical inhibition of polymerases induced with camptothecin, as a result of the collision of the replication fork with damaged DNA or aberrant DNA structures induced with UV (Kim and Huberman 2001; Chastain, Heffernan et al. 2006; Seiler, Conti et al. 2007). This checkpoint aims to inhibit the origin firing and to stabilise the replication fork in case of an assault. Unlike IR, UV produces photoproducts, which block the progression of the replication fork. The ATR/ATRIP complex is recruited to the damage site by RPA coated ssDNA on the stalled replication fork and activated by interacting with both the 9-1-1 (Rad9/Rad1/Hus1) and the Rad17-RFC complexes (Burtelow, Roos-Mattjus et al. 2001; Zou and Elledge 2003; Zou, Liu et al. 2003). At the same time, claspin is phosphorylated and associates with Chk1 in response to the stress. (Kumagai and Dunphy 2000; Chini and Chen 2003; Chastain, Heffernan et al. 2006). To gain full activity, Chk1 may need to interact with Timeless (Tim) and Tim interacting protein (Tipin) (Unsal-Kacmaz, Chastain et al. 2007). Activated Chk1 targets Cdc7/Dbf4 and Cdc25A (Jares, Donaldson et al. 2000; Sorensen, Syljuasen et al. 2003; Sorensen, Syljuasen et al. 2004). The cell tolerates a certain level of DNA damage but activates the checkpoint when the critical threshold is passed (Figure 1.9) and (Shimada, Pasero et al. 2002; Mirkin and Mirkin 2007). In addition to the origin firing, cell may control the rate of fork progression. For example, an increase in the dose of UV radiation slows down the replication further but do not decrease the frequency of

replication events (Chastain, Heffernan et al. 2006). Furthermore, the absence of XRCC3 reduces or abrogates the fork slowing and this phenotype is partially rescued by the RAD51 reconstitution suggesting the involvement of two recombination proteins in the fork slowing regulation (Henry-Mowatt, Jackson et al. 2003). It is likely that, XRCC3 and RAD51 stabilise the fork to maintain its integrity and to allow time for a repair. Alternatively, they may allow replicative bypass of the DNA damage. In the latter case, RAD51 cooperates with RAD54 and promotes fork regression into a chicken foot structure, the DNA synthesis on the nascent lagging strand template, and the restoration of the fork (Bugreev, Rossi et al. 2011). The DNA damage bypass is further reviewed in section 1.3.6.

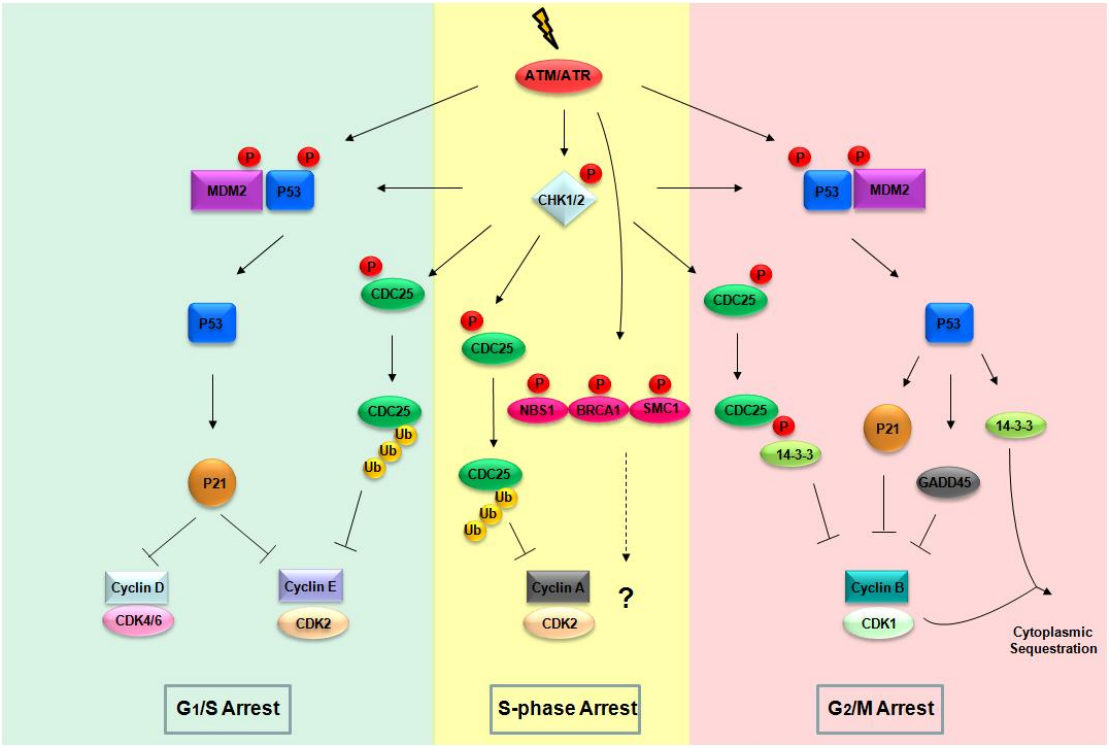


Figure 1.6 The regulation of cell cycle checkpoints. Simplified regulation of three main cell cycle checkpoints including G_1/S, S-phase and G_2/M arrest in response to the DNA damage. After DNA damage ATM/ATR kinases trigger activation of signaling cascades resulting in ultimate restriction of CDKs activity and subsequent arrest or delay of the cell cycle.

1.3.4 Non-Homologous End Joining

NHEJ is a mechanism of DSB which is active throughout the cell cycle. It operates in a template independent manner and predominates during the G_1 and the G_0 cell cycle phases when HR is virtually inactive (Jackson 2002; Rothkamm, Kruger et al. 2003). In response to the assault, a ring-shaped heterodimer Ku70/80 is recruited to the damage site and loaded onto the DNA ends. Ku80 localises to DNA end being distal to the break, whereas Ku70 becomes proximal to the break (Yoo, Kimzey et al. 1999; Walker, Corpina et al. 2001). Next, Ku70/80 recruits the DNA-dependent protein kinase catalytic subunit (DNA-PK_{CS}) to form the active DNA-dependent protein kinase (DNA-PK). DNA-PK_{CS} from the opposite broken DNA ends form a synaptic complex to bring both DNA ends together (DeFazio, Stansel et al. 2002; Weterings and van Gent 2004). Ku additionally interacts with p54/PSF, which potentially increases the effective concentration of DNA ends by stabilising the pairing in the pre-ligation complex (Bladen, Udayakumar et al. 2005; Weterings and Chen 2007). Then, DNA-PK_{CS} autophosphorylates and changes the conformation to allow access of the enzymes, which process and ligate the DNA ends. Full conformational change requires further ATM-mediated phosphorylation (Uematsu, Weterings et al. 2007; Weterings and Chen 2007). This mechanism may protect from premature degradation and from ligation of the DNA termini before the synaptic complex is properly established (Weterings, Verkaik et al. 2003; Block, Yu et al. 2004). In many cases, the post-irradiation DNA ends consist of 3'- or 5'- end overhangs and therefore require processing before they can be properly ligated. The overhangs are removed either by removal of the single stranded DNA part or by synthesis of

complementary strand. Polymerases able to catalyse the complementary strand synthesis were found to accumulate to DSB and to co-localise with the Ku70/80 heterodimer. Those polymerases include the human terminal deoxynucleotidyl transferase (TdT), the DNA polymerase λ, and μ (Mahajan, Gangi-Peterson et al. 1999; Mickelsen, Snyder et al. 1999; Mahajan, Nick McElhinny et al. 2002; Lee, Blanco et al. 2004). By contrast, a resection of overhangs is performed by endonuclease Artemis. Artemis associates with DNA-PK_{CS} and is hyperphosphorylated by both ATM and DNA-PK_{CS} in response to IR (Dahm 2007). Furthermore, processing of the DNA ends may require the addition of 5' phosphate groups, which is mediated by the mammalian polynucleotide kinase (PNK) in a DNA-PK_{CS} and a XRCC4-dependent manner or by the removal of 3' phosphoglycolates performed by tyrosyl-DNA phosphodiesterase (TDP1), PNK and Artemis (Chappell, Hanakahi et al. 2002; Inamdar, Pouliot et al. 2002; Valerie and Povirk 2003; Povirk, Zhou et al. 2007). After overhangs have been removed DNA ends are ligated in a process involving ligase IV and XRCC4. Two proteins form a complex, are recruited to the DSB and are then activated by DNA-Ku to perform ligation (Figure 1.7) and (Nick McElhinny, Snowden et al. 2000). Recent studies, suggest involvement of the XRCC4-like factor (XLF) in a novel mechanism of NHEJ during which non-compatible DNA ends are ligated. In this mechanism, overhanging strands are ligated leaving the other DNA strand unligated, which theoretically may be a target for polymerases (Gu, Lu et al. 2007; Tsai, Kim et al. 2007).

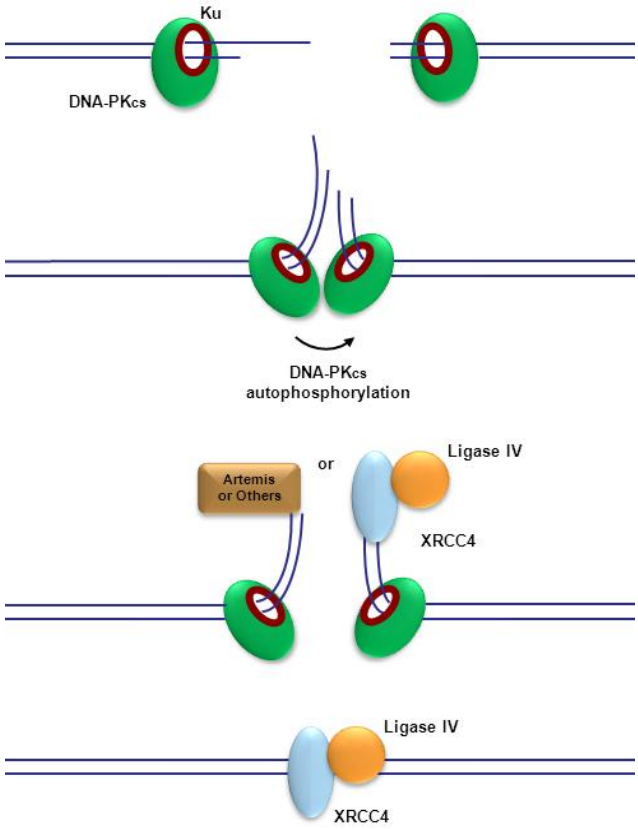


Figure 1.7 Non-Homologous End Joining. Schematic model of the non-homologous end joining mechanism divided into four stages: DSB recognition, DNA-PK activation, DNA ends processing and ligation. Ku heterodimer associates with the DNA ends and facilitates the recruitment of DNA-PK_{cs} to form DNA-PK complex. DNA-PK promotes the DNA end processing and the subsequent ligation of DNA by Ligase IV/XRCC4.

1.3.5 Homologous Recombination

Homologous recombination is an essential mechanism of DSB repair occurring in the S and G_2 phases. Decreased rate of the HR leads to insufficient DNA repair. Cells harboring mutations in BRCA1 or BRCA2, tumour suppressors involved in HR, have increased sensitivity to IR and high susceptibility to breast and ovarian cancers (Powell, Kachnic 2003). Yeast rad51 mutants are viable but very sensitive to IR. Furthermore, murine cells deficient in RAD51 homologue accumulate chromosomal breaks prior to death (Sasaki et al. 1998). By contrast cells from Bloom Syndrome patients have an increase in homologous recombination rate, which leads to a loss of heterozygosity and ultimately gives rise to the cancer (Karow, Wu et al. 2000; Wang, Seki et.al. 2000). HR engages the undamaged template from the sister chromatid to deliver an error-free repair of the DSB lesion. After the damage has been recognised and the checkpoint activated, HR initiates a DNA strand resection. First, CDK2 phosphorylates CtIP to promote interaction with BRCT motif of BRCA1 (Yu, Wu et al. 1998; Huertas and Jackson 2009). Next, CtIP is ubiquitinated by BRCA1 ring domain, which possesses E3 ubiquitin ligase activity. CtIP ubiquitination is required for its chromatin binding and facilitates accumulation of CtIP/BRCA1 complex to the DSB site (Yu, Fu et al. 2006). Alternatively, BRCA1 interacts with protein Abraxas, which recruits RAP80 to BRCA1, bridges interaction between RAP80 and BRCA1 BRCT domain and mediates the localization of BRCA1 to the site of the DNA damage. Both RAP80 and Abraxas are required for DNA damage resistance (Sobhian, Shao 2007; Wang, Matsuoka 2007). Recruited to DNA damage site, CtIP/BRCA1 interacts with MRN and promotes the DNA end resection to create short

ssDNA overhangs (Sartori, Lukas et al. 2007; Chen, Nievera et al. 2008). Then overhangs are targeted for further processing by helicase BLM and two nucleases, Exo1 and Dna2. In the absence of those DNA processing factors, MRN/CtIP resection progresses but is insufficient for complete formation of overhangs (Liao, Toczylowski 2008; Nimonkar, Ozsoy 2008; Zhu, Chung 2008). The DNA overhangs are then coated with Replication Protein A (RPA), which has high affinity for ssDNA and removes secondary structures. (Bochkareva, Korolev et al. 2002; West 2003). BRCA2 interacts with RAD51 through BRC motifs (Wong, Pero et al. 1997; Galkin, Esashi et al. 2005; Shivji, Davies et al. 2006; Tal, Arbel-Goren et al. 2009). Interestingly, BRC repeats promote loading of RAD51 onto ssDNA but also reduce the association with dsDNA (Shivji, Mukund et al. 2009). The assembly of RAD51 nucleoprotein filament catalysed by BRCA2 causes displacement of RPA from ssDNA (Liu, Doty et al. 2010; Seong, Colavito et al. 2009). Next, BRC acts by blocking ATP hydrolysis and by stabilising the active ATP bound to RAD51 on ssDNA, thereby establishing a favorable state for DNA strand exchange (Carreira, Hilario et al. 2009; Shivji, Mukund et al. 2009). Additionally, BRCA2 interacts with multimeric RAD51 through the carboxyl terminal. The interaction between C-terminus and RAD51 depends on CDK phosphorylation of S3291 on BRCA2, and is regulated in both a cell cycle and a DNA damage dependant manner (Esashi, Christ et al. 2005; Esashi, Galkin et al. 2007). According to conflicting literature BRCA2 C-terminus is involved in the replication fork stabilisation and/or in HR. (Ayoub, Rajendra et al. 2009; Hashimoto, Chaudhuri et al. 2010; Schlacher, Christ et al. 2011; Mauro, Rego et al. 2012). The RAD51 nucleoprotein filament invades the sister chromatid

to form a D-loop and to search for a homologous sequence. The homology search happens through random collisions of nucleoprotein filament with the invaded DNA strand. It is still not very clear how RAD51 pre-synaptic filament is disassembled. In yeast Srs2 helicase triggers ATM hydrolysis within the Rad51 filament causing a weakening of the Rad51-DNA interaction and allowing filament disassemble (Antony, Tomko et al. 2009). In mammals homologue of Srs2 has not been identified yet but proteins including: RecQ5, BLM and FANCJ were reported to disrupt RAD51 filaments from ssDNA. By contrast the removal of RAD51 from dsDNA is catalysed by RAD54. (Burgreev, Yu et al. 2007; Hu, Raynard et al. 2007; Sommers, Rawtani et al. 2009). The removal of excess of RAD51 prevents nonspecific association of RAD51 with the bulk chromatin and creates access to the DNA for polymerases, which use 3'- DNA terminus in a D-loop to initiate DNA synthesis (Solinger, Kiianitsa et al. 2002; Xu and Marians 2002; Heyer, Li et al. 2006). DSB is repaired through synthesis-dependent strand annealing (SDSA) or double strand break repair (DSBR) (Figure 1.8) and (San Filippo, Sung et al. 2008). In the SDSA scenario, the invading DNA strand anneals with the complementary ssDNA strand, which is associated with the other double strand break end. The 3'- extension at a D-loop is performed by polymerase η (eta) until the gap is filled (McIlwraith, Vaisman et al. 2005; San Filippo, Sung et al. 2008). Interestingly however, the polymerase η deficient cells do not show obvious defects in HR, leading to the conclusion that other polymerases may be involved. It is speculated that the polymerase ξ is involved in the process because its deficiency is lethal (Paques and Haber 1999). When the repair is finished the newly synthesised DNA strand is

released by sliding Holliday Junction (HJ) in a 3'- end direction. Although many proteins, including: WRN, RAD54, BLM and p53, were shown to play a role in HJ migration during repair, how the DNA strand is released is still unclear (Lee, Cavallo et al. 1997; Mohaghegh, Karow et al. 2001; Bugreev, Mazina et al. 2006; Raynard, Bussen et al. 2006). Finally, DNA nicks are sealed by DNA ligase I and polymerase δ/ε (Batty and Wood 2000). The D-loop is unwound and only non-crossover products are formed (Figure 1.8) and (San Filippo, Sung et al. 2008). In the second pathway, both DNA ends invade a homologous template and form intermediate structure with two HJs. The double Holliday Junction (dHJ) is dissolved by BLM and topoisomerase III α or resolved in a process catalysed by nucleases including GEN1, SLX1-SLX4, Mus81-Eme1/2 giving rise to non-crossover or crossover products (Figure 1.8) and (Chen, Melchionna et al. 2001; Fekairi, Scaglione et al. 2009; Gaillard, Noguchi et al. 2003; Rass, Compton et al. 2010; Raynard, Bussen et al. 2006).

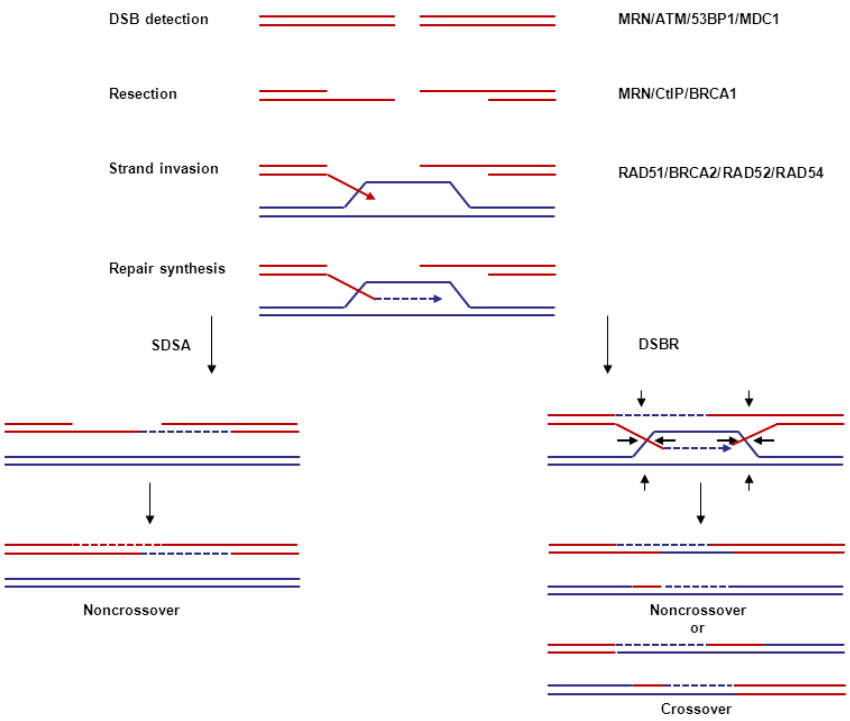


Figure 1.8 Homologous Recombination. Schematic model of the homologous recombination mechanism. DSB is detected by MRN, 53BP1 and MDC1 proteins. Then, the DNA ends are resected by Mre11 and CtIP and generated ssDNA invades the homologous strand in a reaction that is catalysed by RAD51 and BRCA2. HR involves synthesis-dependent strand annealing (SDSA) or double strand repair (DSBR) pathways to resolve the damage. Horizontal arrows refer to non-crossover and vertical arrows to crossover products. Figure adapted from (Yata and Esashi 2009).

1.3.6 DNA Damage Repair During S-Phase

1.3.6.1 Introduction

The replication forks stall when they encounter DNA lesions, secondary DNA structures, template-bound proteins, or due to a lack of deoxyribonucleotides (Mirkin and Mirkin 2007; Budzowska and Kanaar 2009). Cells have evolved two mechanisms to deal with DNA damage during the S-phase: homologous recombination and trans-lesion synthesis (TLS). TLS uses specialised polymerases, which tolerate irregular template structures to replicate DNA over damaged template. This method is error-prone because it incorporates incorrect nucleotides and leads subsequently to mutations (Kunkel, Pavlov et al. 2003; Yang 2003; Budzowska and Kanaar 2009). The mechanism preference is not completely clear but it potentially depends on the type of the damage encountered by forks (Budzowska and Kanaar 2009).

1.3.6.2 HR-Dependent Models of DNA Damage Repair During S-Phase

If the lagging strand of the replication fork is affected, the replication can be restarted with a new Okazaki fragment. This approach leaves a ssDNA gap behind the fork, which is repaired after the replication is finished. Alternatively, the ssDNA gap could be invaded by the undamaged strand and repaired in the HR-dependent manner (Michel, Boubakri et al. 2007; Bugreev, Rossi et al. 2011). In contrast, a DNA damage on the leading strand is resolved through one of the three pathways: fork regression, HR-dependent template strand switching, and DSB-dependent restart (Figure 1.9) and (Budzowska and Kanaar 2009; Mazloum and Holloman 2009; Bugreev, Rossi et al. 2011). The DSB-dependent restart utilises HR when the fork encounters

ssDNA or stalls at the DNA damage for a long period of time. Prolonged stalling may be induced with HU, UV, MMS or CPT and requires Mus81-dependent cleavage of an arm of the fork. The balance between Mus81-dependent fork collapse into DSBs and the alternative repair mechanisms depends on the length of stalling (Doe, Ahn et al. 2002; Ciccia, Constantinou et al. 2003; Whitby, Osman et al. 2003; Hanada, Budzowska et al. 2007; Lambert, Froget et al. 2007; Petermann, Orta et al. 2010). The separated arm of the fork is resected to allow establishment of RAD51 filaments catalysed by BRCA2. Then, RAD51 promotes strand invasion into the sister chromatid to re-establish defective fork (Budzowska and Kanaar 2009). The significance of this model is not clear and according to conflicting data, the Mus81-dependent DSB may be either sufficient to restart the replication, or may be involved in post-replication repair only. In the second scenario, the eukaryotic cells restart through a new origin firing and activate Mus81 only when the checkpoint adapts or leaks (Hanada, Budzowska et al. 2007; Petermann, Orta et al. 2010). Another pathway utilises the HR template switch to restart replication. Despite the damage on the leading strand, helicase continues to unwind the fork for lagging strand synthesis. This creates ssDNA gaps on the leading strand, which can be repaired by HR using undamaged sister chromatid. Alternatively, the fork can reverse into a ‘chicken foot’ structure in order to bypass the block (Figure 1.9) and (Pages and Fuchs 2003; Heller and Marians 2006; Lehmann and Fuchs 2006; Mazloum and Holloman 2009; Bugreev, Rossi et al. 2011). The fork regression is promoted by WRN, BLM and RAD54. The activity of the last is additionally facilitated by RAD51 (Machwe, Xiao et al. 2006; Mazloum and Holloman 2009; Bugreev, Rossi et

al. 2011). RAD51 promotes the accumulation of the ‘chicken foot’ structure and prevents fork restoration. This may be due to a recently discovered role of the RAD51 filament-dependent stabilisation of the regressed fork, which is discussed below (see Section 1.3.6.3) and (Bugreev, Rossi et al. 2011; Schlacher, Christ et al. 2011). In the chicken foot structure, the elongated lagging strand serves as a template for leading strand synthesis and extends the leading strand beyond the point of the DNA damage on the parental strand. Thereafter, the ‘chicken foot’ structure is reset by reversed branch migration into the fork, in which damage is bypassed. (Budzowska and Kanaar 2009; Mazloum and Holloman 2009; Bugreev, Rossi et al. 2011). The chicken foot structure is a hypothesis which has not been confirmed in mammalian cells in vivo. In vivo the chicken foot structure is observed in budding yeast as an effect of defective intra-S checkpoint. In checkpoint-deficient yeast majority of stalling forks collapse and 10% forms chicken foot structures contributing to incomplete replication or cell death (Lopes, Cotta-Ramusino et al. 2001; Sogo, Lopes et al. 2002; Tercero and Diffley 2001).

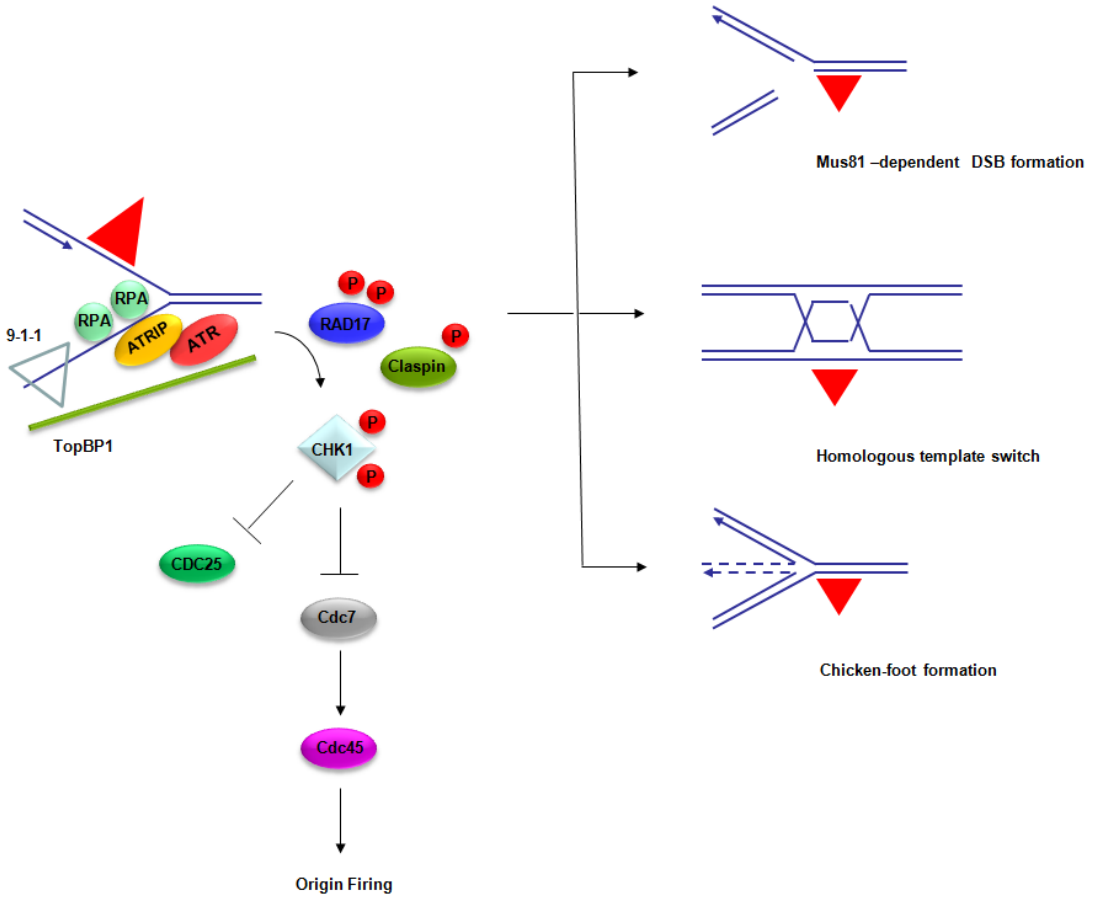


Figure 1.9 The DNA Damage during S-Phase. In response to the lesion, replication fork stalls and activates checkpoint to prevent new replication origin firing. Replication fork bypasses lesion using homologous template switching or regresses into chicken foot structure. Alternatively, after prolonged stalling Mus81 separates the arm from the fork and replication is restarted using HR.

1.3.6.3 Regressed Fork Protection

When the fork reverses into a ‘chicken foot’ structure, the nascent DNA strand is coated with the RAD51 filament. Once established, the RAD51 filament is stabilised by BRCA2. This function of BRCA2 is HR-independent and executed by the C-terminal region of the protein (Lomonosov, Anand et al. 2003; Esashi, Galkin et al. 2007; Hashimoto, Chaudhuri et al. 2010; Schlacher, Christ et al. 2011). The C-terminal of BRCA2 contains the S3291 phosphorylation site, which regulates its affinity to the RAD51 filaments. Low phosphorylation of the C-terminal increases the interaction with the RAD51 filament, whereas the phosphorylation of S3291-BRCA2 has the opposite effect (Esashi, Christ et al. 2005). The phosphorylation of S3291-BRCA2 is regulated in a cell cycle-dependent manner: it falls during the S-phase but increases when cells progress towards mitosis. The cell cycle regulation is overcome by the DNA damage induction, which reduces the S3291-BRCA2 phosphorylation and stimulates interaction with RAD51 in the presence of damage (Esashi, Christ et al. 2005). When the DNA stress is removed, BRCA2 is phosphorylated again and promotes the RAD51 filament disassembly leading to replication restart (Ayoub, Rajendra et al. 2009; Davies and Pellegrini 2007; Esashi, Christ et al. 2005). The S3291-BRCA2 can be phosphorylated by both CDK1/Cyclin B and CDK2/Cyclin A, however the overall status of the phosphorylation may depend also on the activity of phosphatases and factors, which modulate recognition of the substrates by CDKs in cell cycle (Falck, Mailand et al. 2001; Esashi, Christ et al. 2005). In the absence of RAD51 filament, Mre11 promotes fork degradation independently (Hashimoto, Chaudhuri et al. 2010; Schlacher, Christ et al.

2011). Mre11 may also cooperate with other nucleases for leading strand degradation, including WRN, which possesses 3'-5' exonuclease activity stimulated by Mre11 (Cheng, von Kobbe et al. 2004). Degradation of the nascent lagging strand may be facilitated by 5'-3' nucleases EXO1 or CtIP (Mimitou and Symington 2009). BRCA2-deficient cells develop chromosome aberrations such as breaks and radial structures, which may be related to the degradation of unprotected replication forks (Schlacher, Christ et al. 2011).

1.4. Large Tumour Suppressor

1.4.1 Introduction

The Large Tumour Suppressor (LATS) is an evolutionary conserved serine/threonie kinase involved in developmental regulation, apoptosis, cell cycle and cytokinesis, DNA damage repair, and apoptosis (Visser and Yang 2010). It is a human homologue of *Drosophila* dlats/warts tumour suppressor discovered in two independent screens in *Drosophila* in 1995 (Justice, Zilian et al. 1995; Xu, Wang et al. 1995). Dlats and warts encode the same gene and for consistency only warts (wts) will be used in reference to *Drosophila* homologue in this thesis. The warts mutants produced an over-growth phenotype. The medium and strong allele's mutant larvae were much bigger than wild type, whereas the weak allele's flies developed rough eyes, wing held-out and outgrowth on the head. The strong alleles exhibited late embryonic and early larvae lethality, medium, late larvae and pupal lethality, and weak semi-viable lethality (Xu, Wang et al. 1995). The homozygous loss of warts resulted in clones being greatly overgrown, fragmented and rounded in response to irradiation. A rounded shape suggested that cells in warts mutant clones did not divide in a controlled manner and their proliferation was not oriented preferentially. It was also noticeable that irradiated clones developed many overgrown patches on legs or wings. The warts negative cells had very irregular cell shape with cells being domed in epithelium in comparison to being flat in the wild type (Justice, Zilian et al. 1995). The expression of the human LATS1 in mutant flies rescued phenotype including embryonic lethality and developmental defects proving that LATS1 is a

functional homologue of warts (Tao, Zhang et al. 1999). In mammals, mice mutants of Lats1 developed soft tissue sarcomas and ovarian tumours (St John, Tao et al. 1999). In humans, the inactivation of LATS1 was associated with breast cancer, tissue sarcoma, leukemia, lung and esophageal cancers (Hisaoka, Tanaka et al. 2002; Takahashi, Miyoshi et al. 2005; Visser and Yang 2010). In contrast to the majority of tumour suppressors, which are inactivated by combination of LOH of one allele and mutation of the other allele, mutations in LATS1 gene are very rare. LATS1 loses its function due to hypermethylation of the CpG promoter region, which occurs in 56.7% of the tumours. The downregulation of LATS1 resulting from the gene promoter hypermethylation is correlated with aggressive breast tumours distinguished by large tumour size, high lymph node metastasis, negative status of estrogen, and is associated with a poor prognosis (Takahashi, Miyoshi et al. 2005).

1.4.2 Homologues and Molecular Structure

Warts is homologous to the budding yeast dbf2, the fission yeast orb6 and the C. elegance Lats. In mammalian systems, it has homology to LATS1, LATS2, NDR1 and NDR2 in humans and to Lats1 and Lats2 in mice (Figure 1.10) and (Tao, Zhang et al. 1999; Hori, Takaori-Kondo et al. 2000; Yabuta, Fujii et al. 2000). Warts and human LATS1 share 39 % overall sequence similarity with 84 % similarity and 73 % identity over the kinase domain and 42 % similarity and 22 % identity over N-terminal (Tao, Zhang et al. 1999). LATS1 belongs to the AGC kinase family due to the alignments in the sequence of the C-

terminal kinase domain (Pearce, Komander et al. 2010). The AGC group of proteins was named after the protein kinase A, G, and C families (PKA, PKC, PKG). AGC are cytoplasmic Ser/Thr kinases that are regulated by secondary messengers such as cyclic AMP (PKA) or lipids (PKC). The AGC kinases are involved in the regulation of cell growth, differentiation and cell survival. They are activated by phosphorylation of the activation loop and the subsequent relocation of key catalytic and substrate binding regions (Johnson, Noble et al. 1996; Huse and Kuriyan 2002; Nolen, Taylor et al. 2004; Pearce, Komander et al. 2010).

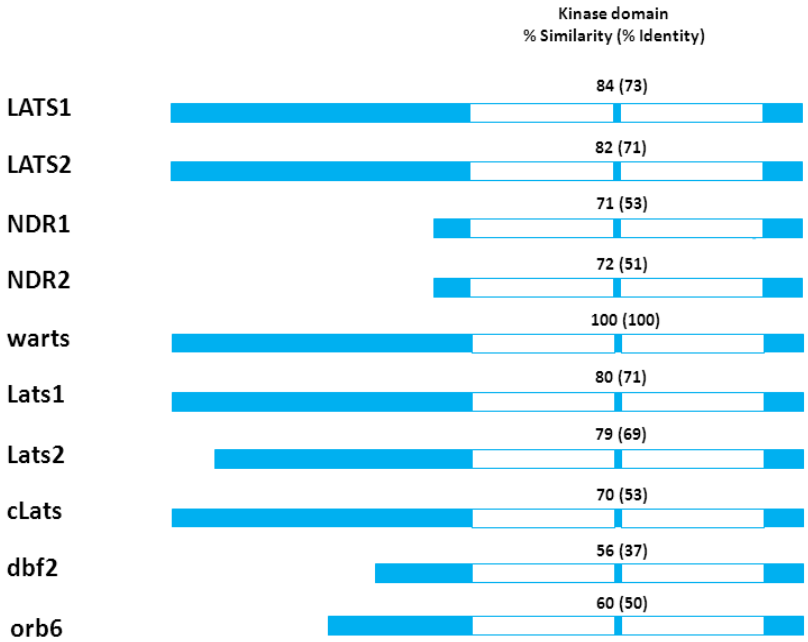


Figure 1.10 LATS Homologues. Evolutionary conserved LATS homologues shown with percentage identity and similarity of the kinase domain to the *Drosophila* warts gene. Figure adapted from (Visser and Yang 2010).

In humans, LATS1 and LATS2 are the closest homologues as demonstrated by their molecular structure (Figure 1.11). LATS1 shares 52 % overall sequence identity with LATS2, with 85 % sequence identity over the kinase domain (Yabuta, Fujii et al. 2000). Their C-terminal kinase domains are conserved, whereas the N-terminals differ substantially, suggesting a functional difference between the homologues. The LATS1 gene is mapped to chromosome 6q24-51 and encodes a large kinase of 160 kDa, whereas LATS2 is located at chromosome 13q11-q12 and expresses protein of 120 kDa (Nishiyama, Hirota et al. 1999; Yabuta, Fujii et al. 2000). Both LATS1 and LATS2 have an insert of 30-60 amino acids in between VII and VIII subdomain, which potentially has an autoinhibitory role (Pearce, Komander et al. 2010). Additionally, LATS kinases have a protein binding domain (PBD),

through which they bind to LIMK1, MOB1 and Zyxin (Hirota, Morisaki et al. 2000; Yang, Yu et al. 2004; Bothos, Tuttle et al. 2005). LATS1 and LATS2 have a PPxY motif (P-proline, X-any amino acid, Y-tyrosine), which binds the WW domains of proteins such as YAP or TAZ (Hao, Chun et al. 2008; Lei, Zhang et al. 2008). LATS1 in its sequence has a region rich in proline called P-stretch, which is potentially involved in protein-protein interactions (Nishiyama, Hirota et al. 1999). LATS2 does not have a P-stretch, however, it possesses proline alanine repeats (PAPA) (Figure 1.11) and (Yabuta, Fujii et al. 2000). The highest expression of LATS1 is observed in the adult ovary, whereas LATS2 is highly expressed in the heart and the muscle (Tao, Zhang et al. 1999; Hori, Takaori-Kondo et al. 2000; Yabuta, Fujii et al. 2000). Differences in the structure as well as different expression patterns suggest that LATS1 and LATS2 have distinct functions.

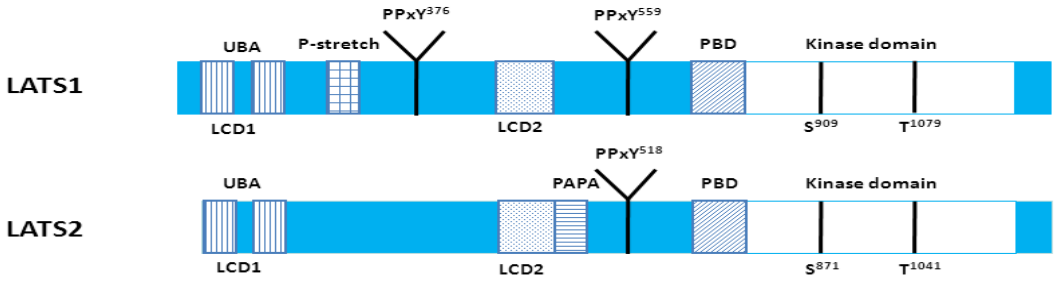


Figure 1.11 Structures of LATS1 and LATS2. LATS1 and LATS2 have conserved domains including kinase domain at C-terminus, Protein Binding Domain (PBD), LATS conserved Domains (LDC1 and LDC2), ubiquitin binding domain (UBA) and PPxY motifs. In addition, LATS1 has a P-stretch, whereas LATS2 possesses a PAPA repeat. Figure adapted from (Visser and Yang 2010).

1.4.3 Developmental Regulation

The LATS kinases play a central role in developmental regulation through their involvement in the growth control hippo pathway (Figure 1.12). The hippo pathway is conserved from *Drosophila* to mammals. In *Drosophila,* Hippo (Hpo), from which the Hippo pathway has its name, the scaffolding adaptor protein Salvador (Sav), Warts (Wts), and Mob as a tumour suppressor (Mats) interact together and transduce signaling downstream (Figure 1.12 a) and (Tao, Zhang et al. 1999; Tapon, Harvey et al. 2002; Harvey, Pfleger et al. 2003; Pantalacci, Tapon et al. 2003; Udan, Kango-Singh et al. 2003; Wu, Huang et al. 2003; Lai, Wei et al. 2005; Wei, Shimizu et al. 2007). The hpo, wts, sav or mats mutants show dramatic tissue overgrowth, whereas the loss of the oncogene Yorki (Yki), the downstream target of warts, is associated with a reduction in tissue growth (Dong, Feldmann et al. 2007). Normally, the tumour suppressor dRASSF, an ortholog of *Drosophila* RASSF, competes with Sav for binding with Hpo and restricts the activity of the latter (Polesello, Huelsmann et al. 2006). In response to signals upstream, four proteins, Hpo, Sav, Wts and Mats complex together and regulate the expression of cell proliferation genes. Hpo autophosphorylates and then activates Sav, Wts and Mats (Glantschnig, Rodan et al. 2002; Wu, Huang et al. 2003; Lai, Wei et al. 2005; Wei, Shimizu et al. 2007). Phosphorylation of Mats enhances the activity of Wts, which in turn phosphorylates Yorki (Yki) at three different sites: S111, S168 and S250 (Wei, Shimizu et al. 2007; Oh and Irvine 2009). Although, the phosphorylation of all three sites contributes to the inhibition of Yki, S168 is particularly important as it facilitates the binding to the 14-3-3 protein and the subsequent cytoplasm retention of the protein (Basu, Totty et

al. 2003; Dong, Feldmann et al. 2007; Zhao, Wei et al. 2007; Hao, Chun et al. 2008; Oh and Irvine 2009). In contrast, when Yki is not phosphorylated, it binds to the transcription factor Scalloped (Sd) and is transported into the nucleus. There, it binds to the DNA and initiates the transcription of the cell proliferation genes including Cyclin E, c-Myc, microRNA bantam, and of genes responsible for preventing apoptosis, including *Drosophila* inhibitor of apoptosis 1 (diap1) (Figure 1.12 a) and (Huang, Wu et al. 2005; Nolo, Morrison et al. 2006; Goulev, Fauny et al. 2008; Stocker 2011). There are potentially three upstream regulatory branches, which activate the Hippo pathway in *Drosophila* including the Ex/Kibra/Mer complex, the Ft-Dachsous (Ds) branch and the apical–basal polarity proteins. Expanded (Ex), Merlin (Mer) and Kibra work upstream of the Hippo core. Phenotypes of the mutants of Ex, Mer of Kibra are mild compared to the mutant phenotypes of wts or hpo. However, phenotypes resulting from the combination of double mutants of ex, mer or kibra are much more significant than the single mutant of hpo (Hamaratoglu, Willecke et al. 2006; Baumgartner, Poernbacher et al. 2010; Genevet, Wehr et al. 2010; Yu, Zheng et al. 2010). Ex/Mer/Kibra connect directly to the Hippo pathway core, Ex interacts with Hpo, Mer and Kibra with Sav (Yu, Zheng et al. 2010). How this interaction regulates Hippo pathway, is still unknown. Additionally, Ex may modulate the activity of Yki by direct binding. This interaction engages the PPxY motif of Ex and WW domain of Yki and potentially, sequesters Yki in cytoplasm (Badouel, Gardano et al. 2009). Fat, which is upstream of Ex/Mer/Kibra, regulates the activity of the Hippo pathway by initiating localisation of Ex (but not Mer) to the apical membrane of epithelial cells (Bennett and Harvey 2006; Silva, Tsatskis et al. 2006;

Willecke, Hamaratoglu et al. 2006). The loss of Fat leads to overproliferation (Bryant, Huettner et al. 1988). Fat is activated upon binding to its ligand Dachsous (Ds), a cadherin from the neighboring cell, which promotes the phosphorylation of intracellular domain of Fat by Casein Kinase 1ε homolog Discs overgrown (Dco) (Clark, Brentrup et al. 1995; Feng and Irvine 2009; Sopko, Silva et al. 2009). In addition to that, Fat works in combination with myosin Dachs, which accumulates to the membrane when Fat is inactive and subsequently downregulates wts through its degradation (Figure 1.12 a) and (Cho, Feng et al. 2006). The third potential regulatory mechanism involves epithelial cell polarity through the large apical membrane protein Crumbs (Crb). Crb works upstream of Ex/Kibra/Mer complex and its overexpression or mutation leads to the activation of Yki and the expression of downstream targets (Ling, Zheng et al. 2010; Robinson, Huang et al. 2010). Crb interacts directly with Ex and facilitates the apical membrane localisation of Ex in epithelial cells. Hypothetically, Crb may play a role in an Ex/Kibra/Mer complex establishment and hence the regulation of hippo pathway (Figure 1.12 a) and (Grzeschik, Parsons et al. 2010; Ling, Zheng et al. 2010). In mammals, the Hippo pathway is more complex than in *Drosophila* and is involved in regulation of cell proliferation and apoptosis (Figure 1.12 b). The main components of mammalian pathway are orthologs of proteins found in flies. In mammals, YAP, TAZ, LATS1/2, MST1/2, Mob, WW45, are orthologs of Yorki, Warts, Hippo and Mats, respectively (Sudol 1994; Creasy and Chernoff 1995; Creasy and Chernoff 1995; Tao, Zhang et al. 1999; Kanai, Marignani et al. 2000; Yabuta, Fujii et al. 2000; Tapon, Harvey et al. 2002; Bichsel, Tamaskovic et al. 2004; Chow, Hao et al. 2010). Mutants of LATS1

result in tissue sarcoma in mice and mutations in MST2 lead to an increased organ size including the liver in mice. Overexpression of YAP causes liver overgrowth and subsequently tumour formation (St John, Tao et al. 1999; Dong, Feldmann et al. 2007; Song, Mak et al. 2010). In addition to YAP, the Hippo pathway in mammals regulates gene expression through the additional transcription co-activator TAZ. YAP and TAZ are similar in structure as well as in function (Kanai, Marignani et al. 2000; Hong and Yaffe 2006; Lei, Zhang et al. 2008). In the absence of a stimulus, MST2 is inactive and bound to the Raf-1 oncoprotein. In response to signalling upstream, RAS effector protein, which belongs to the RASSF family, targets MST and disrupts interaction with Raf-1. (Scheel and Hofmann 2003; O'Neill, Rushworth et al. 2004; O'Neill and Kolch 2005; Matallanas, Romano et al. 2007). The RASSF association and recruitment of MST to the membrane promotes dimerisation of MST and trans-autophosphorylation of its kinase domains (Glantschnig, Rodan et al. 2002; Agathanggelou, Cooper et al. 2005). At the same time Mob1 targets LATS1 to the membrane, where together with Mob1 and the scaffolding protein WW45, LATS1 is phosphorylated by the active MST2. LATS1 gains fully activity when it is phosphorylated at its hydrophobic motif and activation loop. Then it targets S127 on YAP leading to its inhibition and cytoplasmic sequestration (Chan, Nousiainen et al. 2005; Zhao, Wei et al. 2007). In the absence of a stimulus, the Hippo cascade is not activated and does not restrict the transcription co-activators YAP/TAZ. YAP/TAZ target then TEAD and activate the transcription of genes required for cell growth. Interestingly, in mammals YAP/TAZ may not regulate the expression of Cyclin E since the level of the Cyclin is not elevated in WW45 mutant mice (Lee, Kim et al.

2008). A further difference between flies and mammals is that in mammals the LATS-mediated phosphorylation of YAP may induce interaction with the tumour suppressor p73, thereby activating the transcription of the apoptotic genes such as PUMA (Figure 1.12 b) and (see Section 1.4.4) and (Matallanas, Romano et al. 2007).

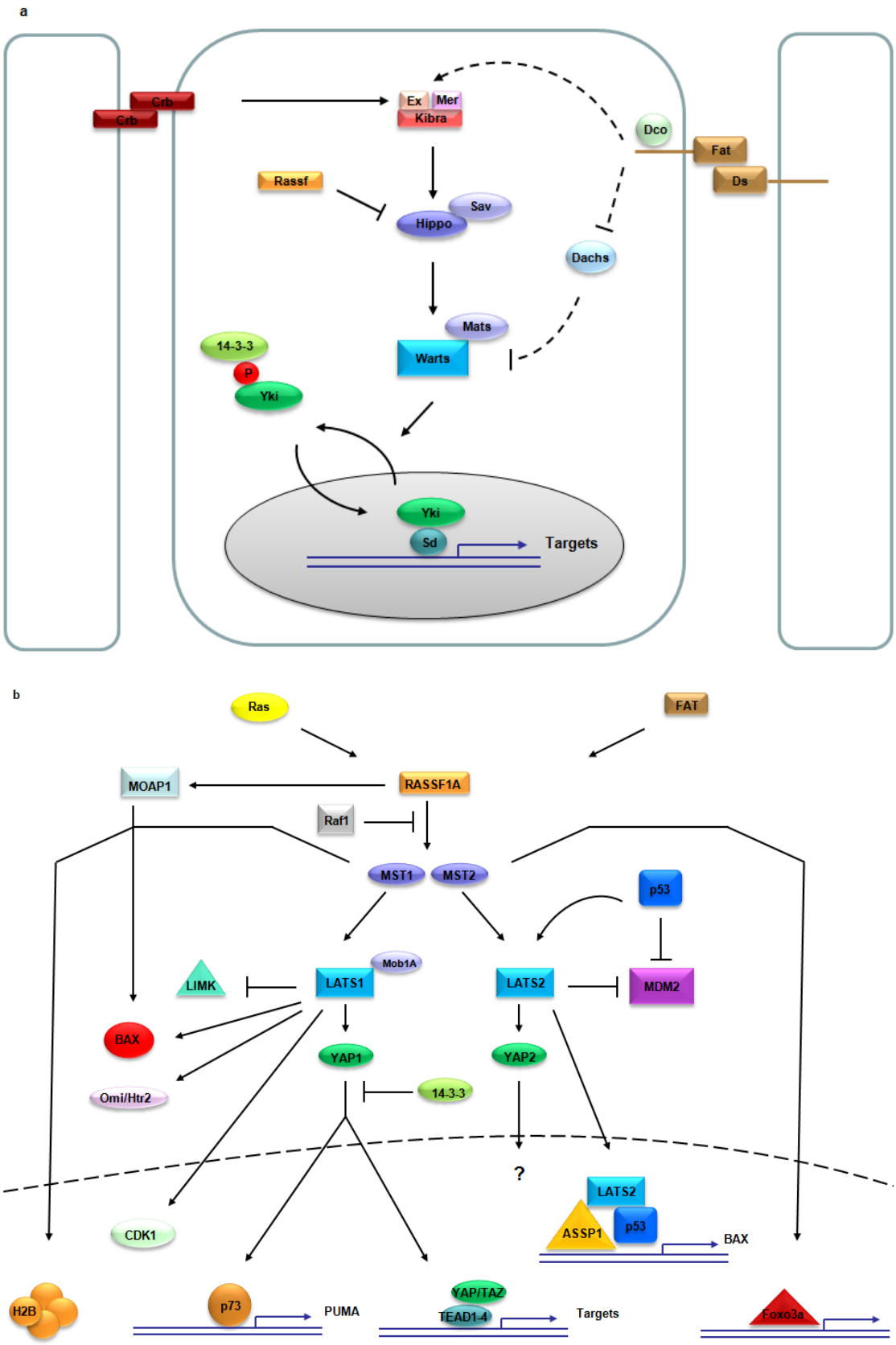


Figure 1.12 The Hippo Pathway. (a) Drosophila and **(b)** Mammals. Detailed description of pathways in the text. Figures adapted from (Halder and Johnson 2011) and (Matallanas, Romano et al. 2008)

1.4.4 Apoptosis

LATS kinases regulate apoptosis through a number of mechanisms. First, overexpression of LATS2 induces apoptosis through downregulation of anti-apoptotic Bcl-2 and Bcl-XL but does not alter levels of apoptotic Bax (Ke, Pei et al. 2004). In contrast, overexpression of LATS1 in cells upregulates levels of Bax and induces apoptosis (Xia, Qi et al. 2002). Furthermore, in response to microtubule damage LATS2 binds MDM2 and inactivates it. This results in p53 activation, which selectively turns on LATS2 transcription, resulting in general upregulation of nuclear LATS2 levels and further stabilisation and induction of p53 (Figure 1.12 b). The activation of p53 leads to transcription of p21 and subsequent G_1 tetraploid checkpoint activation (Aylon, Michael et al. 2006). Interestingly, p53 level is reduced in cells expressing kinase dead LATS1 leading to the abrogation of the G_1 tetraploid checkpoint and subsequent development of polyploidy (Iida, Hirota et al. 2004). In response to oncogenic stress LATS2 phosphorylates ASSP1, proapoptotic p53 transcriptional cofactor and induces its translocation to the nucleus. LATS2 together with ASPP1 relocate p53 towards proapoptotic promoters and induce death of polyploidy cells (Figure 1.12 b) and (Aylon, Ofir-Rosenfeld et al. 2010). Moreover, mutant K-Ras activates proapoptotic RASSF1A-MST2-LATS1 signalling. K-Ras is the only isoform of Ras oncogene able to elicit apoptosis. In reponse to the activation of the pathway LATS1 binds and sequesters MDM2 causing stabilisation of p53 and subsequent apoptosis. This pathway is antagonised by a wild type K-Ras, which inhibits MST2 pathway through activation of AKT (Matallanas, Romano et al. 2011). Furthermore, LATS1 engages the p73 directed transcription of proapoptotic gene PUMA. This stimulation is promoted by RASSF1A expression, serum deprivation or in response to IR (Matallanas, Romano et al. 2007;

Vichalkovski, Gresko et al. 2008; Hamilton, Yee et al. 2009). The activated RASSF1A dissociates Raf1-MST2 complex and subsequently enhances the interaction between MST2 and LATS1. Activated LATS1 phosphorylates YAP1 and promotes its translocation to the nucleus, where YAP1 associates with p73 and transcribes pro-apoptotic PUMA (Figure 1.12 b) and (Matallanas, Romano et al. 2007). Alternatively, upon DNA damage, ATM phosphorylates RASSF1A at Ser131 leading to the activation of both LATS1 and MST2 and the subsequent stabilisation of p73 (Hamilton, Yee et al. 2009). This leads to the transcription of PUMA and the promotion of apoptosis (Yu, Zhang 2008; Hamilton, Yee et al. 2009). The pathway is defective in cell lines harboring A133S RASSF1A polymorphism (Hamilton, Yee et al. 2009). YAP1 promotes apoptosis via co-activation of p73 or exhibits its oncogenic properties when associated with TEAD (Levy, Adamovich et al. 2007; Matallanas, Romano et al. 2007; Zhao, Wei et al. 2007; Ota and Sasaki 2008; Chen, Loh et al. 2010). While both complexes appear to be regulated by LATS1 activation, the resolution of this mechanism is the subject of intense debate (Blandino, Shaul et al. 2009). Moreover, warts downregulates the expression of *Drosophila* Inhibitor of Apoptosis 1 (DIAP1), Cyclin E and micro RNA *bantam* (Harvey, Pfleger et al. 2003; Udan, Kango-Singh et al. 2003; Wu, Huang et al. 2003; Thompson and Cohen 2006). Finally, LATS1 executes apoptosis through the interaction with the pro-apoptotic serine protease Omi. In response to apoptotic stimuli such as DNA damage, Omi translocates from mitochondria to cytoplasm where it interacts with LATS1 (Kuninaka, Nomura et al. 2005). This interaction forces conformational changes of Omi, which opens up the access to the active site of the protease domain and increases its catalytic activity (Kuninaka, Nomura et al. 2005). The activated Omi induces apoptosis through its own protease activity or by cleavage of the Inhibitors of Apoptosis

(IAPs) (Srinivasula, Gupta et al. 2003; Yang, Church-Hajduk et al. 2003; Suzuki, Takahashi-Niki et al. 2004).

1.4.5 Involvement of LATS1 in Cell Cycle

LATS1 inhibits cell proliferation by blocking the G_2/M transition (Yang, Li et al. 2001; Xia, Qi et al. 2002) The G_2/M boundary is primarily regulated by the CDK1/ Cyclin A/B complex. The overexpression of LATS1 reduces the kinase activity of the complex and downregulates Cyclin A and Cyclin B but have no effect on expression of Cyclin E, CDK1 or CDK2 (Xia, Qi et al. 2002). By contrast, the inactivation of warts results in a significant accumulation of Cyclin A but not of Cyclin B in the *Drosophila* eye imaginal discs (Tao, Zhang et al. 1999). In mammals, phosphorylation of LATS1 oscillates with the cell cycle. LATS1 is phosphorylated at the G_2/M boundary and in early prophase and becomes dephosphorylated at the metaphase/anaphase boundary (Nishiyama, Hirota et al. 1999; Tao, Zhang et al. 1999). The activated LATS1 releases the N-terminal from the kinase C-terminal and interacts with CDK1 sequestering the Cyclin A binding (Figure 1.13) and (Tao, Zhang et al. 1999; Turenchalk, St John et al. 1999). The binding is specific to CDK1 since LATS1 does not interact with either CDK2 or CDK4 (Tao, Zhang et al. 1999; Turenchalk, St John et al. 1999). LATS1 does not phosphorylate CDK1 but rather physically restricts the cyclin binding (Turenchalk, St John et al. 1999). The CDK1 complex with LATS1 does not possess any kinase activity as tested on histone H1 (Tao, Zhang et al. 1999). In addition to changes in phosphorylation state, LATS1 changes its localisation within the cell as the cell cycle progresses. During the interphase, it locates to the centrosomes but

then during mitosis it is transferred in a dynamic manner to the mitotic apparatus, including the mitotic spindle and the midbody, where it interacts with a cytoplasmic-dispersed regulator of the actin filament assembly, protein zyxin (Nishiyama, Hirota et al. 1999; Hirota, Morisaki et al. 2000). Zyxin is phosphorylated by CDK1 in mitosis and this phosphorylation enables it to associate with LATS1 on the mitotic apparatus. Microinjections of the truncated form of LATS1 into the cell prolong the mitotic phase, suggesting that LATS1 contributes to the regulation of the mitotic progression through its interaction with zyxin (Hirota, Morisaki et al. 2000). The kinase activity of LATS1 is indispensible to the process, since overexpression of kinase dead LATS1 mutant prolongs the activation of the spindle assemble checkpoint and significantly delays the mitotic progression. This in turn, leads to mitotic slippage and the development of tetraploid cells, which contribute to tumorigenesis (Iida, Hirota et al. 2004). Additionally, silencing of LATS1 abrogates cytokinesis and also contributes to the formation of multinucleated cells (Yang, Yu et al. 2004). This is because LATS1 regulates cytokinesis through direct interaction and the inhibition of LIMK1 (Figure 1.12 b) and (Yang, Yu et al. 2004). LIMK1 is known to modulate actin polymerisation through the inhibition of cofilin. Overexpression of LIMK1 leads to cytokinesis defects and results in polynucleated cells (Amano, Kaji et al. 2002). LATS1-dependent regulation of the LIMK1 activity is important for the complete and equal separation of two cells (Yang, Yu et al. 2004).

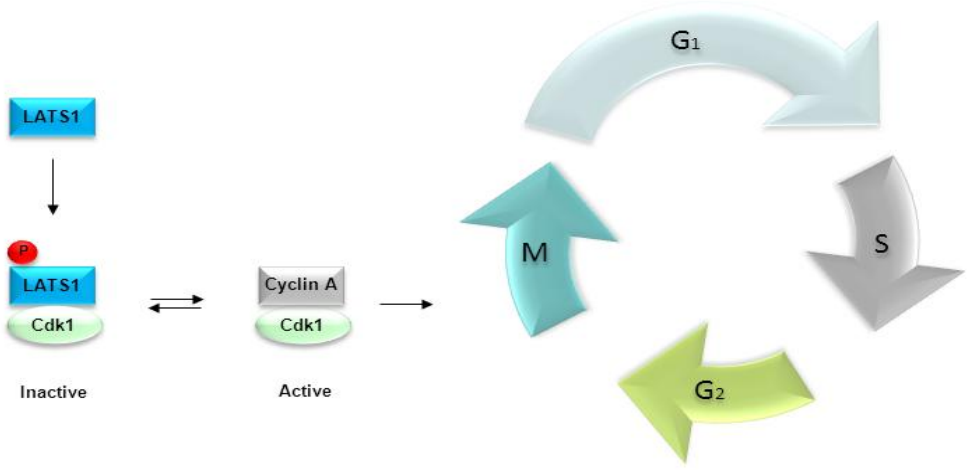


Figure 1.13 The Involvement of LATS1 in the G_2/M Transition. Phosphorylation of Lats1 in early mitosis causes its conformational change and increases the affinity to Cdk1. This interaction sequesters Cyclin A binding to Cdk1 and inactivates the latter inducing G_2/M arrest. Figure adapted from (Turenchalk, St John et al. 1999).

1.5 Aim of the Thesis

The activation of LATS1 is induced by DNA damage in a similar manner to apoptotic signals in that it is dependent on RASSF1A and MST2 (Garth Hamilton December 15, 2009). The activation of LATS1 also appears to be regulated in a cell cycle-dependent manner where phosphorylated LATS1 associates with CDK1 and regulates G_2/M transition. CDKs phosphorylate BRCA2 C-terminus in response to IR and according to conflicting literature, this regulation is involved in HR or/and stabilisation of the replication fork. ATM and ATR substrates analysis revealed the potential role of LATS1 in DNA repair signalling. Depletion of LATS1 showed defects in both the HR and the intra-S checkpoint, suggesting the potential involvement of LATS1 in DSB repair and DNA replication. Therefore, in this project I aim to test whether in response to DNA damage LATS1 complexes with CDK1 or CDK2 thereby regulating BRCA2/RAD51. Additionally, I wanted to understand the significance of this regulation.

.

Chapter 2:
Materials and Methods

2.1 Buffer Compositions

PBS – 137 mM Sodium chloride, 2.7 mM potassium chloride, 10.1 mM sodium phosphate, 1.8 mM potassium phosphate, adjusted to pH 7.4 with HCl

Cryogenic storage media – 20 % FBS, 10 % DMSO, 70 % DMEM

Stripping Buffer - 62.5 mMTris pH 6.8; 2 % w/v SDS; 0.7 % 2-mercaptoethanol

Lysis buffer 1 – 150mM NaCl, 20 mM Hepes, 0.5 mM EDTA, 0.5% NP40, pH=7.5

Lysis buffer 2 – 150 mM KCl, 20 mM Hepes (pH 7.6), 2 mM EGTA, 1.5 mM $MgCl_2$, 50 mM NaF, 01 % NP40, 10 % Glycerol

Inhibitors – 1 mM Na_3VO_4, 20 mM β-glycerophosphate, 1 mM DTT, 25 units/ml Benzonase, Protease inhibitor, 10 mM Benzamidine hydrochloride

Western blot transfer buffer – 20% (v/v) methanol, 0.25 M Tris, 1.92 M glycine

Metaphase spread fixing solution – 75% (v/v) methanol, 25% (v/v) acetic acid

Comet assay lysis buffer – 2.5 M NaCl, 100 mM EDTA, 10 mM Tris, 0.1% DMSO, 0.1% Triton-X, 0.2 M NaOH, pH=10.5

Comet assay electrophoresis buffer – 300 mM NaOH, 1 mM EDTA, 1% DMSO, pH>13

Comet assay neutralization solution –Tris-HCl 500 mM, pH=8

2.2 Tissue Culture

All cancer cell lines including U2OS, HeLa, HT1080 were obtained from the American Type Culture Collection (ATCC, Manassas, VA), the Mouse Embryonic Fibroblasts were obtained from Dr Tian Xu as used previously in (Matallanas, Romano et al. 2007). First, the Human Bone Osteosarcoma Cells (U-2 OS), express a wild type p53 and Rb. Second, HeLa cervical cancer cell line proliferates more rapidly than many other cancer cell lines and are immortal due to the active version of telomerase that prevents telomeres shortening. U2OS and HeLa were utilised in the project due to recorded interaction of LATS1-CDC2 (CDK1) and LATS1 activation upon IR in these cell lines (Tao, Zhang et al. 1999; Matsuoka, Ballif et al. 2007; Hamilton, Yee et al. 2009). HT-1080 are male, human malignant fibrosarcoma cells in which ^{P}S3291-BRCA2 was first observed to be regulated by CDKs (Esashi, Christ et al. 2005). The Mouse Embryonic Fibroblasts were the only non-cancerous cell line used in the process of this research. MEF Lats1$^{-/-}$ had Lats1 genetically ablated and were used when the complete absence of Lats1 was required. Cells were cultured in DMEM medium containing 4.5 g/l glucose (Invitrogen, Carlsbad, CA) with the addition of 10 % foetal bovine serum (HyClone, Logan, UT), streptomycin (100 mg/ml; Invitrogen, Carlsbad, CA) and penicillin (100 units/ml). MEFs were cultured in DMEM medium supplemented additionally with β-mercaptoethanol to final concentration of 55 μM (Sigma-Aldrich, Dorset, UK) and 1% non-essential amino acids (MEN NEAA 100 x; Gibco; Invitrogen). Cell cultures were maintained in incubator (New Brunswick, Galaxy 170R) at 37 °C in water saturated 5 % CO2 95 % air and split twice a week upon reaching confluence. Prior splitting cells were washed twice with

PBS, followed by treatment with 1 ml of 0.25 % trypsin-EDTA (Invitrogen, Carlsbad, CA) for 5 min at 37 °C to detach the cells from the surface of the flask. Depending on growth characteristics, cancerous cells were split 1:5 whereas MEFs 1:3 and re-seeded into flasks containing full DMEM medium as described above.

2.3 Cells Freezing

For longer storage, cells were stored in liquid nitrogen. First, cells were cultured to 80% confluence in T175 flasks, washed twice with PBS and detached from the flask's surface using 2 ml trypsin as described above (see Section 2.2). Afterwards, the cells were re-suspended in 5 ml of DMEM medium, transferred to 15 ml falcon tube, and centrifuged at 700 x g for 10 min. The supernatant was removed and the pellet was washed twice with PBS followed by centrifugation as described above. The washed cell pellet was re-suspended in cryogenic storage medium, divided into 1 ml aliquots in cryovials, and transferred to an isopropanol bath. The isopropanol bath was then placed in -80 °C for a 24 hrs incubation. The slow cooling of isopropanol decreased the formation of ice crystals and improved the recovery rate after thawing. The cryovials were then transferred to liquid nitrogen and stored at -196 °C.

2.4 Cells Thawing

The cryovials were taken from the liquid nitrogen tank, immediately put into dry ice to slow down thawing, and then transferred to the tissue culture room. The cryovials were then placed in 37 °C water bath for 2 min to thaw the cells rapidly. Once the cells thawed, they were transferred to falcon tubes and the DMEM medium was added in a drop-wise manner. The cells were washed once with PBS to remove the freezing medium and centrifuged at 700 x g for 10 min. The cell pellet was re-suspended in complete DMEM, and then the cells were transferred to a T25 flask and incubated at 37 °C.

2.5 siRNA Transfection

The cells were plated onto 96-well, 6-well plates or 10 cm dishes, depending on the experiment, and cultured in an antibiotic-free DMEM medium in order to reach 60% confluence on the day of the transfection. The low confluence aimed to reduce the overgrowth of cells on the day of the assay. The cells were transfected with siRNA at the final concentration of 100 nM as required for LATS1. The protocol below describes the preparation of transfection mix for 1 well of 96-well plate. Those volumes were scaled up to be appropriate for 6-well plate and 10 cm dish as necessary. The amount of 0.5 µl Lipofectamine 2000 (Invitrogen, Carlsbad, CA) was incubated in 25 µl OptiMEM Reduced Serum Medium (Invitrogen, Carlsbad, CA) for 5 min at room temperature (RT). At the same time, 0.15 µl of siRNA was titrated into 25 µl of OptiMEM reduced Serum Medium equivalent to a final concentration of 100 nM. After incubation, the two solutions were combined and incubated

for another 30 min at RT. The transfection mix solution was then diluted in 100 µl of an antibiotic-free DMEM medium to give the desired final concentration of 100 nM and then added to the cells. The cells were incubated for 6 hrs at 37 °C and then the medium was replaced with complete DMEM containing antibiotic. The samples were incubated at 37 °C for 48 hrs prior to further analysis (if not stated otherwise). siRNAs used in the thesis to silence expression of LATS1 in mammalian cells were acquired from Ambion, UK.

Sence sequence	Antisense sequence	siRNA ID
SS' GCCUUGCAGGAAAUUCGAATT	AS' UUCGAAUUUCCUGCAAGGCTT	s17392
SS' CCUCCAUACGAGUCAAUCATT	AS' UGAUUGACUCGUAUGGAGGAA	s17393
SS' GGUUCUGAGAGUAAAAUUATT	AS' UAAUUUUACUCUCAGAACCTC	566

Table 2.1 The List of siRNAs Used in the Project.

2.6 DNA Transfection

2.6.1 DNA Transfection Protocol

Cells were plated onto 6-well plates or 10 cm dishes, depending on the experiment carried our, and in an antibiotic-free DMEM medium in order to reach 60% confluence on the day of the transfection. The low confluence aimed to reduce the overgrowth of cells on the day of the assay. The cells were transfected with plasmid LATS1. On the day of transfection, 2 μg of DNA, 20 μl of PEI (Polysciences, Warrington, PA) and 100 μl of OptiMEM (6-well plate) or 10 μg of DNA, 100 μl PEI and 900 μl of OptiMEM (10 cm dish) were combined in an eppendorf tube and mixed thoroughly. The mix was then incubated at RT for 30 min. At the same time, the cells were covered with 1.8 ml or 9 ml fresh antibiotic-free medium, depending on the size of the plate. After incubation, the DNA mix was added to the cells and the medium was changed 6 hours post-transfection. Transfected cells were then taken to further analysis 24 hrs after the transfection.

2.6.2 Plasmids Used in the Thesis

Human LATS1 cDNA used in the thesis was a kind gift from Dr. Herman Sillje. LATS1 was cloned into pRcCMV vector in frame with sequences that encode 3x myc tags. Construct encoding catalytically inactive kinase LATS1 D846A was created by changing a conserved aspartate to an alanine. Site-directed mutagenesis was performed by PCR with oligonucleotides containing appropriate mutations (Chan, Nousiainen et al. 2005).

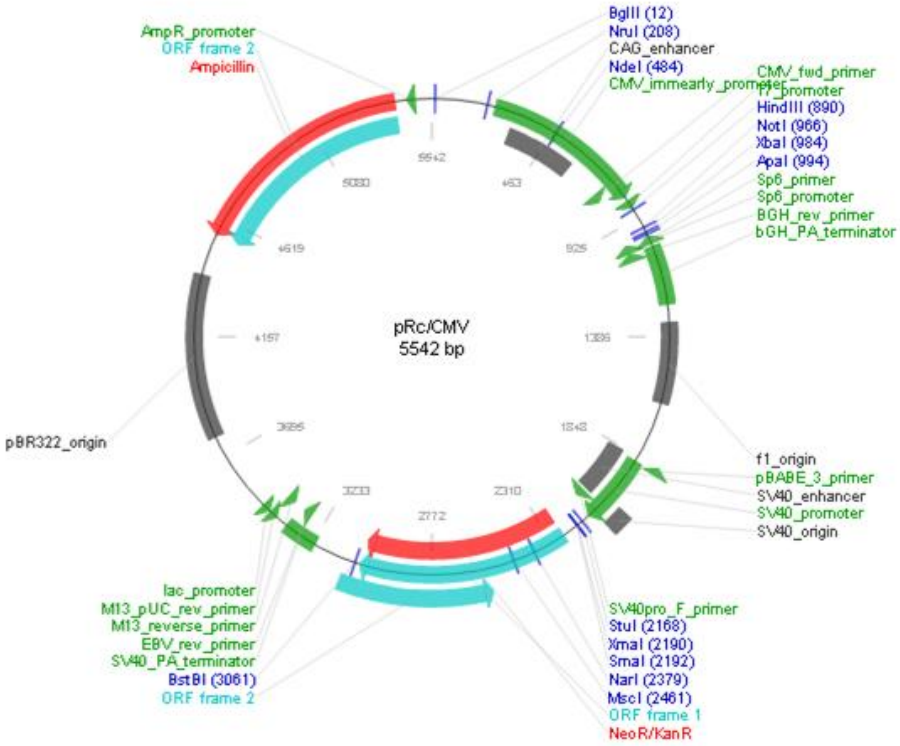


Figure 2.1 Plasmid map of pRc/CMV plasmid. Plasmid was used to transfect LATS1 and LATS1 kinase dead derivative into mammalian cells.

The modified GFP gene (NZ-EGFP) used for recombination assay was created by Dr. Maria Jasin from enhanced GFP gene (EGFP, Clontech). The gene was cloned into pCAGEN plasmid. The SceGFP was constructed by replacing the 34-bp Bcg I fragment from the GFP gene with 34 bp that include 18 bp I-Sce I recognition site. I-Sce I nuclease was expressed in pCβASce from a hCMV enhancer / chicken β-actin promoter (Pierce, Johnson et al. 1999).

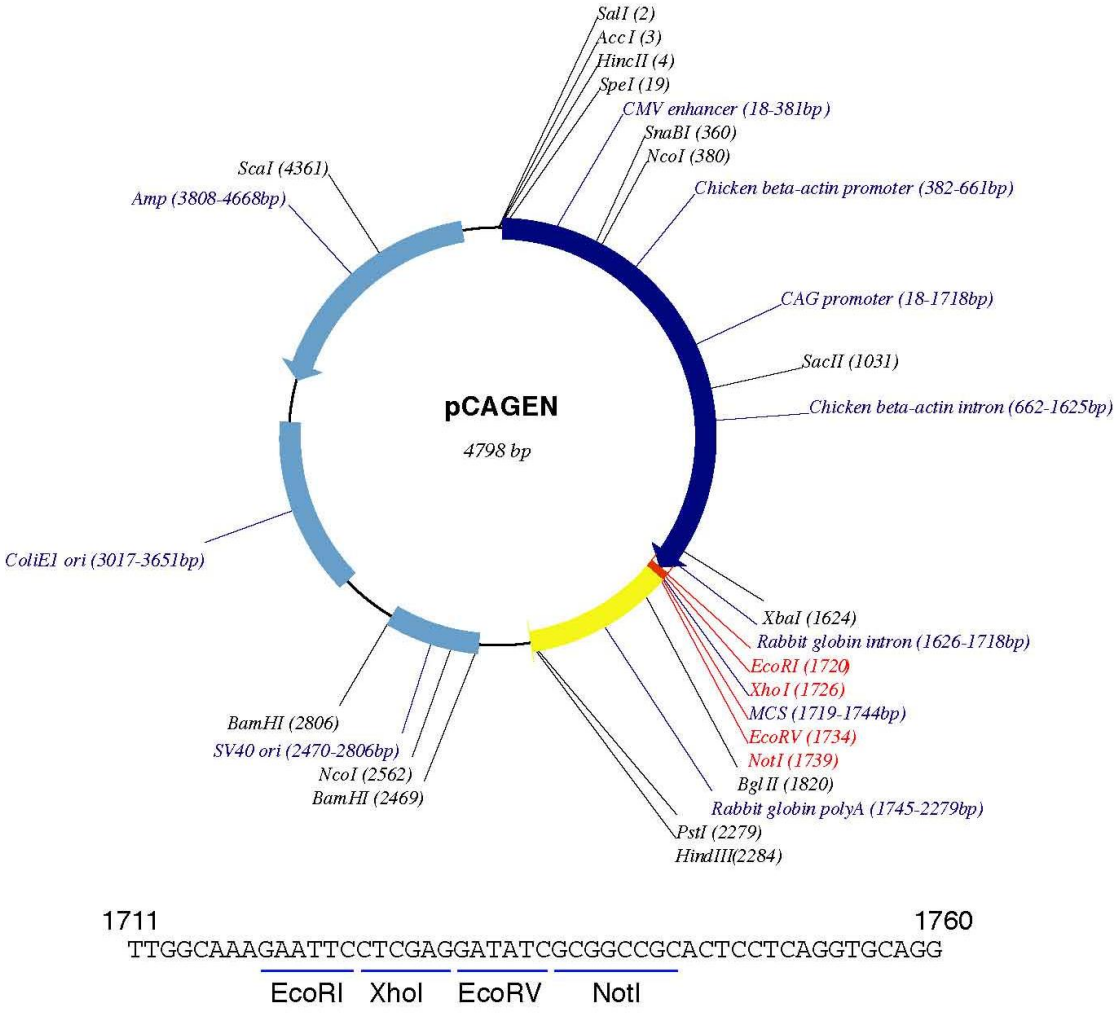


Figure 2.2 Plasmid map of pCAGEN plasmid. Plasmid was used to transfect modified GFP gene into mammalian cells.

2.7 Drug Treatments

2.7.1 Hydroxyurea

Hydroxyurea (HU) depletes the deoxyribonucleotides pool and stalls the replication fork, which after 12 hrs treatment, starts to collapse into DSB and induces HR (Saintigny, Delacote et al. 2001). The cells were incubated in 2 mM hydroxyurea (Sigma-Aldrich, Dorset, UK), diluted in complete DMEM medium for 10 hrs at 37 °C, to induce fork stalling but not collapse of the fork (Saintigny, Delacote et al. 2001). After incubation, the cells were washed twice with PBS and covered with complete DMEM medium and subjected to further analysis.

2.7.2 Nocodazole

Nocodazole was used to induce BRCA2 phosphorylation at S3291, which is observed during the mitotic arrest (Esashi, Christ et al. 2005). Nocodazole is an anti-mitotic drug, which inhibits microtubule polymerisation by binding to β-tubulin. This promotes a spindle assembly checkpoint and arrests cells in prometaphase. The cells were treated with 0.13 µM nocodazole (Sigma-Aldrich, Dorset, UK) and incubated for 16 hrs at 37 °C. After incubation, cells were subjected to further analysis. The G_2/M arrest was verified on western blot using the Cyclin B1 expression as a marker (Figure 5.5).

2.7.3 Colcemid

Colcemid was used to induce chromosome condensation prior to the metaphase spread. Colcemid is a drug, which inhibits microtubule polymerisation and blocks cells in metaphase when chromosomes are formed and the most dens. The cells were treated with 0,27 µM KaryoMAX Colcemid (Invitrogen, Carlsbad, CA) and incubated for 16 hrs at 37 °C. After incubation, the medium from the dish was collected into the falcon tube to minimise the potential loss of detached cells. Subsequently, the remaining cells in the dish were washed with PBS and trypsinised. Samples were treated as described in Section 2.15.

2.8 Cell Irradiation

The cells were treated with Ionising Radiation (IR) while in the exponential growth phase using Mark 1 cesium irradiator to induce DNA damage (J.L. Shepherd, San Fernando, CA) at indicated in the result chapters doses. The control cells were removed from the incubator for the time of irradiation and placed on cold metal plates identical to those used for the irradiation. After the irradiation, the cells were placed on ice to inhibit repair of the DNA damage and then taken to the incubator for further incubation at 37 °C.

2.9 Propidium Iodide (PI) Staining

The cells were cultured in a 10 cm dish in a complete DMEM medium, trypsinised and collected into a 15 ml falcon tube. The cells were then

centrifuged at 250 x g at RT for 5 min. The medium was decanted and the falcon tube containing the cell pellet was vortexed using only the residue remaining in the tube to avoid clumping of cells. Then, a volume of 1 ml of ice cold 70 % ethanol was titrated into the cells while vortexing and the falcon was incubated at -20 °C for a minimum of 30 min. After fixation, the cells were centrifuged at 250 x g at RT for 5 min. The supernatant was decanted, the tube was drained with absorbent paper and the cells were re-hydrated in 1 ml PBS for 2 min. The cells were incubated in 20 µg/ml RNAse diluted in PBS to amplify the signal (PI stains both DNA and RNA) (Invitrogen, Carlsbad, CA) for 30 min at 37 °C. Cells were re-suspended in PBS containing 50 µg/ml propidium iodide (PI) (Invitrogen, Carlsbad, CA) and incubated for 45 min in the dark to allow the stain to develop. The cell cycle profiles were analysed within 2 hrs of staining using Fluorescence-activated cell sorting (FACS) (FACS Calibur, Becton-Dickinson).

2.10 BrdU Staining

The cells were cultured in a 10 cm dish and stained with 20 µM BrdU for 20 min (U2OS and HeLa) or 30 min (MEF) at 37 °C prior to collection. The difference in the incubation time was attributed to the length of the cell cycle of the cell line. The stained cells were protected from light to prevent BrdU deterioration and damages to the chromatin. The cells were washed twice with PBS, trypsinised and collected into a 15 ml falcon tube. The cells were centrifuged at 250 x g at RT for 5 min. The medium was decanted and the falcon tube containing the cell pellet was vortexed using only the residue

remaining in the tube to avoid clumping of the cells. Then, the amount of 1 ml of ice cold 70 % ethanol was titrated to the cells while vortexing and the falcon was incubated at -20 °C for a minimum of 30 min. After fixation, the cells were centrifuged at 250 x g at RT for 5 min. The supernatant was decanted, the tube was drained with absorbent paper and the cell pellet was re-suspended in 1 ml of 2 M HCL containing 0.1 mg/ml pepsin followed by 20 min of incubation at RT. After incubation, the pellet was washed once with PBS and then washed again with 2 % FCS in PBS. The cells were incubated with BrdU primary antibody (BD Bioscience, UK) and diluted with 2 % FCS in PBS (1:1000) for 90 min at RT. After incubation, 1 ml 2% FCS in PBS was added and the cells were centrifuged at 250 x g for 5 min. The pellet was re-suspended in Alexa Fluor 488 secondary antibody diluted 1:200 in 2 % FCS in PBS and incubated for 60 min in the dark. The analysis was accomplished using FACS (FACS Calibur, Becton-Dickinson).

2.11 Cell Lysis

The lysis buffer used for the cell lysis varied between experiments. The cells including U2OS, HeLa and MEFs were lysed using NP40 Lysis Buffer 1 containing inhibitors, whereas the HT1080 cells utilised for the determination of BRCA2 phosphorylation were lysed with Lysis Buffer 2 containing inhibitors (see Section 2.1). The cells were placed on ice and the growth medium was aspirated off. The cells were washed twice with ice cold PBS and covered with lysis buffer. The cells were then scraped from the surface of the dish and gathered on one side using a rubber-tipped cell scraper. The cell lysate was

then transferred to an eppendorf tube and rotated in a cold room for 30 min at 4 °C to allow accurate cell lysis. After rotation, the tubes were centrifuged at 20 000 x g (Eppendorf Centrifuge 5417R; Eppendorf, UK) for 10 min at 4 °C. After the centrifugation, the supernatant was collected and was used for sample preparation.

2.12 Immunoprecipitation

The cells were lysed and cleared with centrifugation at 20 000 x g for 10 min at 4 °C (see Section 2.11). The amount of 50 µl of lysate was collected for input lysate analysis. The remaining volume was applied to Protein G Sepharose beads (Sigma-Aldrich, Dorset, UK) and rotated for 1 h at 4 °C to pre-clear the sample. After rotation, the samples were centrifuged at 700 x g for 5 min at 4 °C and the supernatant was collected to the new eppendorf tube. 3 µl of the desired antibody (Table 2.1) and 10 µl of G Sepharose beads were added to the supernatant and rotated overnight at 4 ^{o}C. After incubation, the cells were washed three times with lysis buffer without inhibitors and the supernatant was aspirated off.

2.13 Electrophoresis

The electrophoresis was achieved using pre-cast NuPAGE gels. The samples were prepared through the addition of a sample buffer (4x) (Invitrogen, Carlsbad, CA) and a NuPAGE reducing agent (10x) (Invitrogen, Carlsbad, CA) to IP or lysis samples. The samples were incubated at 70 °C for 10 min and loaded into the appropriate gel. The analysis of BRCA2 was conducted

using 3-8% Tris-Acetate gel (Invitrogen, Carlsbad, CA). The samples were run in 5 % Tris-Acetate SDS Running buffer (Invitrogen, Carlsbad, CA) at 120 V for approximately 60 min or until the dye front had progressed sufficiently far down the gel. The electrophoresis of the smaller proteins was conducted using NuPAGE 4-12 % Bis-Tris gel (Invitrogen, Carlsbad, CA) and the samples were run in 5 % MOPS SDS running buffer (Invitrogen, Carlsbad, CA) at 150 V for approximately 60 min or until the dye front had progressed sufficiently far down the gel. The electrophoresis was performed in XCellSureLock Mini-Cell Electrophoresis System (Invitrogen, Carlsbad, CA) and gels were subsequently western blotted.

2.14 Western Blotting

The separated proteins with NuPAGE gel (Invitrogen, Carlsbad, CA) were transferred to the PVDF transfer membrane (Immobilon-FL, Millipore, Billerica, MA) by western blotting. The gels were orientated with the membrane as shown in Figure 2.1 with all components wetted in the transfer buffer. The PVDF membrane was primed with an immersion in 100% methanol (Fisher Scientific, Loughborough, UK) prior to use. The air bubbles were eliminated from between the gel and the membrane using a roller prior to applying a current, as the transfer is only efficient where the gel is in direct contact with the membrane. The stack, as shown in Figure 2.1, was then placed within a western blotting transfer tank filled with transfer buffer along with an ice pack to cool the transfer. A voltage of 100 V was applied for 1 h. The transfer condition was different between the NuPAGE gels used. The 3-8

% Tris-Acetate gel with the BRCA2 samples loaded was transferred at 30 V overnight at 4 °C and 4-12 % Bis-Tris gel was transferred at 100 V for 1 h at RT. Following the transfer, the PVDF membranes were blocked in 50 % Odyssey blocking buffer (Li-cor Biosciences, Nebraska, USA) and diluted in PBS. The primary antibodies diluted in Odyssey blocking buffer were incubated at final concentrations as indicated in Table 2.1. Antibody binding was detected using the fluorescent antibodies Alexa Fluor 488 or 680 (Invitrogen, Carlsbad, Ca) on Odyssey Infrared Imaging System (Li-cor Biosciences, Nebraska, USA). To re-probe for different proteins, the membranes were stripped of antibodies prior to re-probing by incubating in a stripping solution for 30 min at 50 °C. After stripping, the membranes were blocked in 50 % blocking buffer diluted with PBS and probed with the desired antibodies.



Figure 2.3 Western Blot Stack. The orientation of the gel and the PVDF membrane between the electrodes separated from electrodes with three sheets of Whatman filter paper and sponges both immersed in transfer buffer with sponges in contact with the electrodes at both interfaces.

2.15 Metaphase Spread

The cells were cultured in 10 cm dishes to reach 80 % confluence and treated with 5 µM KaryoMAX Colcemid Solution (Invitrogen, Carlsbad, CA) for 16 hrs. After incubation, the cells were washed with PBS, trypsinised and collected into the falcon tube. The samples were centrifuged at 700 x g for 10 min. The supernatant was removed and the cell pellet was re-suspended in 9 ml hypotonic buffer (30 mM Na citrate) pre-warmed at 37 °C and titrated while gently vortexing. The cells were then incubated in a hypotonic buffer for 25 min at 37 °C. After incubation, 3 drops of a fresh fixative solution was added to the falcon tube and the cells were centrifuged at 700 x g for 10 min. The supernatant was aspirated off leaving 1 ml over the cell pellet, in which cells were subsequently re-suspended. 11 ml of the fixative solution was titrated while vortexing and the samples were centrifuged at 700 x g for 10 min. The supernatant was decanted and the pellet was re-suspended in 250 µl of fresh fixative solution. At the same time, the slides were washed in methanol and wiped with cotton cloth and subsequently covered with 45 % acetic acid. Immediately after the acetic acid application to the slide surface, the fixed cells were dropped from above on a slide using a pipette. The slides were left to dry overnight and then probed with DAPI 1:1000 from 1 mg/ml stock solution (Invitrogen, Carlsbad, CA).

2.16 Recombination Assay

The recombination substrate DR-GFP was stably transfected into U2OS, MEF *wt* and MEF Lats1 $^{-/-}$ cells following the DNA transfection protocol (see Section

2.6). The concentration of puromycin (Sigma-Aldrich, Dorset, UK) in the medium was experimentally evaluated at 1.5 µg/ml. The cells were selected in the medium with puromycin for 3 weeks. The DR-GFP was kindly received from Dr Maria Jasin. The DR-GFP plasmid consisted of two GFP genes: SceGFP and iGFP. They were mutated and separated by puromycin N-acetyltransferase gene encoding selection marker. SceGFP had engineered in 18-bp I-SCE I endonuclease recognition site, which was built into the BcgI restriction site after the resection of 11 bp from the GFP gene. The I-SCE I recognition site possessed two stop codons, which prevented the expression of the functional GFP protein. The cells were transfeced with I-SCE I endonuclease, which cleaved DR-GFP gene into DSB. The cells with effective HR mechanism repaired the DNA and expressed the functional GFP protein (Pierce, Johnson et al. 1999). The cells selected with puromycin were washed twice with PBS, trypsinised and transferred to a 6-well plate. The MEFs were plated at a concentration of $1x10^5$ and the U2OS at $2x10^5$ cells per well in an antibiotic-free DMEM medium. The next day, the U2OS cells were transfected with non-targeting siRNA and siRNA against LATS1. MEF *Lats1*$^{-/-}$ were transfected with either control plasmid (pcDNA) or hLATS1 (see Sections 2.5 and 2.6). The cells were transfected with I-SCE I endonuclease using Lipofectamine 2000 48 hrs post siRNA and 24 hrs post DNA transfection and subsequently incubated for 48 hrs at 37 °C. After the incubation, the cells were trypsinised, and re-suspended in a complete DMEM medium. The cells were sorted by flow cytometry using two-colour fluorescence. The cells, which were not able to recombine the GFP protein, did not present a green signal but exhibited auto-fluorescence and gathered along the green/orange

diagonal. The cells with the recombined GFP gene produced a green signal and formed a separate population shifted towards FL 1 green fluorescence and FL 2 orange fluorescence.

2.17 Immunofluorescent Assay

The cells were plated onto cover slips in a complete DMEM medium at density of $1x10^5$ MEF and $2x10^5$ U2OS and incubated overnight at 37 °C. The cells were then transfected with DNA or siRNA and subsequently irradiated at the indicated doses. Cells were washed twice with PBS and fixed with 4 % paraformaldehyde in PBS (Sigma-Aldrich, Dorset, UK) for 20 min. Paraformaldehyde was washed away with PBS and the cells were permabilised with 0.3 % Triton-X 100 in PBS (Fisher Scientific, Loughborough, UK) for 10 min. After the cell membrane was permabilised, the cells were blocked with 3 % BSA in PBS (Sigma-Aldrich, Dorset, UK) for 40 min at 4 °C to prevent non-specific protein interactions. The permabilised and blocked cells were incubated with the primary antibodies RAD51 or γH2AX (Table 2.1), diluted 1:1000 in 3 % BSA in PBS and incubated overnight at 4 °C. After the incubation, the cells were washed three times with PBS to remove the non-binded antibodies and subsequently incubated with a secondary rabbit (RAD51) Alexafluor 488 or a mouse (γH2AX) Alexafluor 488 for 1 h at RT in the dark to prevent bleaching of the signal. The cells were washed three times with PBS and probed with DAPI at 1:1000 concentration for 5 min at RT in the dark. DAPI was fully aspirated off and the cover slips were lifted and dried in the dark on the paper towel. The dry coverslips were

then mounted on the slide using a Pro long gold antifade mounting medium (Invitrogen, Carlsbad, CA). After mounting, the medium-solidified slides were analysed on fluorescent microscope Nikon Eclipse 90i (Nikon Instruments, Melville, NY). The cell nucleus were observed using DAPI filter and either RAD51 or γH2AX foci probed with Alexa Fluor 488 using FITC filter. The quantitation of foci was performed using the ImageJ 1.41 software.

2.18 Comet Assay

Comet assay was utilised to determine the extent of DNA damage in the cells post-IR treatment. In this method, the damaged DNA is separated from the intact DNA using electrophoresis and is pulled out from the nucleous in the form of a 'comet tail'. The slides were prepared by lying 600 μl of molten normal melting point agarose (Bio-rad, Hertfordshire, UK) onto the slide surface and left to dry overnight. Concomitantly, the cells were irradiated at the indicated doses and incubated for the desired time at 37 °C. After incubation, the cells were trypsinised and diluted to $2x10^5$ cells/ml in a complete DMEM medium. Then, 250 μl of cell suspension was titrated into 1 ml of molten low melting point agarose (Bio-rad, Hertfordshire, UK) at 37 °C and 1 ml of this solution was applied onto the slide. The slides were placed on ice to facilitate the setting of the agarose. Then, the slides were placed in a coplin jar with freshly prepared cold lysis buffer for 1 h at 4 °C. Post lysis, the slides were transferred to an electrophoresis tank, covered with cool electrophoresis buffer and left for 30 min to let the DNA unwind. Electophoresis was performed at 25 V, 400 mA for 25 min and afterwards the

slides were washed with a neutralisation solution 3 times for 5 min. The slides were left overnight to air dry and stained with SYBR Gold dye for 30 min the following day. The analysis was performed on a Nikon Eclipse 90i microscope and the intensity of the comet tail was measured using Komet 5.5 software.

2.19 Statistical Analysis

I applied standard errors represented by error bars to the bar charts to report accuracy of measurements. First, I calculated the standard deviation using the formula below:

$$SD = \sqrt{\frac{\sum (x - \bar{x})^2}{(n-1)}}$$

x – represents a single measurement i.e. the number of cells with more than 9 foci on one picture

$\bar{x} = \frac{\sum x}{n}$ – the mean i.e. the sum of all cells with more than 9 foci divided by the total number of cells

n – the number of repeats i.e. the number of pictures taken

To acknowledge multiplication of repeats of an experiment, I calculated the standard error using formula below:

$$SE = \frac{SD}{\sqrt{n}}$$

SD – standard deviation

n – the number of repeats i.e. number of times the experiment was repeated

To show the difference in the significance between two different populations I used the *p value,* which was calculated using the *z*-test.

$$z = \frac{(\bar{x}_1 - \bar{x}_2)}{\sqrt{(SE_1)^2 + (SE_2)^2}}$$

$\bar{x}_1$ – the mean of population 1

$\bar{x}_2$ – the mean of population 2

SE_1 – the standard error of population 1

SE_2 – the standard error of population 2

2.20 List of Antibodies Used

Antibody (clone)	Dilution	Species Derivation	Catalogue Number	Company
β-Actin (AC-15)	1:3000	Mouse monoclonal	A1978	Sigma
BRCA2	1:500	Mouse monoclonal	OP-95	Millipore
P-BRCA2	1:1000	Mouse monoclonal	N/A	N/A
BrdU	1:1000	Mouse monoclonal	347580	BD Biosciences
CDK1/cdc2	1:1000	Rabbit polyclonal	06-923	Upstate
CDK2	1:1000	Rabbit polyclonal	07-631	Upstate
CDK3 (3C12)	1:1000	Mouse monoclonal	H00001018M01	Abnova
CyclinA (BF683)	1:1000	Mouse monoclonal	4656	Cell Signaling
CyclinB1 (V152)	1:2000	Mouse monoclonal	4135	Cell Signaling
CyclinE (HE12)	1:1000	Mouse monoclonal	4129	Cell Signaling
γH2AX (JBW301)	1:1000	Mouse monoclonal	05-636	Millipore
LATS1	1:500	Rabbit polyclonal	A300-477A	Bethyl
P54/nrb	1:1000	Rabbit polyclonal	GTX101419	GeneTex
RAD51 (H-92)	1:1000	Rabbit polyclonal	Sc-8349	Santa Cruz
α-Tubulin	1:3000	Mouse monoclonal	Ab4074	Abcam

Table 2.2 The List of Primary Antibodies Used in the Project

Chapter 3:

LATS1 in Cell Cycle Regulation

3.1 Introduction

It has been previously described that the LATS kinases interact with CDKs and restrict cell cycle progression (Tao, Zhang et al. 1999; Turenchalk, St John et al. 1999; Xia, Qi et al. 2002; Li, Pei et al. 2003). In line with this, LATS1 is phosphorylated in a cell-cycle-dependent manner and specifically associates with CDC2 (CDK1) in the early mitosis, although no regulation of the interaction was observed. This interaction sequesters CDK1 by blocking Cyclin A binding and prevents the G_2/M transition (Tao, Zhang et al. 1999; Xia, Qi et al. 2002). In addition to that, LATS2 has been shown to be involved in the regulation of the G_1/S transition through the modulation of CDK2/Cyclin E activity (Li, Pei et al. 2003). CDKs are tightly regulated to ensure the fidelity of cell replication and are intimately controlled by a number of checkpoints during the cell cycle, most notably in response to the presence of DNA damage. The LATS kinases have been described to be activated in response to a number of upstream signals (see Sections 1.4.3 and 1.4.4), including recently, DSBs in the DNA (Hamilton, Yee et al. 2009). We wanted to determine whether DNA damage-induced activation of LATS1 can promote an interaction with CDKs and can result in cell cycle regulation.

3.2 LATS1 Interaction with CDK1 and CDK2 in Response to IR

Overexpressed LATS kinases were previously shown to associate with CDKs constitutively (see Section 1.4.5) and (Tao, Zhang et al. 1999; Xia, Qi et al. 2002; Li, Pei et al. 2003). LATS1 has since been described to be activated by cell-cell contact and DNA damage (see Sections 1.4.3 and 1.4.4) and (Zhao, Wei et al. 2007; Ota and Sasaki 2008; Hamilton, Yee et al. 2009). We first wanted to establish whether the interaction with CDKs could be detected at the endogenous level and whether it is regulated in response to DNA damage. To test this, we exposed U2OS cells to 4 Gy IR and performed immunoprecipitation using the anti-LATS1 antibody and subsequently analysed samples for the presence of endogenous CDK1 or CDK2 by western blot. IR induces double strand breaks in the DNA, which recruit and activate ATM. The activation of ATM triggers checkpoints that halt the cell cycle in order to elicit DNA repair processes and guard against the replication of damaged cells. LATS1 responds to ATM-dependent stimulation of RASSF1A and MST2 signalling (Hamilton, Yee et al. 2009). In unperturbed cycling cells, immunoprecipitated LATS1 did not associate with either CDK1 or CDK2, however, the interaction was readily induced 4 hrs after the induction of DNA damage with IR (Figure 3.1).

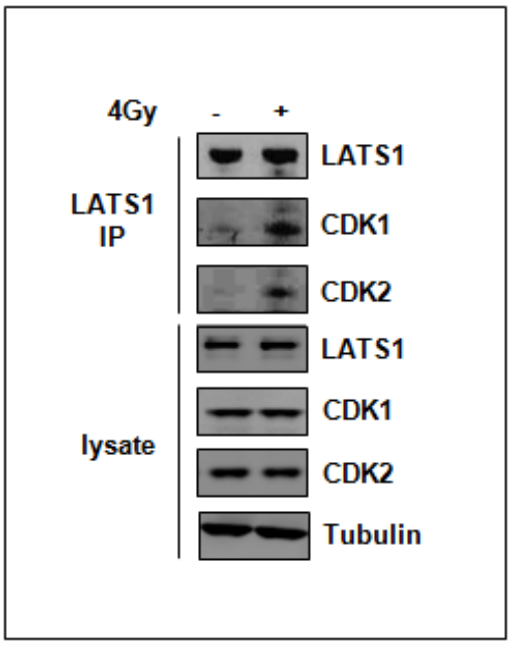


Figure 3.1 LATS1 Associates with CDK1 and CDK2 in Response to IR in U2OS cells. The Western blot analysis of LATS1 IP and lysate. U2OS cells were cultured to 30 % confluence, treated with 4 Gy IR and subsequently lysed 4 hrs post DNA damage induction. Lysates were immunoprecipitated with LATS1 antibody conjugated to G Sepharose beads, western blotted and probed with indicated antibodies. The interactions were visualised using Odyssey scanner (Li-cor).

The IR-induced association suggested that the interaction between CDKs and LATS1 depends on the activation status (Figure 3.1). Next, we wanted to determine whether the additional stimuli that activate LATS1 could also promote the association. LATS1 has been described to associate with its substrate YAP in high cell density (see Section 1.4.3) and (Zhao, Wei et al. 2007; Ota and Sasaki 2008). To determine if this signal could also activate LATS1-CDK binding, U2OS cells were cultured to full confluence. Cells were lysed at the indicated time points and the cell extracts were immunoprecipitated with the LATS1 antibody. The samples were western blotted and incubated with CDK1, CDK2 and CDK3 antibodies (Figure 3.2).

Immunoprecipitates indicated that LATS1 interacted specifically with CDK1 and CDK2, but not with CDK3 in confluent cultures. This observation suggested that activation of LATS1 by cell density promoted a specific interaction with both CDK1 and CDK2, in contrast to the previously reported association of overexpressed LATS1 with only CDK1 (Figure 3.2) and (Tao, Zhang et al. 1999). No additional binding was observed upon exposure to IR, indicating that two signals did not drive an additive association. Surprisingly, the association of both CDK1 and CDK2 decreased at 1 h and 2 hrs after IR. However, in agreement with the timing observed in Figure 3.1, the LATS1-CDK complexes appeared to increase at 4 hrs after the DNA damage despite the initial reduction (Figure 3.2). While the regulation in response to cell density raised interesting questions regarding the regulation of the cell cycle exit upon reaching confluence, at that point it was decided to focus on the DNA damage as a direct signal that could induce LATS1-CDK interactions. Interestingly, and in agreement with previous reports, no cyclins were detected in LATS1 IPs suggesting that LATS1 binded to CDK1 and CDK2 and not to CDK/cyclin complexes (Figure 3.2). Therefore, it is possible that LATS1 modulates the activity of both CDK1 and CDK2 in a DNA damage-dependent manner by keeping the bound kinases inactive through restricting the binding of cyclins.

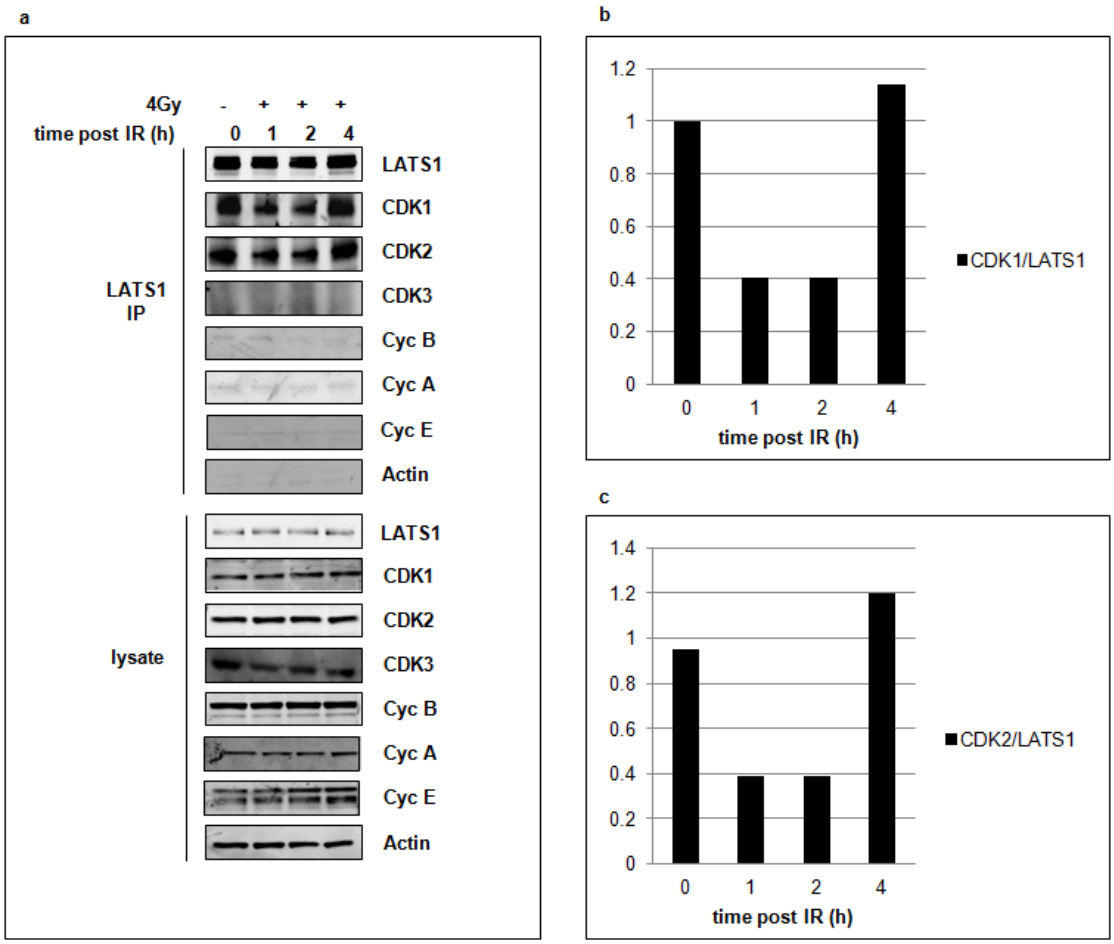


Figure 3.2 Association of LATS1 with CDK1 and CDK2 in Confluent U2OS Cultures is Regulated in an IR-Dependent Manner. (a) The Western blot analysis of LATS1 IP and lysate. Cells were cultured to 90% confluence, irradiated with 4 Gy and incubated at 37 °C for 1 h, 2 hrs and 4 hrs. The sample labelled 0 was not treated with IR. The cells were lysed at the indicated time points and lysates were immunoprecipitated with G Sepharose beads conjugated to LATS1 antibody. The blots were incubated with antibodies as indicated and visualised using Odyssey scanner (Li-cor). **(b)** The bar chart representing the ratio of quantitated bands of CDK1/LATS1 from the Western Blot on the left. **(c)** The bar chart representing the ratio of quantitated bands of CDK1/LATS1 from the Western Blot on the left.

3.3 Optimisation of Transfection of siRNA

In order to determine whether the interaction has a physiological relevance to the DNA damage checkpoint regulation of CDKs, we wanted to remove LATS1 by siRNA. To establish conditions for effective knockdown of LATS1 in U2OS cells, the cells were transfected with an increasing concentration of siRNA targeted to LATS1 using Lipofectamine 2000 as a transfection reagent. Lipofectamine 2000 was used throughout all siRNA transfections utilised in this thesis. A number of siRNAs was tested, including siRNA against LATS1 id: 566 and Silencer Select siRNAs id: 17932; id: 17933. Silencer Select was advertised as siRNA that is 100-fold more effective than normal siRNA because of reduced off-target activity and up to 90% efficiency. The most effective depletion of LATS1 was achieved 48 hrs post-transfection with a final concentration of 100 nM of siRNA and Lipofectamine 2000 diluted as recommended by the manufacturer (see Section 2.5). There was no significant difference in the efficiency of depletion of LATS1 between the different types of siRNAs (Figure 3.3 a). To further validate siRNA depletion, a LATS1 IP was performed (Figure 3.3 b). First, cells were transfected with siLATS1 id: 566 and incubated for 48 hrs. We observed successful depletion of LATS1 in the cell lysates but not in the LATS1 IP samples. The amount of LATS1 detected in the IP samples transfected with siRNA was significantly lower than in the non-treated cells but still detectable with a LATS1 antibody (Figure 3.3 b). To rule out potential effects of incomplete LATS1 knockdown, we employed Mouse Embryonic Fibroblasts genetically depleted of Lats1 ($Lats1^{-/-}$ MEFs) in this research project.

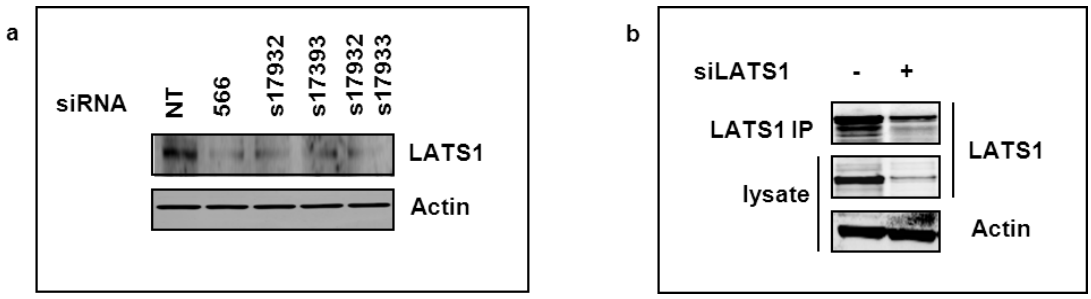


Figure 3.3 siRNA Transfection Optimisation. (a) Lysate analysis for LATS1 expression after a siRNA treatment. U2OS cells were cultured to 30 % confluence and transfected using Lipofectamine 2000 with non-targeting (NT) and siRNA against LATS1 (566, s17932, s17933) at final concentration of 100 nM. The transfected cells were incubated at 37 °C for 48 hrs prior to the lysis. The samples were western blotted, incubated with LATS1 and Actin antibodies and visualised using Odyssey scanner (Li-cor); **(b)** LATS1 IP. U2OS cells were transfected with siRNA id: 566 against LATS1 and incubated at 37 °C for 48 hrs. The cells were lysed and immunoprecipitated with G Sepharose beads conjugated to the LATS1 antibody. The samples were western blotted and probed with the indicated antibodies.

3.4 The Accumulation of LATS1-Deficient Cells in the G_2 Phase after IR

The cell cycle profiles were analysed in the presence and in the absence of LATS1 to ascertain whether the DNA damage-dependent interaction between LATS1 and CDK1 and CDK2 could influence the cell cycle regulation (Figure 3.1). Both U2OS and HeLa cells were transfected with either non-targeting siRNA (siNT) or siRNA against LATS1 (siLATS1) for 48 hrs and exposed to 4 Gy. The cells were fixed at the indicated time points and stained with propidium iodide (PI). The stained and fixed cells were then sorted using FACS based on their DNA content to determine the number of cells in the distinct phases of the cell cycle (Figure 3.4). As would be expected of cells with effective DNA damage checkpoints, the G_2/M population of U2OS cells transfected with siNT increased from 14.6 % to 30 % within 12 hrs of exposure to IR (Figure 3.4). The cells deficient of LATS1 displayed similar cell cycle profiles prior to IR, however in contrast to siNT, the population at G_2/M raised to 41 % 12 hrs after exposure to IR and continued to increase further to 45.3 % at 24 hrs (Figure 3.4). This suggested that any potential failure to engage CDK1 did not affect the G_2/M checkpoint, in fact the G_2/M checkpoint appeared to be exacerbated. Interestingly, the control cells displayed consistently slightly lower G_1 phase in the absence of LATS1 (Figure 3.4). The enhanced entry into the S-phase in cells depleted of LATS1 might have been caused by the absence of LATS1 proteolytic fragments generated by Omi which inhibit G_1/S transition (Kuninaka, Iida et al. 2007). However, the arrest at G_2/M indicated that despite variations in the S-phase entry, the cells

failed to resolve a G_2 checkpoint, which implied the accumulation of DNA damage.

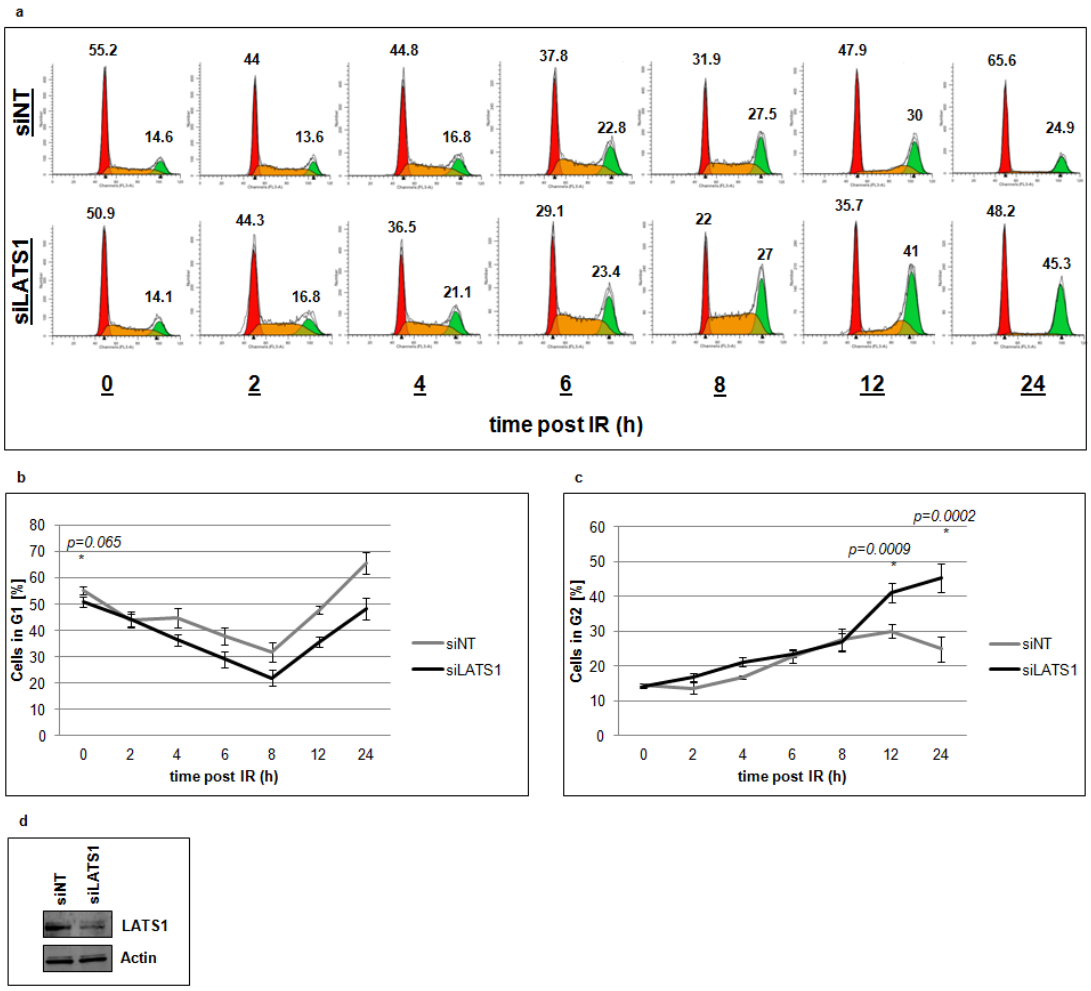


Figure 3.4 Defects in the Cell Cycle Distribution in the Absence of LATS1 Post IR in U2OS Cells. (a) The cell cycle profile analysis. The cells were transfected with either non-targeting siRNA (siNT) or siRNA against LATS1 (siLATS1) and irradiated with 4 Gy 48 hrs post transfection. Cells were fixed at indicated time points and stained with propidium iodide (PI) for 30 min. The samples were read on FACS and analysed using FlowJo software. The values above peaks indicate the percentage of the total events within the peak. The profiles are plotted as FL3-A (Fluorescence area) on x-axis against a number of events counted on the y-axis. **(b)** The chart representing the percentage of cells in G_1 phase after IR as a function of time. **(c)** The chart representing the percentage of cells in G_2 phase after IR as a function of time. **(d)** The Wester Blot showing efficiency of siRNA-mediated knockdown of LATS1. The figure represents n=3 repeats. P value refers to the data point indicated with the asterix.

Similarly to the observations in U2OS cells (Figure 3.4), HeLa cells depleted of LATS1 displayed a significantly increased G_2/M population compared to siNT transfected cells, albeit at earlier time points after induction of DNA damage (Figure 3.5). The most significant difference in proportion of G_2/M cells, 15.4 % for siNT vs. 27.5 % for siLATS1 respectively, was observed 6 hrs after the induction of the DNA damage. The effects observed in both U2OS and HeLa cells were not due to off-target effects of the siRNA as similar results were obtained with distinct siRNA targeting LATS1. HeLa cells did not maintain a G_2/M arrest and returned to a normal cell cycle profile after 24 hrs, which might have been due to a less efficient siRNA-mediated knockdown of LATS1 compared to the U2OS cells. Similar to U2OS, HeLa profiles depleted of LATS1 initially displayed fewer cells in G_1 suggesting a weaker G_1/S cell cycle checkpoint (Figure 3.5).

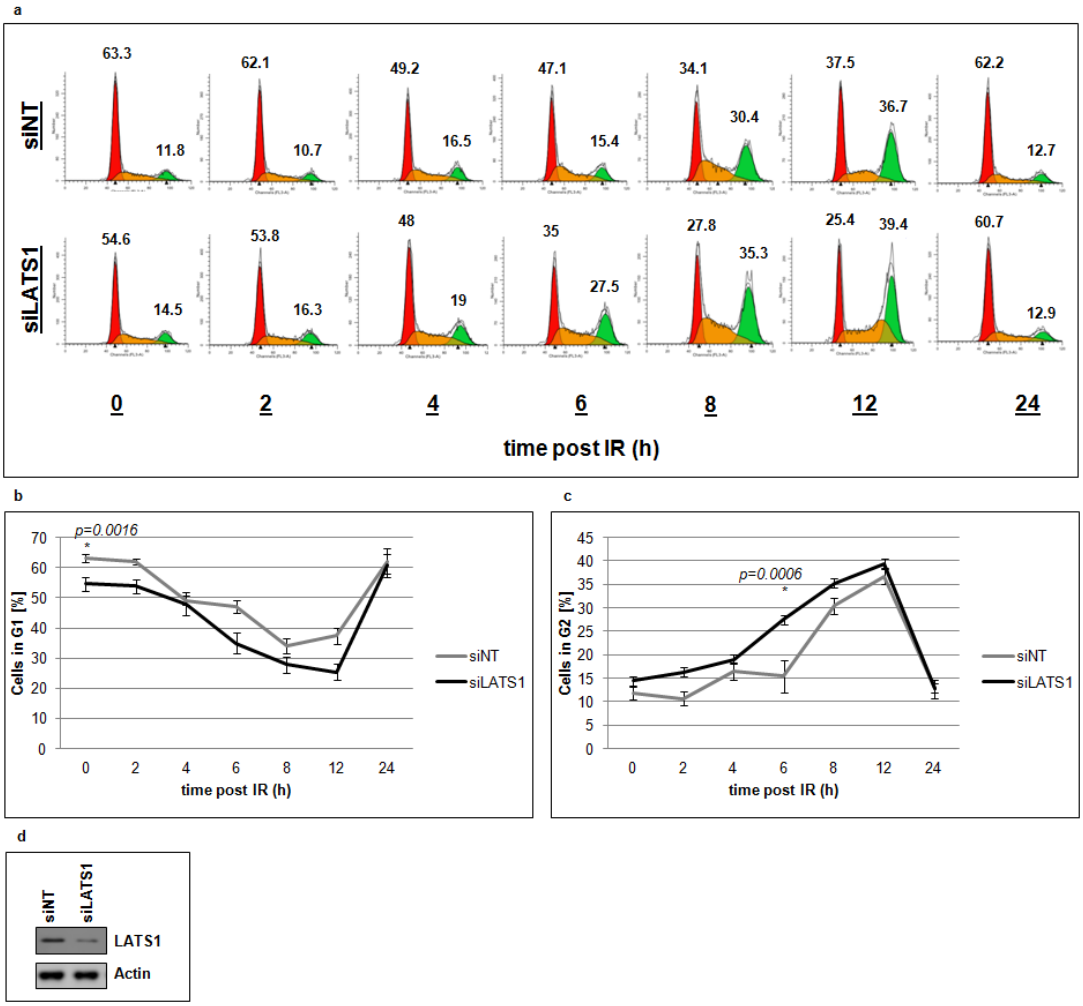


Figure 3.5 Defects in the Cell Cycle Distribution in the Absence of LATS1 Post IR in HeLa Cells. (a) The cell cycle profile analysis. The cells were transfected with either non-targeting siRNA (siNT) or siRNA against LATS1 (siLATS1) and irradiated with 4 Gy 48 hrs post transfection. Cells were fixed at indicated time points and stained with propidium iodide (PI) for 30 min. The samples were read on FACS and analysed using FlowJo software. The values above peaks indicate the percentage of the total events within the peak. Profiles are plotted as FL3-A (Fluorescence area) on x-axis against a number of events counted on the y-axis. **(b)** The chart representing the percentage of cells in G_1 phase after IR as a function of time. **(c)** The chart representing the percentage of cells in G_2 phase after IR as a function of time. **(d)** The Wester Blot showing efficiency of siRNA-mediated knockdown of LATS1. The figure represents n=3 repeats. P value refers to the data point indicated with the asterix.

To ensure these results were attributable to LATS1, we next employed mouse embryonic fibroblasts (MEFs) that were genetically ablated of the Lats1 (mouse LATS1) gene. Asynchronously cycling MEFs were irradiated with 10 Gy, stained with PI and fixed at the indicated time points (Figure 3.6). In agreement with observations in U2OS (Figure 3.4) and HeLa cells (Figure 3.5), a greater degree of *Lats1*$^{-/-}$ fibroblasts accumulated in G_2/M compared to *wt* cells. Similarly, cell cycle profiles displayed a consistently reduced number of cells in the G_1 phase and accumulated in G_2/M within 6 hrs of IR (Figure 3.6).

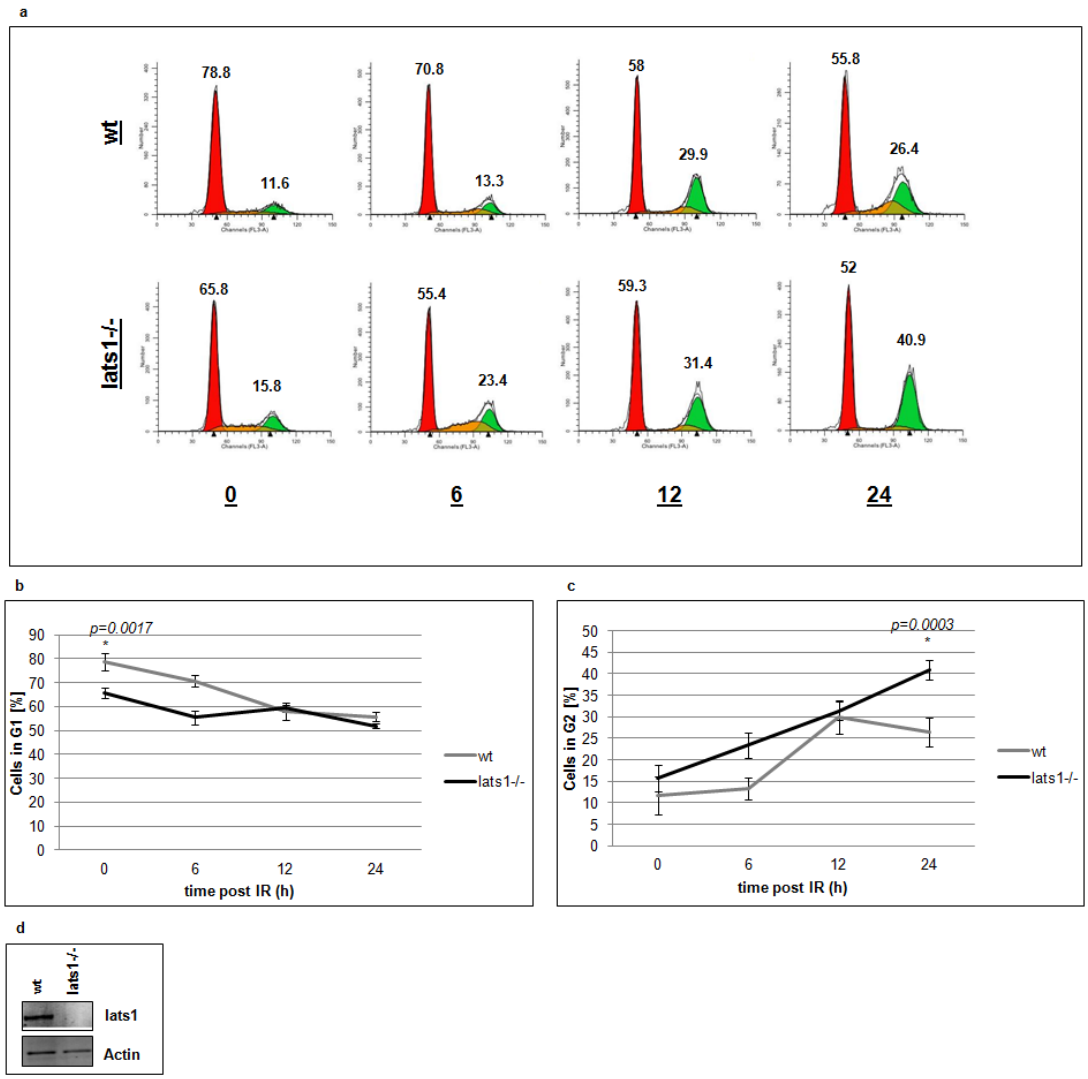


Figure 3.6 Defects in the Cell Cycle Distribution in the Absence of Lats1 Post IR in MEFs. (a) The cell cycle profile analysis. MEF *wt* and *Lats1*$^{-/-}$ were cultured and irradiated with 10 Gy. The cells were fixed at the indicated time points and stained with propidium iodide (PI) for 30 min. The samples were read on FACS and analysed using FlowJo software. The values above peaks indicate the percentage of the total events within the peak. Profiles are plotted as FL3-A (Fluorescence area) on x-axis against a number of events counted on the y-axis. **(b)** The chart representing the percentage of cells in G_1 phase after IR as a function of time. **(c)** The chart representing the percentage of cells in G_2 phase after IR as a function of time. **(d)** The Wester Blot showing efficiency of siRNA-mediated knockdown of LATS1. The figure represents n=3 repeats. P value refers to the data point indicated with the asterix.

3.5 The Accumulation of LATS1-Deficient Cells in the S-Phase after IR

We next wanted to investigate whether there were intrinsic defects in the S-phase progression due to the LATS1-mediated restriction of CDK2 activity (Figure 3.1). Both U2OS (Figure 3.7) and HeLa (Figure 3.8) cells were transfected with either non-targeting siRNA (siNT) or siRNA against LATS1 (siLATS1) and incubated for 48 hrs. The cells were irradiated with 4 Gy and stained with BrdU to indicate active replication, and fixed at the indicated time points for FACS analysis. The cell cycle profile of U2OS cells treated with siLATS1 indicated a higher number of cells actively incorporating BrdU, which further increased at 2 hrs to 8 hrs post IR (Figure 3.7). Similar results were obtained in HeLa cells at 6 hrs, however, these results were less obvious, potentially due to the insufficient ablation by siRNA (Figure 3.8). Together, the data demonstrated that the LATS1 appeared to restrict the S-phase entry in response to the DNA damage but did not affect the ability of cells to progress with active BrdU incorporation.

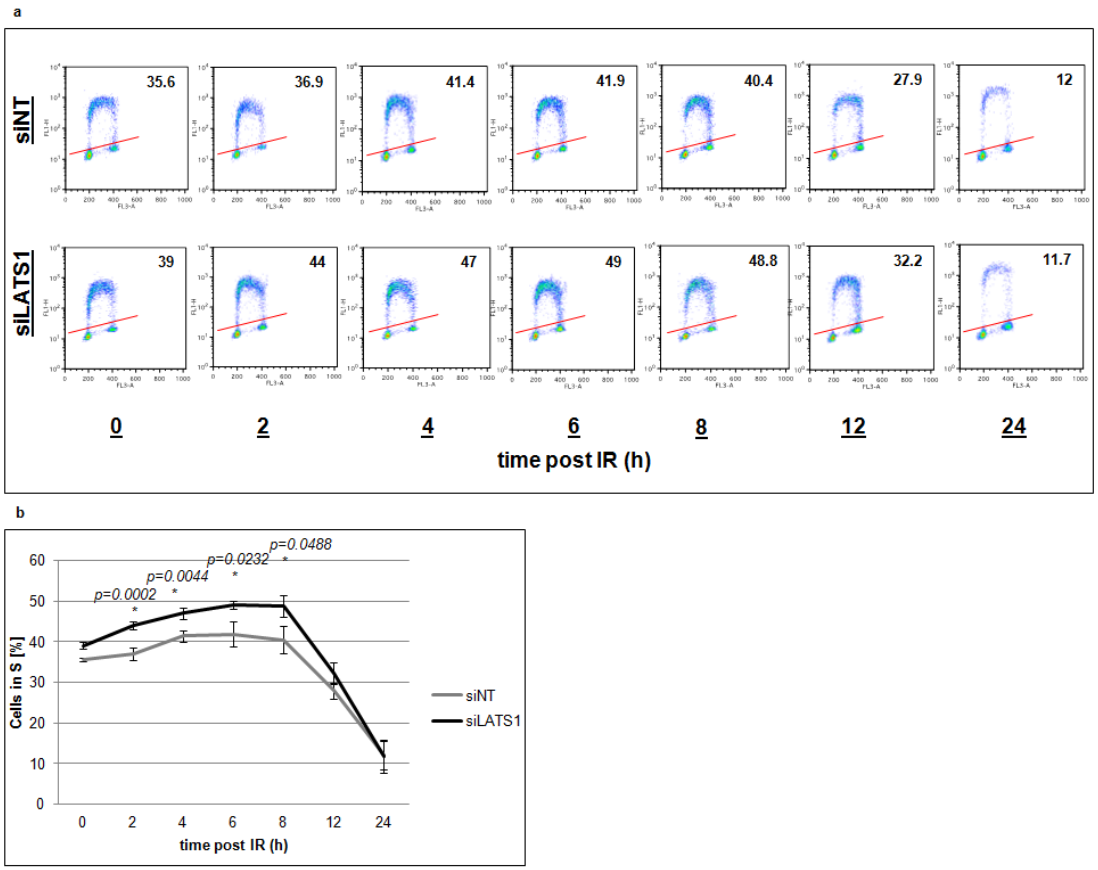


Figure 3.7 Defects in the S-Phase Distribution in the Absence of LATS1 in U2OS Cells. (a) The S-phase profile analysis. The cells were transfected with either non-targeting siRNA (siNT) or siRNA against LATS1 (siLATS1) and irradiated with 4 Gy 48 hrs post transfection. The cells were stained for 30 min with BrdU and fixed at the indicated time points. The samples were read on FACS and analysed using FlowJo software. The values in the top right corner indicate the percentage of cells in the S-phase. The red bar represents a boundary between cells in the S-phase and the G_1 or G_2 populations. Profiles are plotted as FL3-A (Fluorescence area) on x-axis against a number of events counted on the y-axis. **(b)** The chart representing the percentage of cells in S-phase after IR as a function of time. The figure represents n=3 repeats. P value refers to the data point indicated with the asterix.

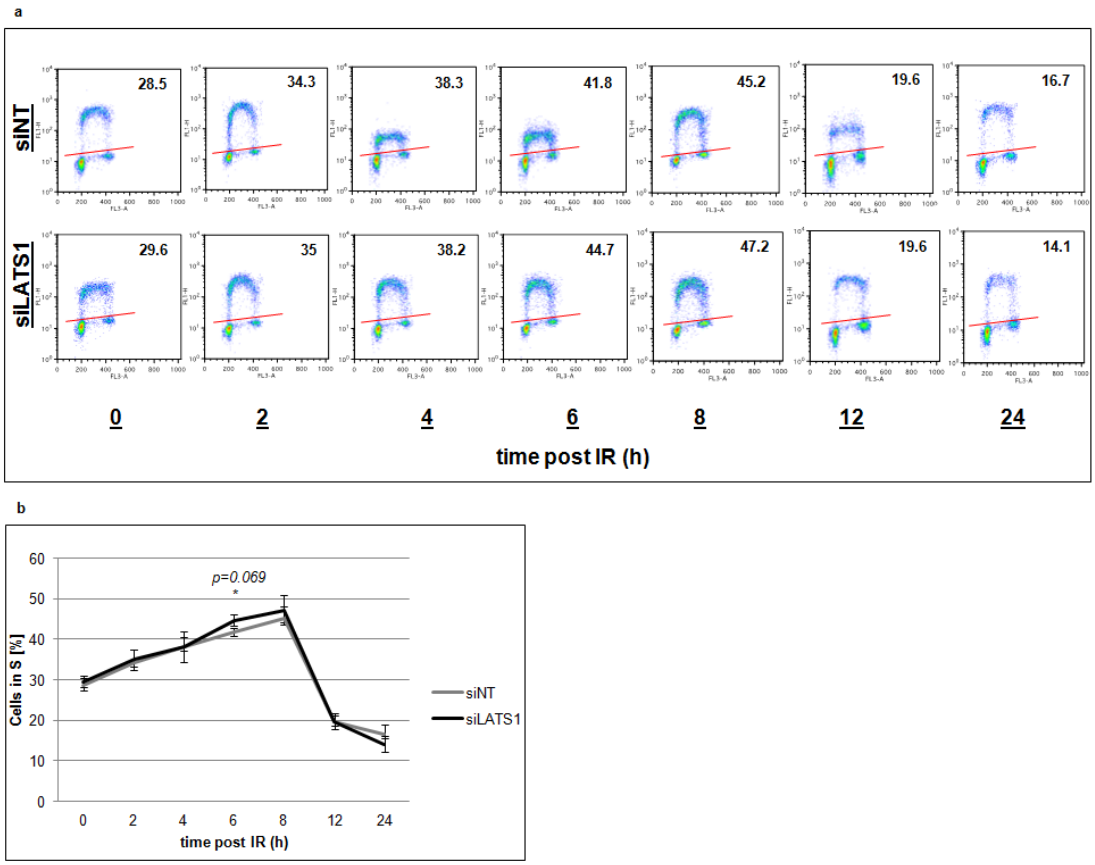


Figure 3.8 Defects in the S-Phase Distribution in the Absence of LATS1 in HeLa Cells. (a) The S-phase profile analysis. The cells were transfected with either non-targeting siRNA (siNT) or siRNA against LATS1 (siLATS1) and irradiated with 4 Gy 48 hrs post transfection. The cells were stained for 30 min with BrdU and fixed at indicated time points. The samples were read on FACS and analysed using FlowJo software. The values in the top right corner indicate the percentage of cells in the S-phase. The red bar represents a boundary between cells in the S-phase and the G_1 or G_2 populations. Profiles are plotted as FL3-A (Fluorescence area) on x-axis against a number of events counted on the y-axis. **(b)** The chart representing the percentage of cells in S-phase after IR as a function of time. The figure represents n=3 repeats. P value refers to the data point indicated with the asterix.

To further examine the effects on the S-phase distribution observed in U2OS (Figure 3.7) and HeLa cells (Figure 3.8), we again utilised *Lats1*$^{-/-}$ MEFs. Although a measureable G_1 arrest upon exposure to 10 Gy was not discernible by FACS (Figure 3.6), incorporation of BrdU indicated that control MEFs did restrict S-phase entry 6 hrs after DNA damage (Figure 3.9). Results also suggested that after sufficient time to complete DNA repair has elapsed (i.e. 24 hrs), cells appeared to re-enter cell cycle (Figure 3.9). In contrast, *Lats1*$^{-/-}$ cells continued to enter and accumulate in S-phase 6 h after exposure to DNA damage and failed to re-enter cycle as indicated by the lack of BrdU incorporation at 24 hrs (Figure 3.9).

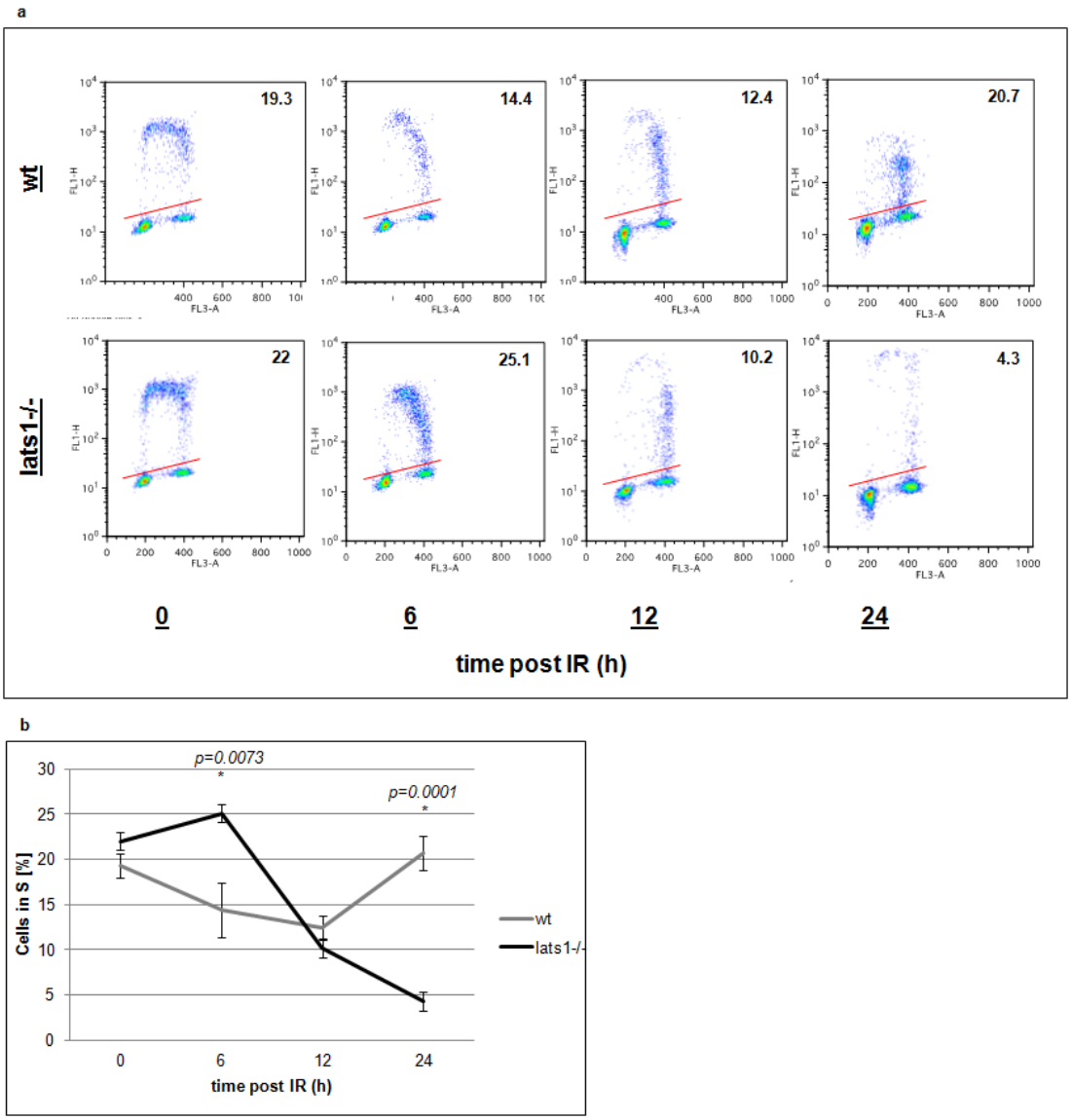


Figure 3.9 Defects in the S-Phase Distribution in the Absence of Lats1 in MEFs. (a) The S-phase profile analysis. MEF *wt* and *Lats1*$^{-/-}$ were cultured and irradiated with 10 Gy. The cells were stained for 30 min with BrdU and fixed at the indicated time points. The samples were read on FACS and analysed using FlowJo software. The values in the top right corner indicate the percentage of cells in the S-phase. The red bar represents a boundary between cells in the S-phase and the G_1 or G_2 populations. Profiles are plotted as FL3-A (Fluorescence area) on x-axis against a number of events counted on the y-axis. **(b)** The chart representing the percentage of cells in S-phase after IR as a function of time. The figure represents n=3 repeats. P value refers to the data point indicated with the asterix.

3.6 Discussion

LATS1 is phosphorylated during the prophase and the metaphase and is found to be associated with CDK1 in the mitotic cells. Whether this interaction is restricted to mitotic cells, has not been clarified and in this chapter we did not observe interaction of LATS1 with either CDK1 or CDK2 in the cycling cells (Figure 3.1) and (Tao, Zhang et al. 1999). The lack of an obvious interaction with CDK1 might have been attributed to the low proportion of cells undergoing mitosis. However, we reasoned that LATS1 may require to be activated in order to associate with CDKs. As LATS1 kinase activity was reported to be triggered by cell density, we assessed the association in confluent cultures and observed LATS1 co-immunoprecipitation with both CDK1 and CDK2, but not with CDK3 (Figure 3.2) and (see Section 1.4.3) and (Zhao, Wei et al. 2007; Ota and Sasaki 2008). No cyclins were detected in the LATS1/CDKs immuno-complex when the blots were probed with antibodies against Cyclin A, B1 or E indicating that, in line with previous reports, LATS1 negatively regulated CDKs by keeping bound kinases in an inactive state (Figure 3.2) and (Tao, Zhang et al. 1999). The induction of the DNA double strand breaks activates the ATM-RASSF1A-MST2 signalling leading to the stimulation of LATS1 (Hamilton, Yee et al. 2009). In response to IR, CDKs co-immunoprecipitated with LATS1 within 4 hrs of inducing the DNA damage (Figures 3.1). Interestingly, in confluent cultures where the interaction between LATS1 and CDKs was induced, no additive effect was observed and CDKs appeared to dissociate from LATS1 after IR (Figure 3.2). While this implied a potentially interesting crosstalk between the DNA damage signalling and the pathways that sense cell density, it also suggested that LATS1-

dependent regulation of CDKs may not be required soon after the DNA damage. These observations demonstrated that the previously described interaction between LATS1 and CDK1 may be regulated in a DNA damage-dependent manner. Moreover, we expanded the previously described ability to associate with CDK1 to a DNA damage-promoted association with CDK2. Furthermore, the depletion of LATS1 led to alteration of the G_1/S boundary resulting in the reduction of G_1 population in non-irradiated cells (Figures 3.4, 3.5 and 3.6). LATS1 may potentially regulate the G_1/S transition through a similar mechanism to its human homologue LATS2, which promotes the silencing of E2F target genes expression through the modulation of the DREAM complex. Furthermore, LATS2 has been suggested to restrict the G_1/S transition through inhibition of CDK2/Cyclin E kinase, although no direct association was found (Li, Pei et al. 2003; Tschop, Conery et al. 2011). The CDK2/Cyclin E activity is required to allow the S-phase entry by inactivating Rb, a direct inhibitor of E2F transcription. As we now observed LATS1-mediated regulation of CDK2, the regulation of the G_1/S boundary may involve facets of the regulation previously attributed to an overexpressed LATS2 (Li, Pei et al. 2003). In addition to a weakened G_1/S boundary, the data indicated that LATS1 is required to prevent a G_2/M arrest in response to the DNA damage (Figure 3.7 and 3.9). We observed exacerbated G_2/M arrest in LATS1-deficient cells exposed to IR, which suggested that the association of LATS1 with CDK1 did not drive a DNA damage G_2/M checkpoint. The most likely explanation was that LATS1-depleted cells remained in G_2 due to an increased amount of the DNA damage that was the result of the failure to respond to the checkpoint activation or the defective DNA repair during the S-

phase. Therefore, we reasoned that the variation in the response of the irradiated cells might have been attributed to LATS1 restricting CDK2 activity. To address these questions, the next chapter focuses on monitoring levels of the DNA damage and repair in the absence of LATS1.

Chapter 4:
LATS1 in DNA Damage

4.1 Introduction

The previous chapter revealed aberrations in the cell cycle progression in cells deficient in LATS1. In the absence of LATS1, cells harbouring DNA damage appeared to increase in the S-phase population (Figures 3.7 and 3.9) and subsequently accumulated in the G_2/M (Figures 3.4 and 3.6). Ionising radiation (IR) introduces a number of lesions to the DNA, including double-strand breaks (DSB), single-strand breaks (SSB), base damage and DNA-protein cross-links (Ward 1988; Su, Meador et al. 2010). During the S-phase, the DNA replication forks stall, regress or collapse when they encounter damage. The DSBs generated from collapsed forks can be repaired by HR, the main DNA damage repair mechanism during the S-phase (see Section 1.3.6) and (Hanada, Budzowska et al. 2007; Lambert, Froget et al. 2007). In the absence of LATS1, the cells displayed a weakened DNA damage checkpoint at the G_1/S boundary with more cells appearing in the S-phase. At later time points following the DNA damage, we observed that cells accumulated in the G_2/M in the absence of LATS1 (Figures 3.4 and 3.6). Therefore, restriction of CDK2/Cyclin E activity may be required to prevent replication and allow the DNA repair process to complete repair. To address this, we ascertained whether the cells display DNA repair defects at the same time that we observed variations in the S-Phase progression and entry into the G_2/M.

4.2 Retardation of the DNA Repair in the Absence of LATS1

To assess whether cells depleted of LATS1 were less efficient at repairing DNA damage, we determined the extent of the DNA damage remaining at different time points after the exposure to IR using the alkaline comet assay. The alkaline condition of the assay measure the presence of both SSB and DSB. *Lats1*$^{-/-}$ and control MEFs were exposed to 10 Gy IR and trypsinised at the indicated time points. The trypsinised cells were then re-suspended in a low melting point agarose, applied to slides and subsequently lysed for 1 h. The slides were then subjected to electrophoresis and treated with the nucleic acid stain SYBR Gold. The analysis was performed using Komet 5.5 software (Figure 4.1). In this assay, the intact nuclear DNA forms a bright 'comet head' structure and the fragmented unrepaired DNA is visualised as a migrating 'comet tail'. To assess the progression of the DNA damage repair, we quantified the fluorescent intensity of the tail fraction of the DNA and represented it as a percentage of the total nuclear DNA. The proportion of the total DNA in the comet tail was below detection in the control cells but increased to approximately 40 % immediately after treatment with 10 Gy IR in both *wt* and *Lats1*$^{-/-}$ MEFs (Figure 4.1). Both cell lines reduced their comet tail by 3 hrs after DNA damage induction, with the *wt* MEFs resolving the damage more efficiently than the MEFs lacking Lats1, the percentages were 8 % and 18 % respectively (Figure 4.1). The variation in the comet tail DNA indicated that in the absence of Lats1 cells repair DNA less efficiently comparing to wt (Figure 4.1). The data from Comet assay together with the observations in Chapter 3 suggested that the cells progressing through the S-phase in the absence of Lats1 were likely to be doing so with elevated DNA damage

(Figures 3.7, 3.9 and 4.1). The DNA damage was negligible in both cases 24 hrs after IR. While the comet assay was a definitive detection of DNA damage, we next wanted to address the same question with a more sensitive measurement. Therefore, we examined the biochemical markers of the DNA double strand breaks (DSBs).

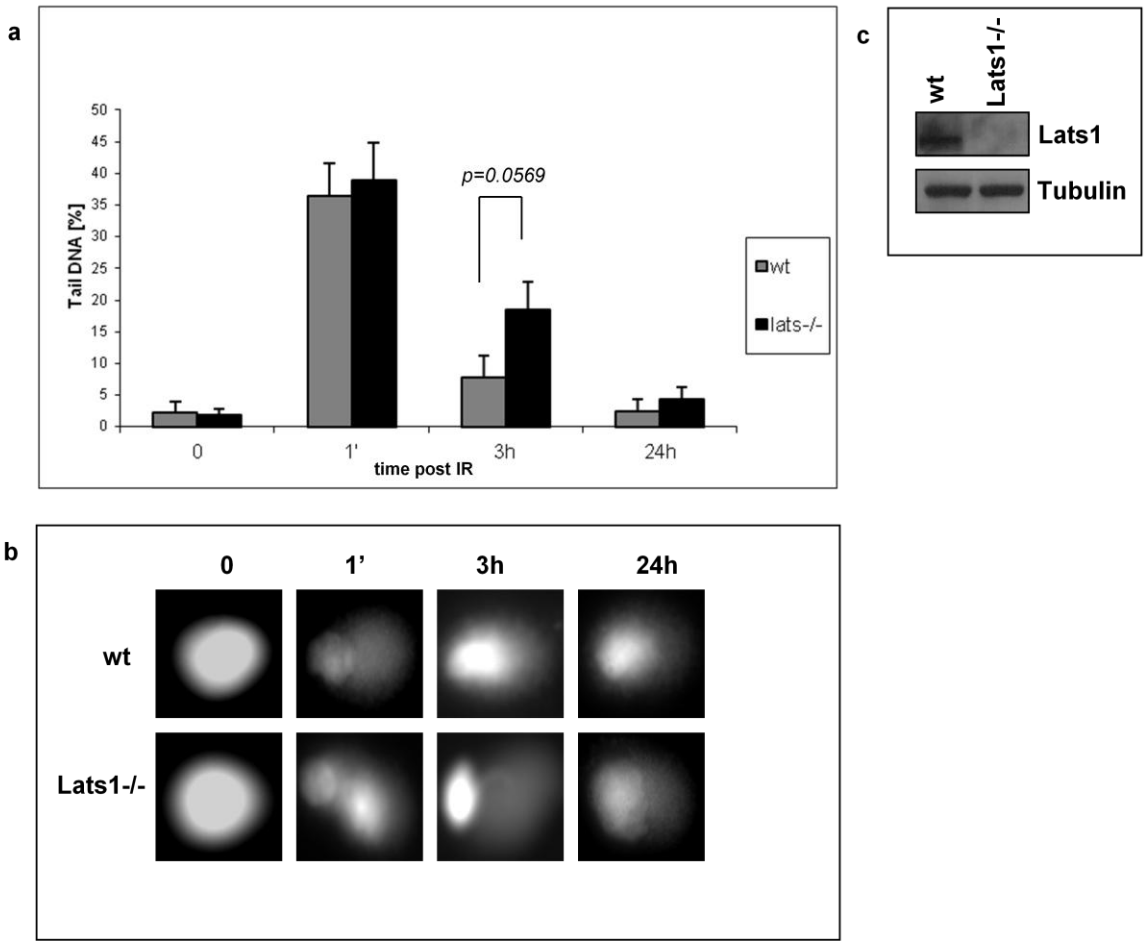


Figure 4.1 DNA Repair is Retarded in the Absence of LATS1. The alkaline comet assay; quantitation of DNA in a tail of the comet. MEF *wt* and MEF *Lats1*$^{-/-}$ were cultured to 30% confluence. Cells were irradiated with 10 Gy and incubated at 37 °C for 1 min, 3 hrs and 24 hrs. The sample labelled 0 was not irradiated. **(a)** The bar chart represents the percentage of overall DNA in the comet tail. The comets were quantitated using 'Komet 5.5' software. This figure represents n=3 repeats. **(b)** The representative pictures of comets were taken with microscope Nikon 90i. **(c)** The Western blot showing level of expression of Lats1.

4.3 The Persistence of Phosphorylation of H2AX after IR in the Absence of LATS1

We reasoned that the differential kinetics of the comet tail resolution (Figure 4.1) might have been responsible for the increased G_2/M arrest of cells lacking LATS1 (Chapter 3). To obtain a more sensitive measurement of DSBs, we next monitored levels of phosphorylation of the variant histone H2AX (γH2AX). H2AX is a marker of double strand breaks (DSBs) generated by exogenous damage i.e. IR (Rogakou, Pilch et al. 1998; Burma, Chen et al. 2001). Since the comet assay suggested that LATS1 was required for the resolution of the DNA damage, we attempted to discern whether the DNA was being repaired by measuring phosphorylation of H2AX. In correlation with the comet tail analysis, 3-6 hrs after exposure to the DNA damage the LATS1 expressing cells demonstrated a noticeable reduction in the γH2AX levels whereas *Lats1*$^{-/-}$ failed to appreciably reduce levels at these time points. Furthermore, *Lats1*$^{-/-}$ MEFs failed to resolve γH2AX up to 24 hrs post exposure to 10 Gy IR (Figure 4.2). The reconstitution of *Lats1*$^{-/-}$ MEFs with either hLATS1 or a kinase dead derivative (hLATS1 KD) restored the levels of γH2AX to levels equivalent to control MEFs (Figure 4.2). This indicated that similarly to association with CDKs, the LATS1 kinase activity was not required for the DNA damage resolution (Tao, Zhang et al. 1999). The analysis also revealed elevated γH2AX in non-irradiated *Lats1*$^{-/-}$ MEFs, compared to control fibroblasts, indicating a potential inherent genomic instability of these cells (Figure 4.2). To ensure that the defects in the DNA damage were not a consequence of a genomically unstable phenotype, we monitored the

chromosome in the metaphase spread and did not observe any obvious general defects (Appendix S1). Furthermore, the effects we observed could be rescued by reconstituting the *Lats1*$^{-/-}$ MEFs with LATS1 expressing plasmids. Interestingly, while the comet tails did not show unresolved DNA damage 24 hrs post IR (Figure 4.1), the more sensitive measurement of γH2AX in *Lats1*$^{-/-}$ MEFs indicated that these cells indeed had unrepaired damage that was likely promoting the G_2/M arrest observed in Chapter 3.

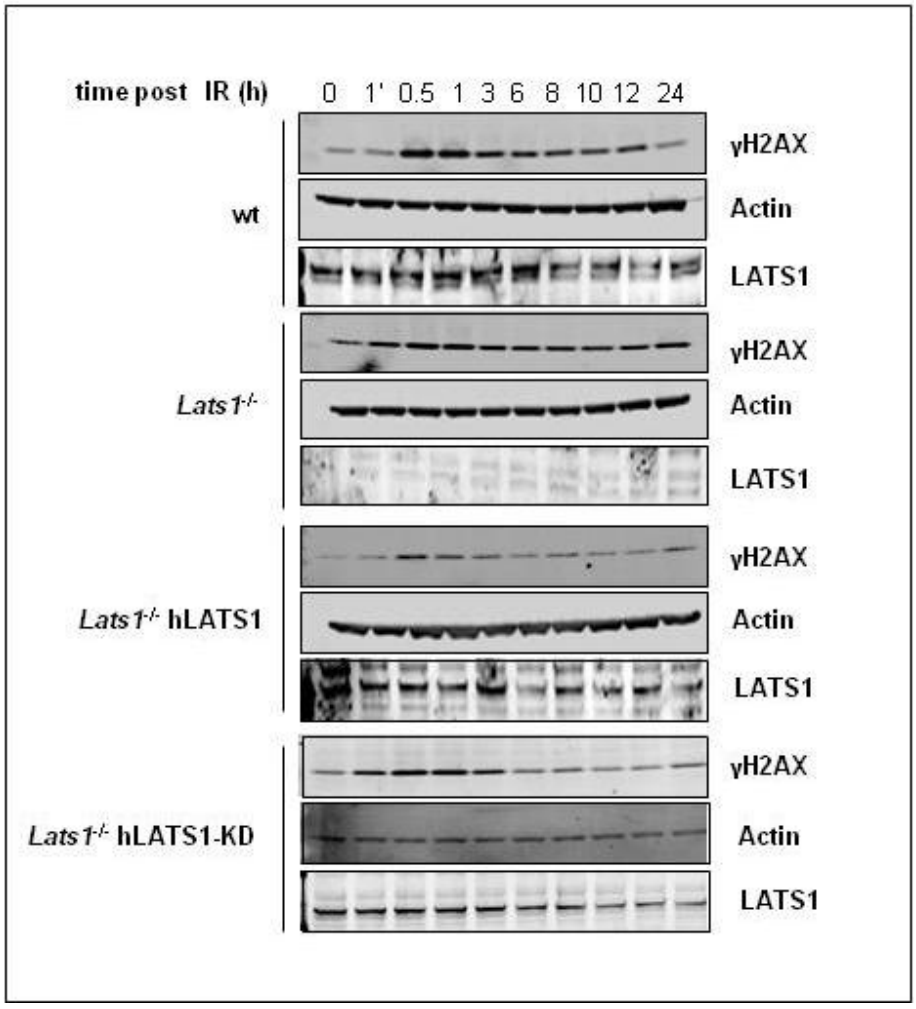


Figure 4.2 The Absence of LATS1 Causes Persistence of Phosphorylation of H2AX Post IR in MEFs. The Western blot analysis of γH2AX levels in MEF *wt*, MEF *Lats1*$^{-/-}$ and MEF *Lats1*$^{-/-}$ reconstituted with hLATS1 or hLATS1-KD. The cells were cultured to 30 % confluence. MEF *Lats1*$^{-/-}$ were transfected with 10 µg of either hLATS1 or hLATS1 kinase dead referred as hLATS1-KD. 24 hrs after transfection the cells were irradiated with 10 Gy and incubated at 37 °C for 1 min, 30 min and 1, 3, 6, 8, 10, 12 and 24 hrs. The sample labelled 0 was not irradiated. The blots were probed with the indicated antibodies and visualised using Odyssey scanner (Li-cor).

To corroborate the results in MEFs, U2OS cells were treated with either non-targeting siRNA (siNT) or siRNA targeted against LATS1 (siLATS1) (Figure 4.3). The cells were exposed to 4 Gy IR at 48 hrs after the transfection with siRNAs and were lysed at the indicated time points post IR. The phosphorylation of H2AX was not detected in non-irradiated U2OS *wt* or cells transfected with either siNT or siLATS1. γH2AX was apparent after 30 min exposure to 4 Gy IR with initial resolution observed from 2 hrs and completely resolved at 8 hrs post IR in *wt* and siNT (Figure 4.3). In contrast to *wt* and siNT, the cells depleted of LATS1 established γH2AX immediately after IR, which persisted up to 12 hrs (Figure 4.3). Importantly, at 24 hrs γH2AX was reduced but still detectable in U2OS cells depleted of LATS1 (Figure 4.3) but was much more evident in *Lats1*$^{-/-}$ fibroblasts (Figure 4.2). This variation might have been attributed to different cell types (fibroblast vs. epithelial cancer cell), complete vs. partial ablation of LATS1 or alternatively due to *Lats1*$^{-/-}$ MEFs containing a degree of endogenous damage due to genomic instability. In line with this later idea, the elevated levels of γH2AX in *Lats1*$^{-/-}$ MEFs (Figure 4.2) were not observed in U2OS siLATS1 (Figure 4.3), suggesting that cells might have accumulated DNA damage in prolonged absence of LATS1. Whether this was due to the increased endogenous damage or simply a failure to repair the DNA, was not clear.

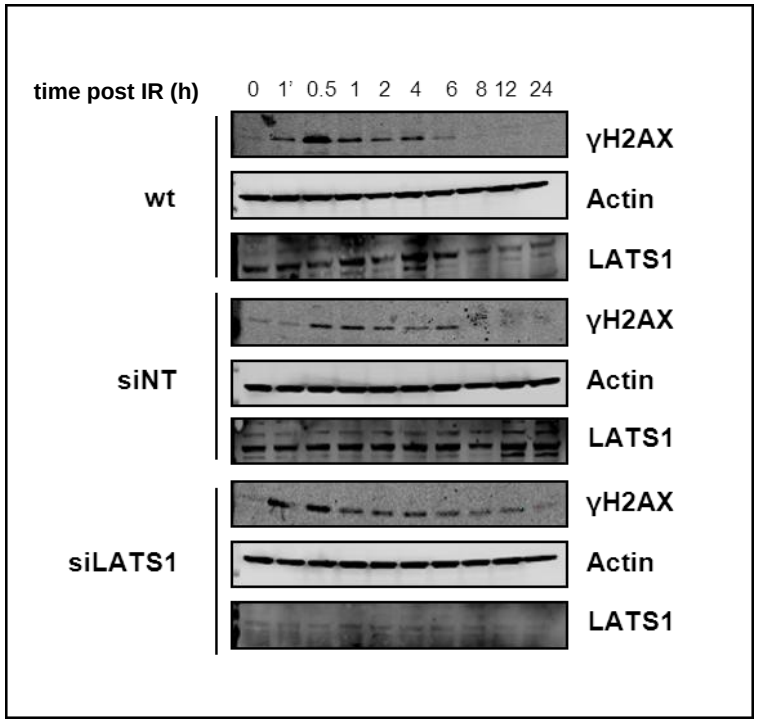


Figure 4.3 The Absence of LATS1 Causes Persistence of Phosphorylation of H2AX Post IR in U2OS Cells. The Western blot analysis of γH2AX levels in U2OS wt, siNT and siLATS1 cells. U2OS cells were cultured to 30% confluence. U2OS were transfected with either non-targeting (siNT) or LATS1 siRNA. 48 hrs after the transfection the cells were irradiated with 4 Gy and incubated at 37 °C for 1 min, 30 min and 1, 2, 4, 6, 10, 12 and 24 hrs. The sample labelled 0 was not irradiated. The blots were probed with the indicated antibodies and visualised using Odyssey scanner (Li-cor).

4.4 The Persistence of the γH2AX Foci Post IR in the Absence of LATS1

The western blot analysis of the phosphorylation status of histone H2AX highlighted the involvement of LATS1 in the DNA damage repair (Figures 4.2 and 4.3). The H2AX histones are phosphorylated in response to DSBs and provide scaffolding for the repair proteins directly adjacent to the DSB. Accumulation of γH2AX promotes the formation of foci around DSBs, which can be visualised by fluorescence microscopy. The γH2AX focus has been described to correspond 1:1 with an unrepaired DSB (see Section 1.3.2) and (Rogakou, Pilch et al. 1998; Burma, Chen et al. 2001). To verify the kinetics of the DNA damage resolution, we determined the extent of the γH2AX foci formation. The U2OS cells were cultured on cover slips to 30 % confluence and were subsequently transfected with non-targeting (siNT) and siRNA against LATS1 (siLATS1). The irradiated cells were fixed at the indicated time points and probed with an antibody against γH2AX (Figures 4.4 and 4.5). To assess the extent of the γH2AX foci resolution and to differentiate the cells with the basal level of γH2AX, only cells with more than 9 foci were included in the statistics (Figure 4.4). Statistics was based on approximately 1000 cells per condition and experiment was repeated three times. As expected, few cells displayed γH2AX foci prior to IR and 100 % of cells efficiently formed more than 9 foci in response to 4 Gy IR (Figure 4.4). In agreement with data from γH2AX western blot analysis (Figures 4.2 and 4.3), U2OS depleted of LATS1 demonstrated persistence of the γH2AX foci 24 hrs after IR (Figure 4.4). Interestingly, while the numbers of cells displaying γH2AX foci at 4 hrs

did not appear to vary upon ablation of LATS1, varying levels of γH2AX were discernible by western blot (Figures 4.2 and 4.3). Upon further analysis, we noticed that the number of γH2AX foci per cell varied dramatically (Figure 4.5). In the absence of LATS1, there was an average of 80 foci per cell 4 hrs post IR, 2.5 fold more than in cells transfected with siNT. Thus, even though the initial DNA damage insult of 4Gy IR was the same in all cases, this provided strong evidence that the absence of LATS1 inhibited the repair of lesions that were decorated with γH2AX. However, despite the elevated damage, the *Lats1*$^{-/-}$ cells complete the S-phase and continued into the G_2/M without resolving this damage. One potential explanation is that the DNA repair is not initiated at these DSBs and therefore we next addressed the DNA repair directly.

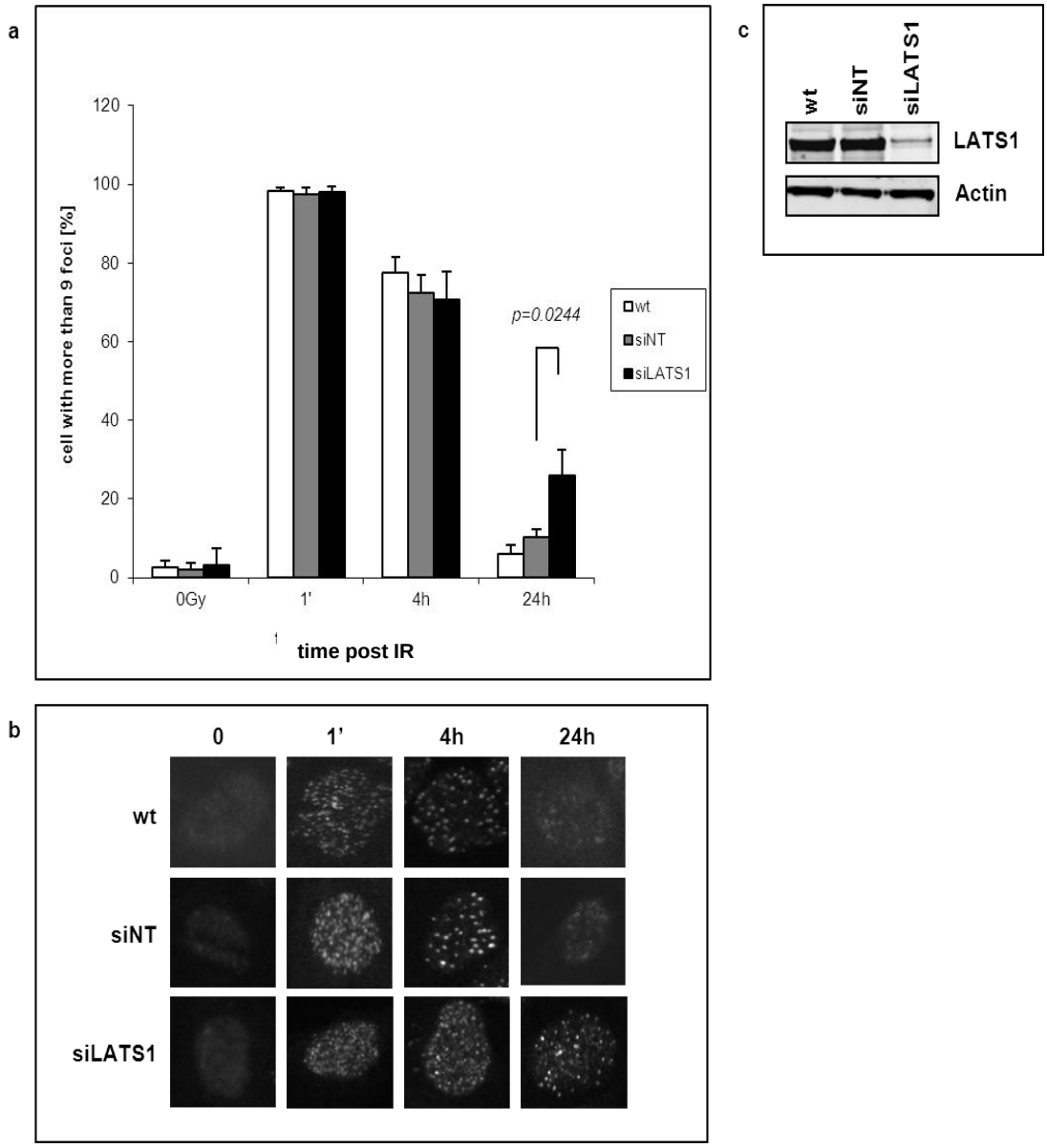


Figure 4.4 γH2AX Foci Persist in the Absence of LATS1 Post IR in U2OS Cells. (a) Quantitation of cells with more than 9 γH2AX foci. The cells were cultured on cover slips and transfected with non-targeting (siNT) and LATS1 siRNA (siLATS1). The sample labelled *wt* was not transfected. 48 hrs after the transfection the cells were irradiated with 4 Gy and incubated at 37 °C for 1 minute, 4 hrs and 24 hrs. The samples labelled 0 Gy were not irradiated. After the incubation, the cells were fixed, probed with an antibody against γH2AX and visualised with secondary fluorescent antibody Alexa 488 and DAPI. The pictures were taken using Nikon 90i microscope with DAPI as well as FITC cubes. The cells were counted manually using ImageJ with 'cell count' plug-in installed. The cells with more than 9 γH2AX foci were treated as positive cells and included in the statistics. **(b)** Representative pictures taken using FITC cube showing γH2AX foci in *wt* U2OS and cells transfected with siNT and siLATS1 without irradiation and 1 min, 4 hrs and 24 hrs after IR. **(c)** Western blot analysis showing efficiency of the LATS1 knockdown.

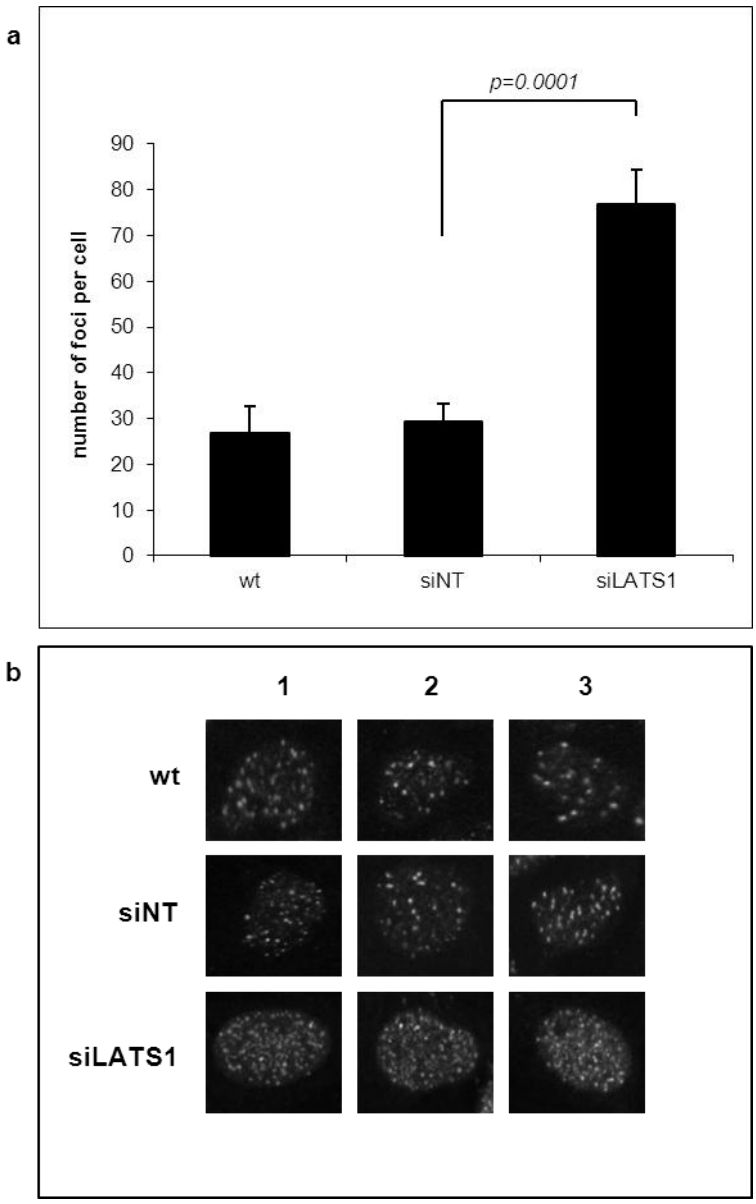


Figure 4.5 Difference in γH2AX Foci Resolution 4 hrs Post IR in U2OS Cells. (a) Chart representing difference in number of γH2AX foci per cell in *wt*, siNT or siLATS1 U2OS cells 4 hrs post 4 Gy IR **(b)** Representative pictures of 3 different cells with γH2AX foci per condition.

4.5 RAD51 Foci Formation Defects in the Absence of LATS1

As outlined above, DSBs occur as a direct product of radiation ion tracts, a combination of closely located SSB, or arise from replication defects when the replication forks encounter lesions, base modifications or cross-links. Due to the availability of a homologous template, homologous recombination (HR) is the main repair mechanism of cells in the S-phase and the G_2 as this permits an error-free repair (Ward 1988; Hanada, Budzowska et al. 2007; Lambert, Froget et al. 2007; Su, Meador et al. 2010). The resolution of DSBs by HR requires the repair proteins BRCA2 and formation of RAD51 filaments on the ssDNA overhangs to initiate the strand invasion of the sister chromatid (see Section 1.3.5). We reasoned that the additional γH2AX foci observed in Figure 4.5 above, might have been due to a failure in the initiation of HR repair, and therefore we measured the influence of LATS1 on the RAD51 foci formation. First, mouse embryonic fibroblasts were cultured on cover slips. Control fibroblasts and *Lats1*$^{-/-}$ MEFs transected with either control plasmid (pcDNA), hLATS1 or the kinase dead derivative (hLATS1 KD) were irradiated with 10 Gy and fixed 4 hrs post IR (Figure 4.6). To differentiate from background levels, only cells with more than 9 RAD51 foci were included in analysis. Statistics was based on approximately 1000 cells per condition and experiment was repeated three times. *Wt* MEFs robustly formed RAD51 foci in response to 10 Gy IR, whereas there were substantially fewer *Lats1*$^{-/-}$ cells establishing RAD51 foci in response to the same stimulus. Reconstitution of *Lats1*$^{-/-}$ with either hLATS1 or hLATS1 KD led to a significant increase in the number of cells with RAD51 foci, suggesting that cells expressing LATS1 were more likely to initiate repair (Figure 4.6). There was no statistical

difference between hLATS1 and its kinase dead derivative in the number of RAD51 foci, as observed in the resolution of γH2AX (Figure 4.2), suggesting that the LATS1 kinase activity was also not required for the regulation of RAD51 foci (Figure 4.6). Together, this indicated that the failure to efficiently regulate RAD51 directly correlated with the persistence of the γH2AX foci.

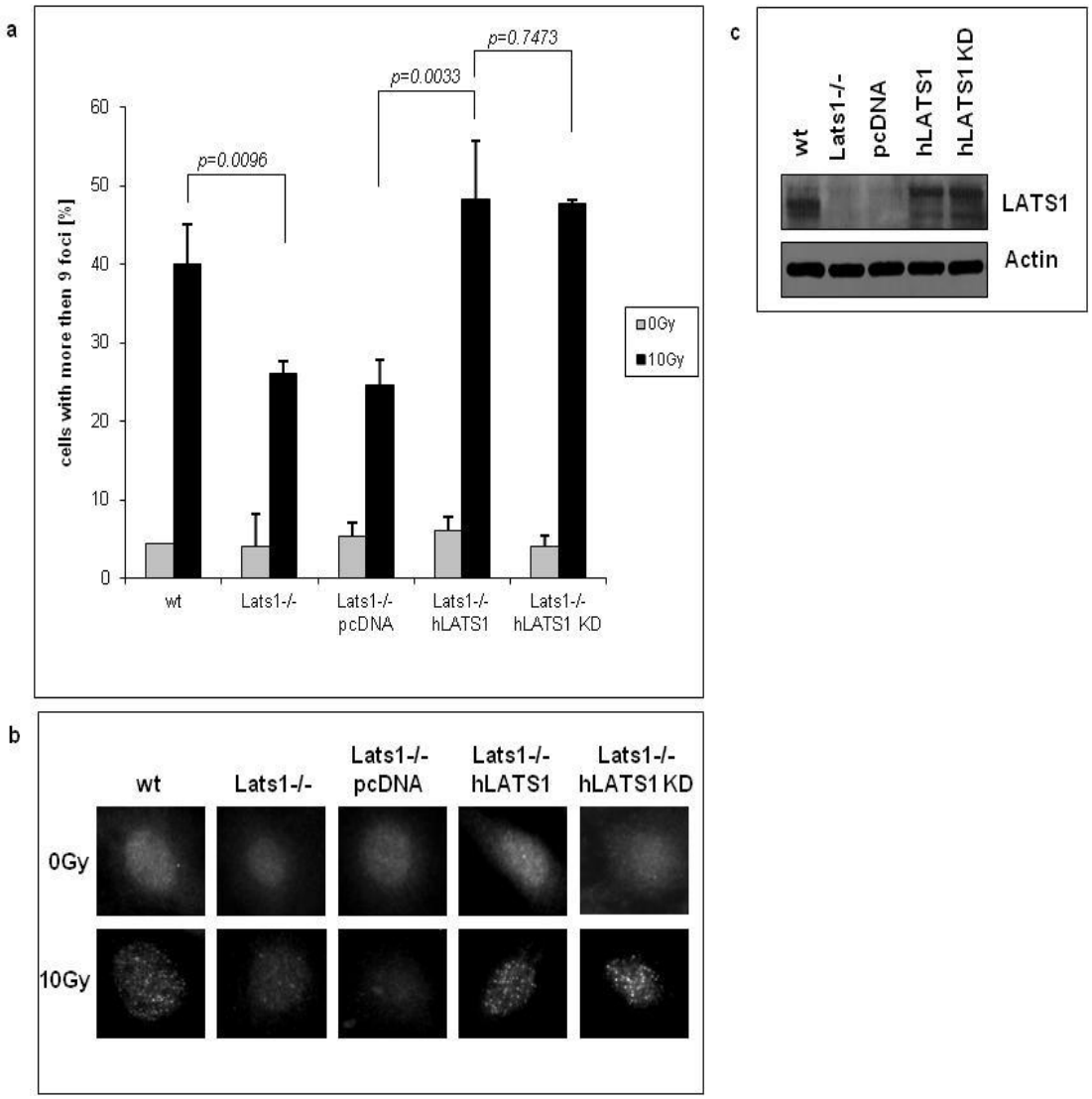


Figure 4.6 RAD51 Foci Formation Defects in the Absence of LATS1 Post IR in MEFs. (a) Quantitation of cells exhibiting more than 9 RAD51 foci per cell. MEF *wt* and MEF *Lats1*$^{-/-}$ were cultured on cover slips. MEF *Lats1*$^{-/-}$ were transfected with either control plasmid (pcDNA) or hLATS1 or hLATS1 kinase dead (hLATS KD). The sample labelled *wt* was not transfected. 24 hrs after transfection, the cells were irradiated with 10 Gy and incubated for 4 hrs at 37°C. The samples labelled 0 Gy were not irradiated. After incubation the cells were fixed, probed with antibody against RAD51 and visualised with a secondary fluorescent antibody Alexa 488 and DAPI. Pictures were taken using Nikon 90i microscope with DAPI and FITC cubes. The cells were counted manually using ImageJ with 'cell count' plug-in installed. Cells with more than 9 RAD51 foci were treated as positive cells and included in the statistics. **(b)** Representative pictures of cells with RAD51 foci. **(c)** The Western blot showing efficiency of hLATS1 and hLATS1-KD transfection.

In agreement with results obtained from MEFs (Figure 4.6), siRNA depletion of LATS1 in U2OS led to a similar decrease in the number of cells with more than 9 RAD51 foci, from 51 % (siNT) to 34 % (siLATS1) 4 hrs after exposure to IR. The experiment was repeated three times and the statistics was based on 1000 cells per condition (Figure 4.7).

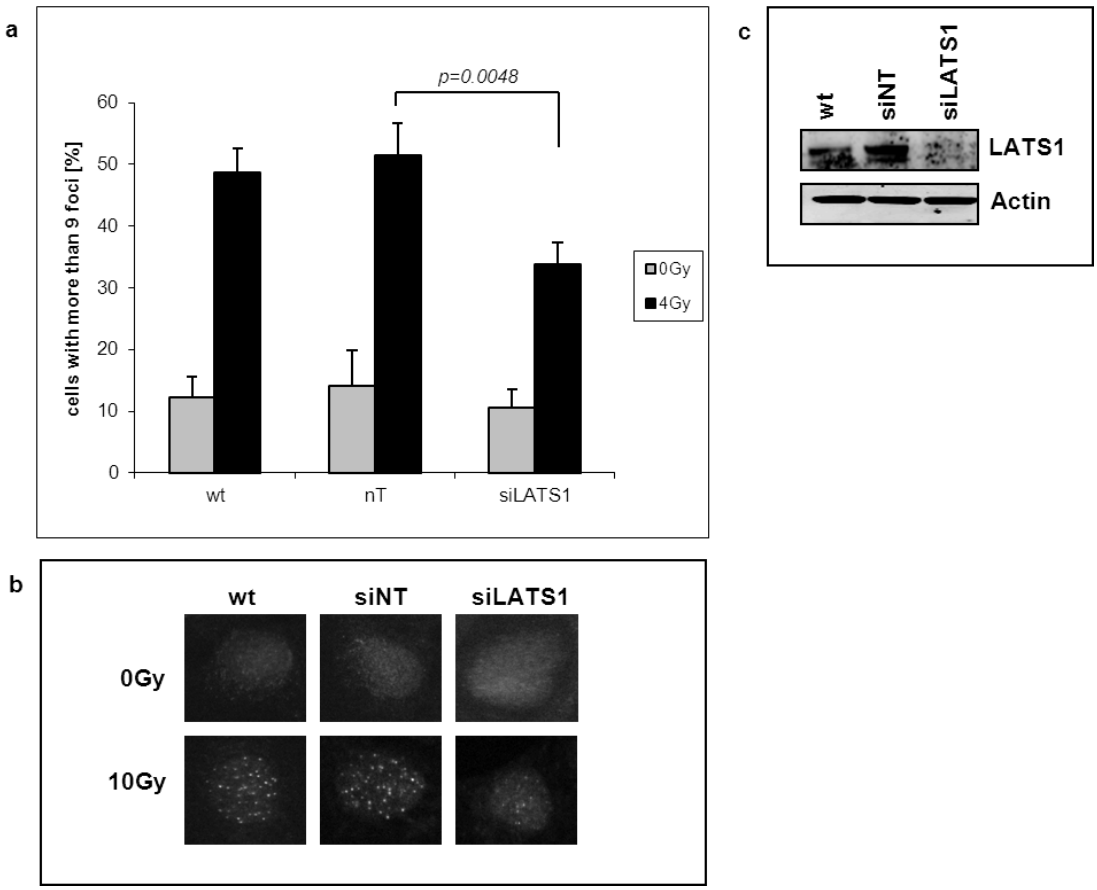


Figure 4.7 RAD51 Foci Formation Defects in the Absence of LATS1 Post IR in U2OS Cells. (a) Quantitation of cells exhibiting more than 9 RAD51 foci per cell. U2OS cells were cultured on cover slips and transfected with non-targeting (siNT) and LATS1 siRNA (siLATS1). The sample labelled *wt* was not transfected. 48 hrs after transfection, the cells were irradiated with 4 Gy and incubated for 4 hrs at 37 °C. The samples labelled 0 Gy were not irradiated. After incubation, the cells were fixed, probed with an antibody against RAD51 and visualised with a secondary fluorescent antibody Alexa 488 and DAPI. Pictures were taken using Nikon 90i microscope with DAPI and FITC cubes. The cells were counted manually using ImageJ with 'cell count' plug-in installed. Cells with more than 9 RAD51 foci were treated as positive cells and included in the statistics. **(b)** Representative pictures of cells with RAD51 foci. **(c)** The Western blot showing efficiency of LATS1 depletion.

Activation of LATS1 in response to IR requires MST2 (Hamilton, Yee et al. 2009). However, the mitogenic stimulation can suppress the MST2 activity through the AKT-dependent phosphorylation (Romano, Matallanas et al. 2010). The mitogenic signals can also influence the cell cycle progression and checkpoints. Therefore, to rule out the contribution of these signals, we cultured siNT and siLATS1 transfected U2OS cells in 0.1 % FBS medium for 16 hrs prior to 4 Gy IR (Figure 4.8). We based statistics on approximately 1000 cells per condition and repeated experiment three times. The depletion of LATS1 led to a significant decrease in the number of cells with more than 9 RAD51 foci from 45 % (siNT) to 29 % (siLATS1) (Figure 4.8) to a similar extent as in 10 % FBS (Figure 4.7). This led to the conclusion that the depletion of growth factors from the medium did not affect the LATS1-dependent RAD51 foci regulation.

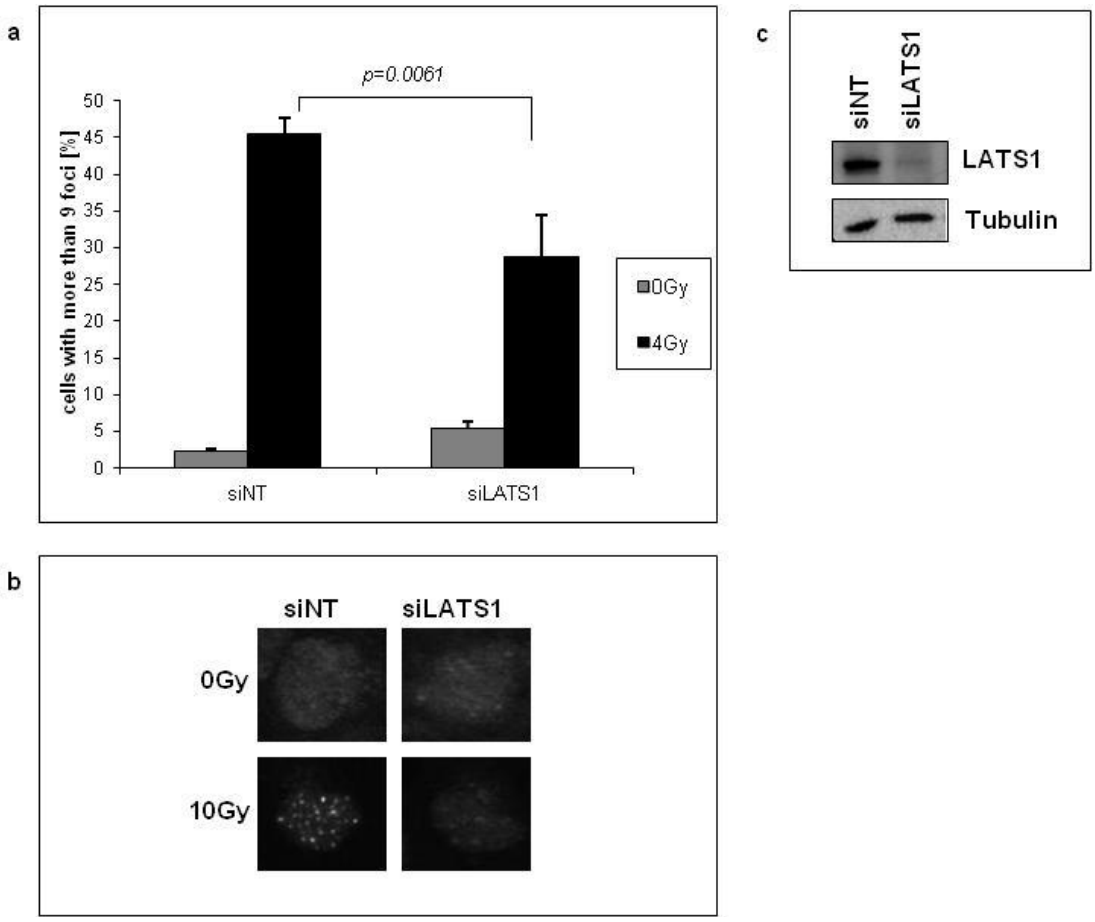


Figure 4.8 RAD51 Foci Formation Defects in the Absence of LATS1 Post IR in U2OS Cells Cultured in a Starving Medium. (a) Quantitation of cells exhibiting more than 9 RAD51 foci per cell. U2OS cells were cultured on cover slips and transfected with non-targeting (siNT) and siRNA against LATS1 (siLATS1). 32 hrs post transfection, the medium was changed to a medium containing 0.1 % FBS. 48 hrs after the transfection and 16 hrs after the change of the medium the cells were irradiated with 4 Gy and incubated 4 hrs at 37 °C. The samples labelled 0 Gy were not irradiated. After the incubation, the cells were fixed, probed with an antibody against RAD51 and visualised with a secondary fluorescent antibody Alexa 488 and DAPI. Pictures were taken using Nikon 90i microscope with DAPI and FITC cubes. The cells were counted manually using ImageJ with 'cell count' plug-in installed. Cells with more than 9 RAD51 foci were treated as positive cells and included in the statistics. **(b)** Representative pictures of cells with RAD51 foci. **(c)** The Western blot showing efficiency of LATS1 depletion.

4.6 The Lack of Effect on HR in the Absence of LATS1

To determine whether the failure to accumulate RAD51 foci in the absence of LATS1 indicates an inability to activate HR, we utilised a recombination assay, which directly addresses the ability to recombine a functional copy of the green fluorescent protein (GFP) (Pierce, Johnson et al. 1999). The gene encoding for GFP has an engineered sequence producing a nonsense transcript that can be cleaved by the I-SCE I nuclease. The gene is encoded on a plasmid that contains a resistance marker. Stably transfected U2OS cells were selected by incubating with puromycin. The DNA cleavage was subsequently induced with I-SCE I nuclease and the cells with efficient HR should be able to repair the cleavage site, which would result in the expression of a sense transcript and the GFP protein. The fluorescent cells can then be counted by Fluorescence Activated Cell Sorting (FACS). However, the defects in the DNA repair ability would leave the cell unable to recombine the GFP gene and fail to produce a functional protein. As expected, the cells with no RAD51 were unable to repair the DNA. Surprisingly, there was no statistical difference between siNT and the cells transfected with siLATS1, implying that HR was not defective in the absence of LATS1 (Figure 4.9). To verify these results, we also constructed the *Lats1*$^{-/-}$ and *wt* MEFs to stably express the recombination assay plasmid. In line with the results in U2OS cells, we observed a limited variation in the ability to promote HR between these cells and no dependence on the LATS1 expression (data not shown). Together, these results indicated that, although LATS1 regulation appeared to be required to limit the DNA damage through

regulation of the RAD51 foci, surprisingly, this did not affect HR directly as indicated by the assay.

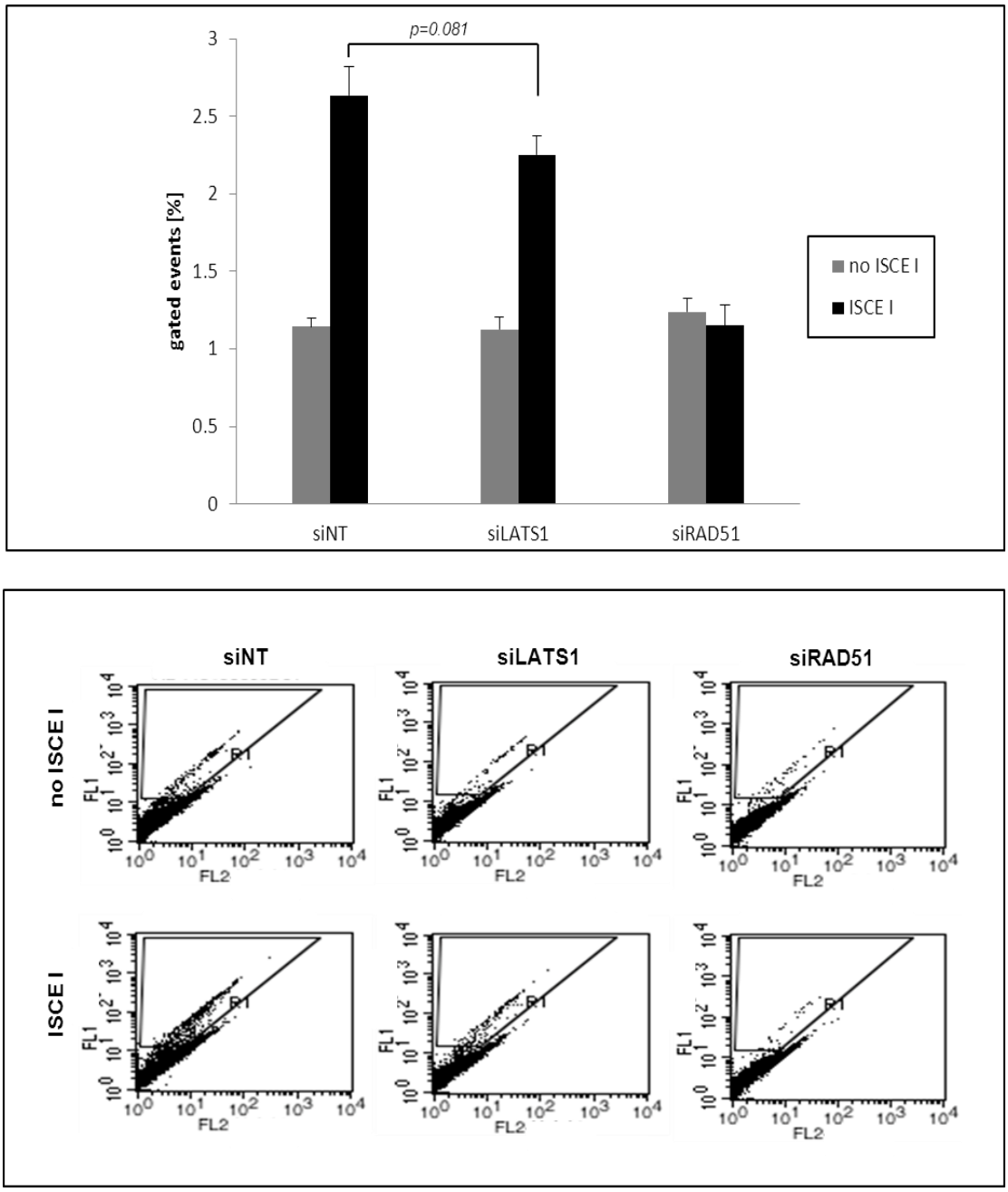


Figure 4.9 HR is Not Affected in the Absence of LATS1 in U2OS Cells. (a) The recombination assay with DR-GFP; quantitation of the recombination events gated. U2OS cells expressing modified GFP plasmid were treated with non-targeting siRNA (siNT), siRNA against LATS1 (siLATS1) and RAD51 (siRAD51). 24 hrs after siRNA treatment cells were transfected with plasmid containing I-SCE I nuclease and incubated for further 48 hrs at 37 °C. 72 hrs post siRNA and 48 hrs post I-SCE I the transfection cells were trypsinised and analysed on FACS based on emitted green signal. **(b)** Representative plots analysed on CellQuest Pro software.

4.7 Discussion

In this chapter we provided evidence that the IR induced G_2/M arrest observed in Chapter 3, was due to elevated DNA damage as measured by the comet assay and γH2AX (Figures 4.1, 4.2, 4.3 and 4.4). In addition to that, defects in the DNA damage repair were displayed in a similar time frame to variations in the S-phase progression and entry into G_2/M. Thus, LATS1-mediated regulation of active in the S-phase CDK2 might have been required to prevent or resolve DNA damage and to allow the efficient transit through G_2 and the completion of the cell cycle. We surmised that the most likely explanation for this phenomenon was that IR induced DSBs were not efficiently repaired in the absence of LATS1 and indeed, we observed defects in the RAD51 foci formation, which would indicate a defective HR (Figures 4.6, 4.7 and 4.8). However, the commonly used assay designed to directly measure HR failed to indicate any variation in the absence of LATS1 (Figure 4.9). The assay is designed to measure gene conversion events only and cannot detect other types of recombination (Pierce, Jasin et al. 1999). Due to the limitations of the method used, the involvement of LATS1 in HR could not be entirely excluded. As the HR did not appear to be affected despite differences in RAD51 foci, the most plausible explanation remaining was that the elevated DNA damage was occurring due to the improper stabilisation of RAD51 filament on the stalled, at IR-induced damage, fork that reversed into 'chicken foot' structure, was degraded and formed DNA breaks (see Section 1.3.6). If the LATS1-CDK2 regulation was specific to RAD51 at replication forks, this might explained why HR was not affected. However, as discussed above more comprehensive analysis would be required to exclude entirely

involvement of LATS1 in HR. The reports that describe the RAD51-dependent protection of the replication forks also highlight that CDK2 imparts a negative regulation of the stabilisation of the protective RAD51 filament (Esashi, Christ et al. 2005; Schlacher, Christ et al. 2011).Therefore, we reasoned that it may be this specific activity of CDK2 that LATS1 may be regulating. Taken together, in the absence of LATS1, CDK2 may restrict the RAD51 filament stabilisation on the regressed replication fork leading to an increased fork degradation, induction of breaks and thus elevated number of γH2AX (Figure 4.5). There might have been additional HR defects in LATS1 null cells that could contribute to the elevated damage, however these could not be discerned by an I-SCE1 assay. Nevertheless, the excessive damage in the absence of LATS1 after IR might have been potentially due to the degraded forks, which formed DNA breaks and therefore generated the G_2/M arrest.

.

Chapter 5:

The LATS1 Regulation of BRCA2 Phosphorylation

5.1 Introduction

In the previous chapters, we suggested that the LATS1-mediated control of the CDK2 activity may potentially be responsible for appropriate protection of the nascent DNA strand at the regressed fork in response to IR-induced damage. The absence of this mechanism allowed cells to accumulate damage through a failure to promote RAD51 foci, potentially indicating failure to stabilise a RAD51 filament and protect the stalled replication fork from degradation. Surprisingly, HR did not appear to be affected by the loss of LATS1, which suggested that the CDK2-mediated inhibition of the RAD51 filaments stabilisation at the stalled forks, might have been a source of the increased damage. The RAD51 filament established on the regressed fork protects the nascent DNA strand from Mre11-dependent degradation and because the replication fork exerts force on the DNA, the filament requires stabilisation. The stabilisation is utilised by the BRCA2 C-terminal domain, which role in HR is still controversial (Postow, Crisona et al. 2001; Schlacher, Christ et al. 2011; Mauro, Rego et al. 2012). Without the RAD51 filament stabilisation, these forks are degraded and form breaks, which may be responsible for the elevated γH2AX observed after IR (Figures 4.2, 4.3 and 4.4). Both CDK1 and CDK2 phosphorylate S3291 located within the C-terminus of BRCA2, abrogating the interaction with the RAD51 filament (Esashi, Christ et al. 2005; Schlacher, Christ et al. 2011). The results so far implied that, LATS1-CDK2 interaction might be functioning in the regulation of BRCA2 at the stalled replication forks (Figure 3.1).

5.2 The LATS1 Requirement for the RAD51 Foci Formation in Response to Fork Stalling

To test our hypothesis that LATS1 is involved in the regulation of BRCA2-dependent stabilisation of RAD51 filaments, we induced stalling of replication forks with hydroxyurea (Figure 5.1). Hydroxyurea is a drug, which reduces the synthesis of deoxyribonucleotides by inactivating ribonucleotide reductase. It forms a free radical nitroxide, which inhibits the active site of the enzyme (Yarbro 1992). The reduction of the deoxyribonucleotides pool causes a replication fork stalling, which can, after prolonged treatment i.e. 12 hrs, collapse into DSB (Saintigny, Delacote et al. 2001; Hanada, Budzowska et al. 2007; Schlacher, Christ et al. 2011). To induce fork stalling but not a collapse, U2OS cells were transfected with either siNT or siLATS1 and treated with 2 mM hydroxyurea for 10 hrs prior to the fixation. Statistics was based on approximately 1000 cells per condition and experiment was repeated three times. In response to the hydroxyurea treatment 40 % of the LATS1-deficient cells established more than 9 RAD51 foci per cell in comparison to 54 % of the control cells (Figure 5.1). This implied that the LATS1 regulation was important for RAD51 foci formation during the replication fork stalling.

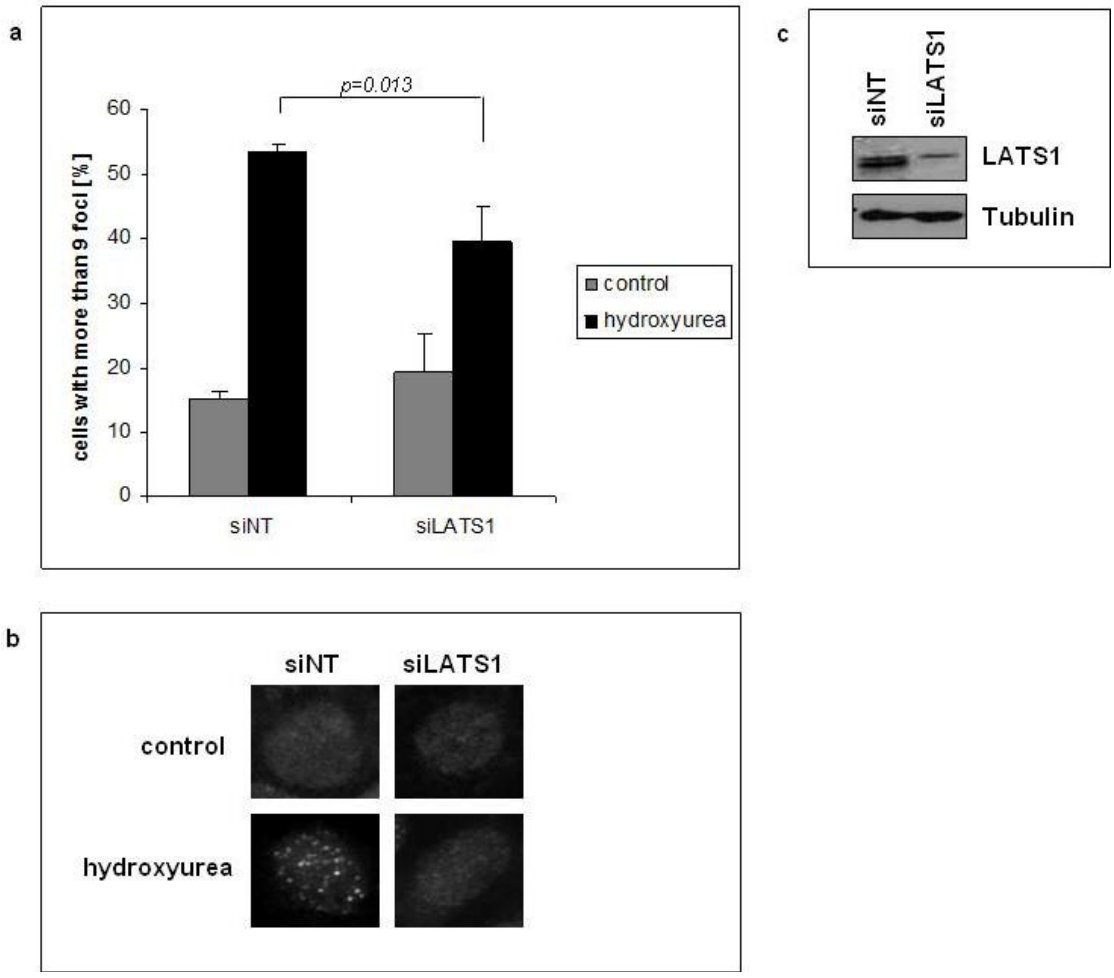


Figure 5.1 RAD51 Foci Formation Defects in the Absence of LATS1 in U2OS Cells Treated with Hydroxyurea. (a) Quantitation of cells exhibiting more than 9 RAD51 foci per cell. U2OS cells were cultured on cover slips and transfected with non-targeting (siNT) and siRNA against LATS1. 38 hrs post transfection, hydroxyurea was added to the cells to induce stalling of the replication forks. The cells were incubated for 10 hrs at 37 °C, after which the medium was changed with the normal culture medium. The samples labelled control were not treated with hydroxyurea. After incubation, the cells were fixed, probed with antibody against RAD51 and visualised with a secondary fluorescent antibody Alexa 488 and DAPI. Pictures were taken using Nikon 90i microscope with DAPI and FITC cubes. The cells were counted manually using ImageJ with 'cell count' plug-in installed. The cells with approximately more than 9 RAD51 foci were treated as positive cells and included in the statistics. **(b)** Representative pictures of cells with RAD51 foci. **(c)** The Western blot showing efficiency of LATS1 depletion.

5.3 The LATS1 Regulation of the CDK2 and BRCA2 Interaction

To test our hypothesis that the defects we observed in the RAD51 foci formation (see Section 4.5 and Figure 5.1) were due to the LATS1-dependent regulation of BRCA2, we determined the ability of CDK2 to associate with BRCA2 by IP. First, U2OS cells were cultured to 30 % confluence and transfected with either siNT or siLATS1 for 48 hrs and subsequently exposed to 4 Gy IR. In addition to that, *wt* and *Lats1*$^{-/-}$ MEFs were exposed to 10 Gy IR and similarly maintained for 4 hrs post IR. The cell lysates were immunoprecipitated using CDK1 or CDK2 antibodies conjugated to G Sepharose beads and analysed by western blot. In the unperturbed U2OS cells, CDK2 efficiently co-immunoprecipitated with BRCA2 and the association was lost upon the DNA damage, correlating with a requirement for the BRCA2 activity and less inhibitory phosphorylation upon the DNA damage (Figure 5.2) and (Esashi, Christ et al. 2005). Depletion of LATS1 did not dramatically affect the ability of CDK2 to associate with BRCA2, however, the interaction was maintained and failed to dissociate upon damage (Figure 5.2). This suggested that LATS1 was required to restrict the inhibitory association of CDK2 with BRCA2 in response to the DNA breaks. We did not detect an interaction between BRCA2 and CDK1 (data not shown), however, as mentioned above, this was likely due to the low number of cells in mitosis.

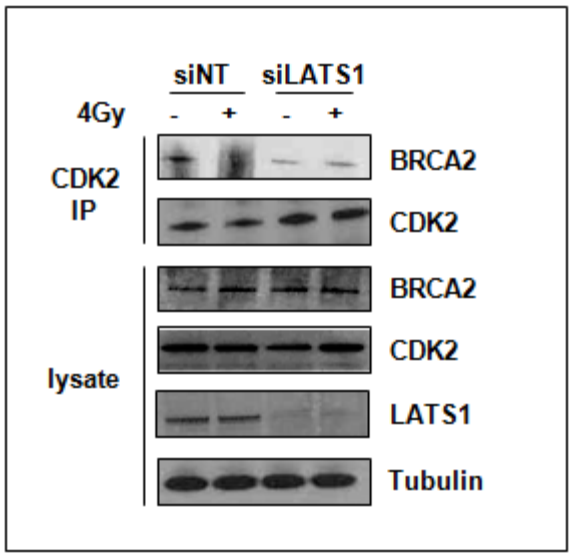


Figure 5.2 The Association Between BRCA2 and CDK2 is regulated in an IR-Dependent Manner and Depends on LATS1 in U2OS Cells. The Western blot analysis of CDK2 IP and lysate. U2OS cells were cultured to 30% confluence, transfected with either non-targeting (siNT) or siRNA against LATS1 (siLATS1), treated with 4 Gy IR and subsequently lysed 4 hrs post the DNA damage induction. The lysates were incubated with the CDK2 antibody conjugated to G Sepharose beads, western blotted and probed with the indicated antibodies. The interactions were visualised using Odyssey scanner (Li-cor).

We next wanted to confirm these results in *Lats1*$^{-/-}$ MEFs. In agreement with the results in the tumor cell lines (Figure 5.2), Brca2 co-immunoprecipitated with Cdk2 in the non-irradiated *wt* and *Lats1*$^{-/-}$ MEFs (Figure 5.3). The interaction between Brca2 and Cdk2 was lost after exposing the *wt* MEF to IR but was constitutive in *Lats1*$^{-/-}$ MEFs (Figure 5.3). Interestingly, the high level of association between Cdk2 and Brca2 appeared unusual to MEFs (Figure 5.3) since it was not observed in tumor cells of human origin (Figure 5.2). This might have been due to either a difference in the mouse vs. human regulatory system or alternatively, might have highlighted a variation between epithelial tumour cells and normal fibroblasts.

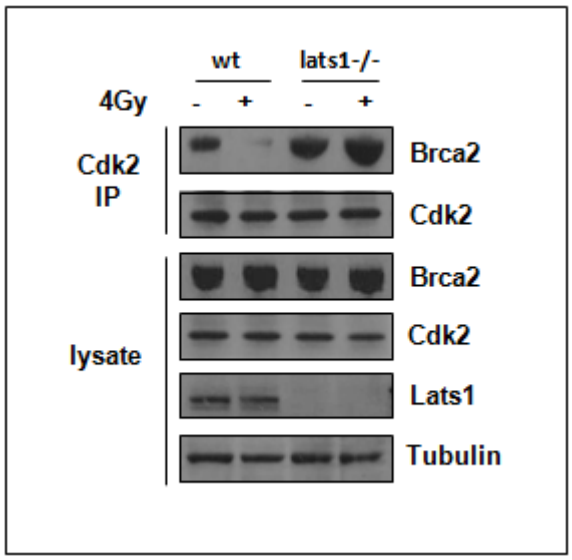


Figure 5.3 The Association Between Brca2 and Cdk2 is Regulated in an IR-Dependent Manner and Depends on LATS1 in MEFs. The Western blot analysis of Cdk2 IP and lysate. MEFs were cultured to 30% confluence, treated with 10 Gy IR and subsequently lysed 4 hrs post DNA the damage induction. The lysates were incubated with the Cdk2 antibody conjugated to G Sepharose beads, western blotted and probed with the indicated antibodies. The interactions were visualised using Odyssey scanner (Li-cor).

5.4 The BRCA2 Phosphorylation Increase in the Absence of LATS1

To confirm that the interaction between CDK2 and BRCA2 was determining phosphorylation of S3291-BRCA2, we utilised HT1080 cells, in which the regulation of BRCA2 phosphorylation by CDK was previously shown (Esashi, Christ et al. 2005). The unsynchronised HT1080 cells were transfected with siNT, siLATS1 or siLATS1 and reconstituted with a plasmid expressing hLATS1. The cell extracts were then analysed for levels of the CDK2-mediated phosphorylation site on BRCA2 by western blotting with a specific antibody directed against phospho-S3291-BRCA2 (^{P}S3291-BRCA2). As expected, the ^{P}S3291-BRCA2 was low in the control cells but substantially increased after LATS1 depletion. The overexpression of LATS1 reduced ^{P}S3291-BRCA2 to the level observed in HT1080 transfected with siNT (Figure 5.4).

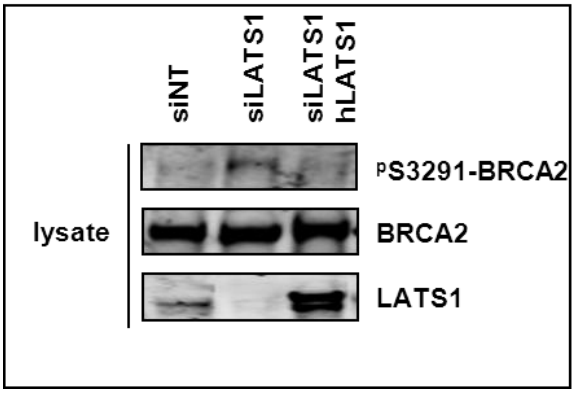


Figure 5.4 BRCA2 Increases the Phosphorylation on S3291 in the Absence of LATS1 in HT1080 Cells. The Western blot analysis of lysates for BRCA2 phosphorylation on S3291. HT1080 cells were cultured to 30 % confluence and transfected with either non-targeting (siNT) or siRNA against LATS1 (siLATS1). siLATS1 U2OS were transfected with hLATS1 48 hrs post siRNA treatment. The samples treated with siRNA were lysed 48 hrs post treatment and the cells reconstituted with hLATS1 24 hrs post transfection. The samples were western blotted, probed with indicated antibodies and visualised using Odyssey scanner (Li-cor).

5.5 The LATS1 Regulation of the DNA Damage-Induced Phosphorylation of BRCA2

S3291-BRCA2 has been described to be phosphorylated during mitosis and to be involved in the replication stress (see Section 1.3.6.3) and (Esashi, Christ et al. 2005; Schlacher, Christ et al. 2011). Having determined that the levels of ^{P}S3291-BRCA2 are higher in the absence of LATS1 (Figure 5.4), we next wanted to analyse whether the DNA damage activation of LATS1 was involved in the regulation. To test this, HT1080 cells were transfected with either siNT or siLATS1 in the presence or absence of hLATS1 and the level of ^{P}S3291-BRCA2 was determined by western blot. As observed in Figure 5.4, ^{P}S3291-BRCA2 was absent in the controls but readily detected in the lysates depleted of LATS1 and reduced to control levels in the cells transfected with

hLATS1. Additionaly, the results above suggested that the kinetics of LATS1-CDK2 interaction occured within 4 hrs of the DNA damage (Figure 3.1), therefore, we monitored the extent of ^{P}S3291-BRCA2 over a similar time course. In the cells that contained LATS1, we observed that the background levels of phosphorylation disappeared, while in the absence of LATS1, ^{P}S3291-BRCA persisted for much longer. Due to the effects on the cell cycle distribution outlined in Chapter 3, these results could be indicative of a varying extent of cells entering G_2/M. To verify whether ^{P}S3291-BRCA2 kinetics vary in a LATS1-dependent manner post IR, we took avantage of the fact that ^{P}S3291-BRCA2 was readily observed in nocodazole arrested (mitotic) cells due to the activity of CDK1 (Esashi, Christ et al. 2005). Furthermore, we have shown in Figure 3.1 that CDK1 is regulated in a LATS1-dependent manner. As expected, the cells blocked in mitosis upon treatment with nocodazole, exhibit higher levels of BRCA2 phosphorylation in comparison to the non-arrested cells (Figure 5.5). While phosphorylation of S3291-BRCA2 increased in the arrested cells, the absence of LATS1 exacerbated the overall levels of phosphorylation. Similarily to the results in the cycling cells, phosphorylation of BRCA2 decreased in mitotic cells exposed to IR in a LATS1-dependent manner (Figure 5.5). In the absence of LATS1, the unrestricted CDK1 activity led to constitutive phosphorylation of S3291-BRCA2 that remained even after 5 hours of IR, in striking contrast to the cells reconstituted with LATS1 (Figure 5.5). These observations confirmed that both the CDK1 and CDK2-mediated phosphorylation of BRCA2 was controlled by LATS1 in response to the DNA damage.

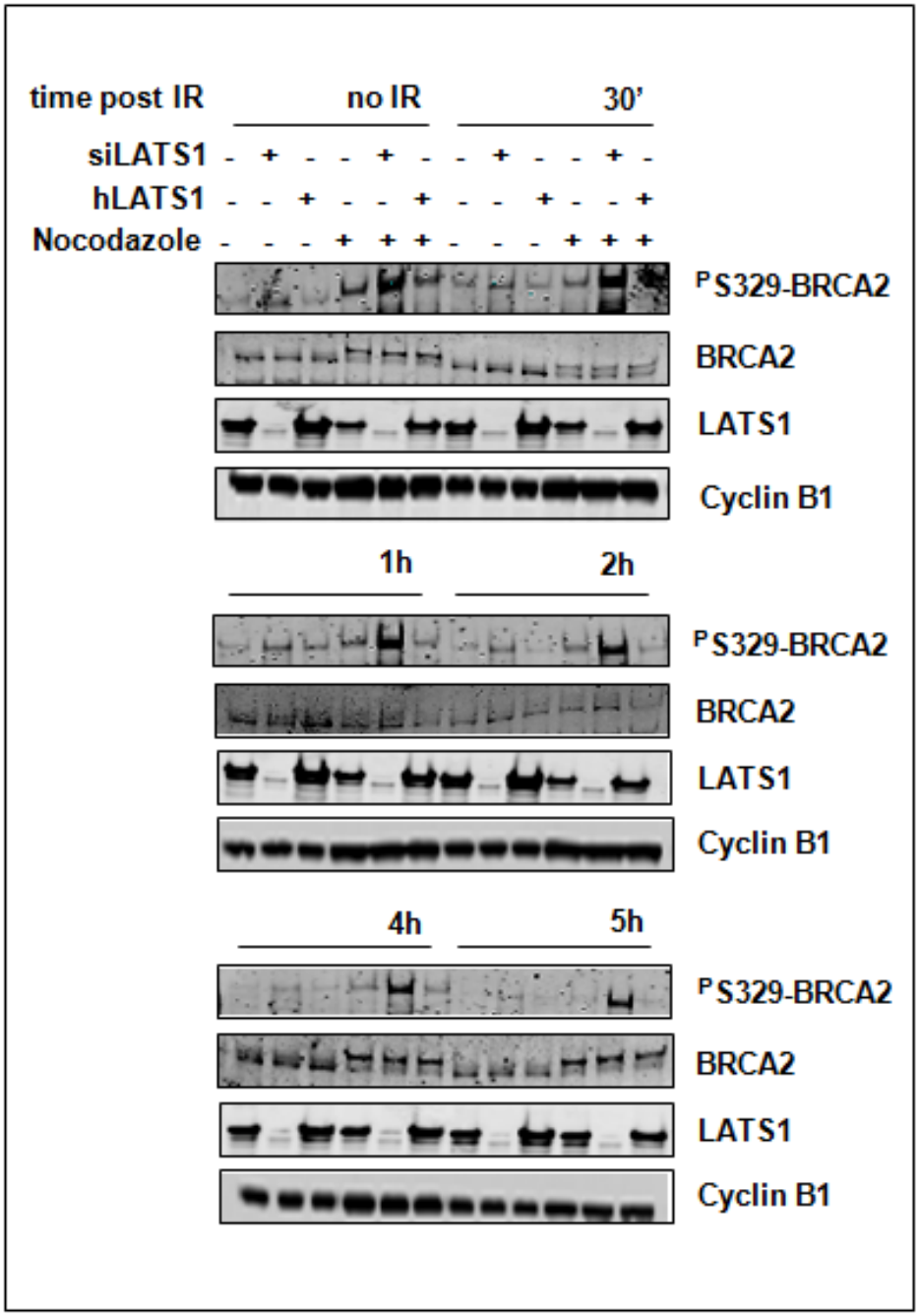


Figure 5.5 BRCA2 Maintains the Phosphorylation on S3291 in the Absence of LATS1 Post IR in HT1080 Cells. The Western blot analysis of lysates for BRCA2 phosphorylation on S3291 in irradiated cells. HT1080 cells were cultured to 30 % confluence and transfected with either siRNA against LATS1 (siLATS1) or hLATS1 plasmid. The cells were incubated with nocodazole 0.13 µM for 16 h prior to IR and lysed at indicated time points post 4 Gy treatment. The samples were western blotted and probed with the indicated antibodies.

5.6 Discussion

In Chapters 3 and 4, we suggested that the LATS1-mediated regulation of CDK2 played a role in limiting the IR-induced DNA damage. In Chapter 4 we proposed that LATS1 regulated a specific function of CDK2 that appeared to be required to promote a substantial fraction of RAD51 foci induced after IR. The LATS1-dependent regulation of RAD51 together with results from the comet assays, HR assay and the γH2AX foci, suggested the degraded replication forks as a potential source of the elevated damage. This led to our working hypothesis that the regulation of LATS1-CDK2 may be important to allow BRCA2 stabilisation of RAD51 filaments established on the reversed into 'chicken foot' structure replication forks, providing protection from degradation and subsequent DNA breaks. In this chapter, we verified that LATS1 plays an important role in promoting RAD51 foci in response to the enforced fork stalling by HU (Figure 5.1). We reasoned that these results agreed with the role of RAD51 on fork stability and might explain the excess damage in the absence of LATS1 that I observed above (Figures 4.2, 4.3, 4.4 and 4.5). Therefore, when replication fork encounters IR-induced lesion, it stalls and reverses into 'chicken foot' structure. The nascent DNA strand on regressed fork is potentially protected from degradation in a LATS1-dependent manner, until repair of DNA damage is finished. The proper regulation of the regressed forks protection limits pausing in G_2/M. BRCA2 is required to stabilise the RAD51 filaments on the regressed replication forks, an activity that is regulated by phosphorylation status of S3291 located at carboxyl terminal of the protein. CDK1/Cyclin B and CDK2/Cyclin A have been described to phosphorylate S3291-BRCA2 and ablate the ability to

interact with RAD51 (Esashi, Christ et al. 2005). In this chapter, we have shown that LATS1 regulated the CDK2-BRCA2 association and was responsible for restricting the phosphorylation of S3291-BRCA2 in response to the DNA damage. In MEFs, the Cdk2-Brca2 (mCDK2-mBRCA2) interaction was considerably stronger potentially due to the complete genetic ablation of LATS1 compared to the lower efficiency of siRNA (Figure 5.3). The ablation of LATS1 led to a constitutive association of CDK2 with BRCA2 and a persistence of ^{P}S3291-BRCA2 (Figures 5.2, 5.3, 5.4 and 5.5). Taken together, the data led to a hypothesis that in response to IR, LATS1 associates with CDK1 or CDK2 sequestering them from the partner cyclins (Figures 3.1 and 3.2), and subsequently leading to the reduction of ^{P}S3291-BRCA2 (Figure 5.5). This activation requirement implies that the proposed stalling of the replication forks may also promote the DNA damage signal that activates LATS1. DSB signalling via ATM has been described to activate LATS1, however, ATR displays a similar substrate activation and may also stimulate LATS1 indirectly, via RASSF1A, or directly by phosphorylation of LATS1 itself (Matsuoka, Ballif et al. 2007; Hamilton, Yee et al. 2009). ATR is activated by ssDNA at the stalled replication fork and may potentially explain the regulation in non-irradiated cells (see Section 1.3.3.3). There are likely to be additional factors that regulate CDK activity and as a result, ^{P}S3291-BRCA2, however it is tantalising to suggest that these may be regulatory events in the vicinity of the replication forks. Furthermore, the CDK-dependent phosphorylation of S3291 may additionally be reduced by phosphatases or in response to the DNA damage induced checkpoints, which are known to inhibit the activity of

CDKs and may also be involved at the stalled replication forks (Falck, Mailand et al. 2001).

Chapter 6:
General Discussion

This thesis describes the involvement of LATS1 in the DNA damage signalling. We identified a novel pathway, through which LATS1 regulates the phosphorylation of carboxyl-terminus of BRCA2 in response to IR. The involvement of LATS1 in the DNA damage repair was first suggested in genome-wide ATM and ATR substrate analysis. The depletion of LATS1 led to defects in the DNA damage repair, elevated levels of γH2AX post damage and impaired G_2/M and intra-S checkpoints after IR (Matsuoka, Ballif et al. 2007). Recent studies have revealed that ATM signalling can activate LATS1 via a cascade through RASSF1A and MST2 and engage YAP1 in the stabilisation of p73 in response to the DNA damaging factors: exposure to IR or cisplatin treatment (Hamilton, Yee et al. 2009). Additionally, LATS1 can be induced by MST2 in response to cell-cell contact leading to cytoplasmic sequestration of YAP and the subsequent restriction of the cell proliferation. LATS1 is also phosphorylated in a cell-cycle-dependent manner and specifically associates with CDC2 (CDK1) in early mitosis, although no regulation of the interaction has been observed. This interaction sequesters CDK1, blocking the Cyclin A binding and prevents the G_2/M transition (Tao, Zhang et al. 1999; Xia, Qi et al. 2002). We demonstrated that LATS1 associated specifically with CDK1 and CDK2, but not with CDK3 in response to either IR or in confluent cultures (Figures 3.1 and 3.2). We did not observe a cyclin binding while CDK was co-immunoprecipitated with LATS1, suggesting that LATS1 might have restricted the kinase activity of CDKs (Figure 3.2). Additionally, we showed that this interaction might have not been required shortly after the DNA damage (Figure 3.2). Our data is not in conflict with previous reports since similarly to Tao *et.al.,* we did not observe an

interaction between LATS1 and CDK2 (nor CDK1) in the absence of IR (Figure 3.1) and (Tao, Zhang et al. 1999). We additionally recorded that in the absence of LATS1, the cells displayed lower G_1 and elevated S-phase in response to IR (Figures 3.4, 3.5, 3.6, 3.7 and 3.9). This suggested that LATS1 may be involved in the regulation of G_1/S boundary through the modulation of CDK2/Cyclin E, restricting the S-phase entry in response to the DNA damage, attributed initially to LATS2 (Figures 3.1, 3.2, 3.7 and 3.9) and (Li, Pei et al. 2003). Alternatively, the faster progression of cells from G_1 to the S-phase in LATS1-depleted cells may be credited to the absence of LATS1 proteolytic fragments generated by Omi, which act as inhibitors of the G_1/S transition (Kuninaka, Iida et al. 2007). Finally, LATS1 may be involved in a mechanism similar to LATS2, silencing E2F target genes through the modulation of the DREAM complex (Kuninaka, Iida et al. 2007; Tschop, Conery et al. 2011). Interestingly, cells, which violated the G_1/S boundary and increased in the S-phase population in the absence of LATS1, accumulated in the G_2/M phase after IR (Figures 3.4, 3.6, 3.7 and 3.9). According to previous reports, LATS1 induces the G_2/M checkpoint through the restriction of the kinase activity of CDK1 (Xia, Qi et al. 2002). Our data showed, however, an exacerbated G_2/M arrest in the absence of LATS1, suggesting that the checkpoint does not fully depend on the association of LATS1 with CDK1 and was properly activated in response to the DNA damage. Moreover, we observed accumulation of cell deficient in LATS1 in the S-phase. We excluded involvement of the LATS1-dependent regulation of CDK2 in the context of the intra-S checkpoint because although LATS1 is a target of ATM signalling, its absence led to the accumulation of cells in the S-phase, unlike cells with mutations in the

proteins involved in the regulation (Young and Painter 1989; Falck, Petrini et al. 2002; Yazdi, Wang et al. 2002; Matsuoka, Ballif et al. 2007; Hamilton, Yee et al. 2009). Furthermore, LATS1 interacted with CDK2 and restricted cyclin binding in response to IR (Figures 3.1 and 3.2) This however, was not synonymous with the inhibitory effects of Chk1/2 on CDK2/Cyclin E in response to IR during the S-phase because depletion of LATS1 resulted in a higher proportion of cells in S-phase (Figures 3.1, 3.2, 3.7, 3.8 and 3.9) and (Falck, Petrini et al. 2002). Therefore, we reasoned that the variation in response of the irradiated cells could be attributed to LATS1 restricting the CDK2 activity during the S-phase leading to defective DNA damage repair. We next confirmed that the cells depleted of LATS1 were indeed less efficient at repairing the DNA damage and reasoned that this was the main cause of the G_2/M arrest (Figures 3.4, 3.6 and 4.1). Furthermore, our data indicated elevated levels of γH2AX in the absence of LATS1, which were synonymous with either DNA damage or replication defects (Figures 4.2, 4.3, 4.4 and 4.5) and (Rogakou, Pilch et al. 1998; Ward and Chen 2001; Sirbu, Couch et al. 2011). The H2AX histones are phosphorylated by either ATM or ATR in response to the DNA double strand breaks or the replication fork stalling respectively (Burma, Chen et al. 2001; Stucki, Clapperton et al. 2005). When the stress is resolved, the phosphorylation on the histones is removed by phosphatase 2A (PP2A) (Chowdhury, Keogh et al. 2005; Kim, Minter-Dykhouse et al. 2006); (Sirbu, Couch et al. 2011). In line with a failure to resolve the γH2AX phosphorylation, we observed defects in the RAD51 foci formation in the absence of LATS1 (Figures 4.6, 4.7 and 4.8). The RAD51 proteins are involved in the processing of DSB through HR and according to

recent studies, also protect from nucleolytic degradation the nascent DNA strand at the regressed replication fork (Esashi, Galkin et al. 2007; San Filippo, Sung et al. 2008; Schlacher, Christ et al. 2011). Our data revealed that the RAD51 defects did not translate into an impairment of the homologous recombination, suggesting a role of LATS1 in the RAD51 filament stabilisation at the stalled replication fork (Figure 4.9) and (Petermann, Orta et al. 2010; Schlacher, Christ et al. 2011). Our hypothesis was further confirmed by observation of the RAD51 foci defects as being important during the replication stalling (Figure 5.1). The replication fork stalls and reverses into a 'chicken foot' structure when it encounters the DNA damage. After the lesion is bypassed, the fork is restored and the replication continues (Bugreev, Rossi et al. 2011); (Lambert, Froget et al. 2007; Budzowska and Kanaar 2009). The nascent DNA strand of the regressed fork is coated with RAD51 filament. Once established, the RAD51 filament is stabilised by carboxyl-terminal of BRCA2 and protects the nascent DNA strand from Mre11-dependent degradation and subsequent breaks and chromosomal instability (Lomonosov, Anand et al. 2003; Esashi, Christ et al. 2005; Esashi, Galkin et al. 2007; Schlacher, Christ et al. 2011). Therefore, the absence of LATS1 appears to leave cells accumulating damage potentially indicating failure to stabilise the RAD51 filament at the regressed replication fork. This leads to the fork degradation, increase in DNA damage and subsequent G_2/M arrest. The phosphorylation of S3291 located within the C-terminus of BRCA2 is regulated in a cell cycle-dependent manner or in response to IR (Figure 5.5) and (Esashi, Christ et al. 2005; Schlacher, Christ et al. 2011). Both CDK1/Cyclin B and CDK2/Cyclin A phosphorylate S3291 on

BRCA2, abrogating the interaction with RAD51 filament (Esashi, Christ et al. 2005; Schlacher, Christ et al. 2011). We reasoned that LATS1 may regulate the BRCA2 phosphorylation by controlling the CDK2 kinase activity. This is due to two reasons. First, the ablation of LATS1 increased phosphorylation on BRCA2 (Figures 5.4 and 5.5). Second, in the absence of LATS1, CDK2 failed to dissociate from BRCA2 in response to IR (Figures 5.2 and 5.3). In theory, the absence of LATS1-dependent protection of the regressed replication fork, would lead to deleterious consequences even in non-irradiated cells where the fork encounters spontaneous DNA damage (Lomonosov, Anand et al. 2003; Schlacher, Christ et al. 2011). We did not notice, however, genomic instability in LATS1 negative cells, which led to conclusion that LATS1-dependent regulation of phosphorylation of S3291-BRCA2 may be supported by an alternative pathway (Appendix S1). This idea was further supported by the decrease of ^{P}S3291-BRCA2 5 hrs post IR in the absence of LATS1 (Figure 5.5). It is possible that in the absence of LATS1, S3291-BRCA2 is dephosphorylated by phosphatase or is regulated in response to Chk1/2 signalling, which also restricts CDKs. In addition to that, it was recently suggested that phosphorylation status of BRCA2 C-terminus may be regulated by p21 in response to DNA damage (Falck, Mailand et al. 2001; Esashi, Christ et al. 2005; Mauro, Rego et al. 2012). The hypothesis put forward in this thesis may also help to explain the observed S-phase accumulation of cells deficient in LATS1 in response to IR (Figures 3.7 and 3.9). In line with this idea, the accumulation may be associated with replication defects of the fork, which encounters the DNA damage created directly in the S-phase by IR or because of the DNA damage inherited from

G_1 phase due to the impaired G_1/S checkpoint (Figures 3.4, 3.5 and 3.6). Defects in the LATS1 signalling may deplete the ability of BRCA2 to protect the genomic stability and give rise to aberrations during the replication, including quadriradial chromosomes and chromatid breaks. These may be a challenge for the repair mechanism and could lead to persistent damage and the subsequent G_2/M arrest (Patel, Yu et al. 1998; Scully and Livingston 2000). Those structures may contribute towards the production of gross chromosomal rearrangements (GCR) including translocations or deletions leading to carcinogenesis (Yu, Koehler et al. 2000). Moreover, the absence of LATS1 expression decreases the YAP-dependent apoptosis leaving the organism with reduced ability to remove cells with extensive DNA damage (O'Neill, Rushworth et al. 2004; O'Neill and Kolch 2005; Matallanas, Romano et al. 2007). Therefore, the regulation described in this thesis may guard chromosome integrity and be indispensable for the carcinogenesis prevention. The low expression of LATS1 or the defects in LATS1 activation may be valid markers for cancer predispositions. Patients with a low expression of LATS1 or with RASSF1A polymorphism may not be treated with drugs, which exploit defects in the DSB repair, including PARP inhibitors. This is due to the fact that LATS1 may not be required for the HR-dependent activity of BRCA2 and this treatment would potentially be ineffective. Furthermore, therapeutics, which increase the regression of the replication fork may not be a treatment possibility as cancer cells, in which LATS1 expression is depleted, would produce extensive DNA damage due to the degraded forks. This would however contribute towards mutations since cells with depleted ability to stabilise RAD51 filament do not lose viability (Schlacher, Christ et al. 2011).

LATS1 is involved in stabilisation of p73 through the activation of YAP. The LATS1-dependent activation of YAP and the subsequent apoptosis is stimulated, similarly to stabilisation of the RAD51 filament on the regressed replication fork, by ATM. This raises an interesting question of how the cell balances the fork stabilisation vs. the apoptosis activation and may be a direction of future research.

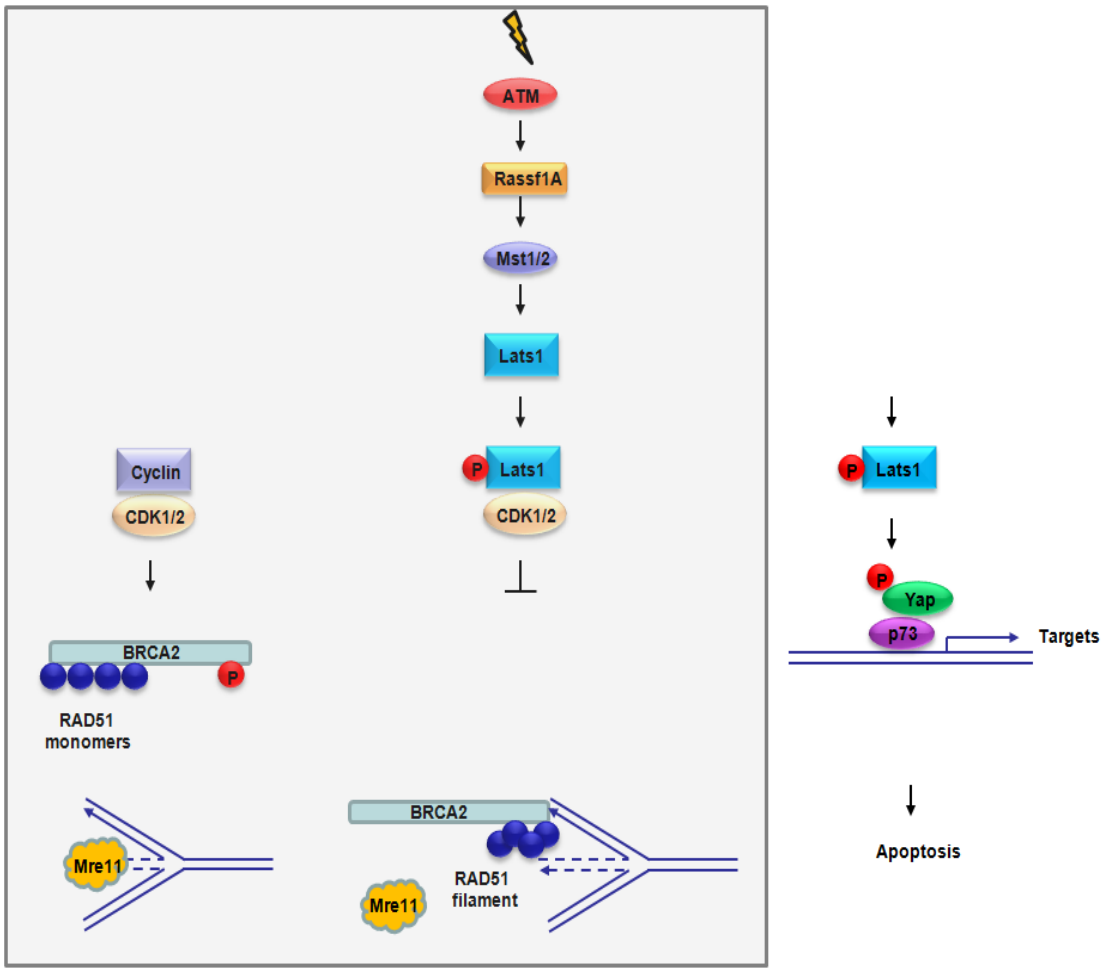
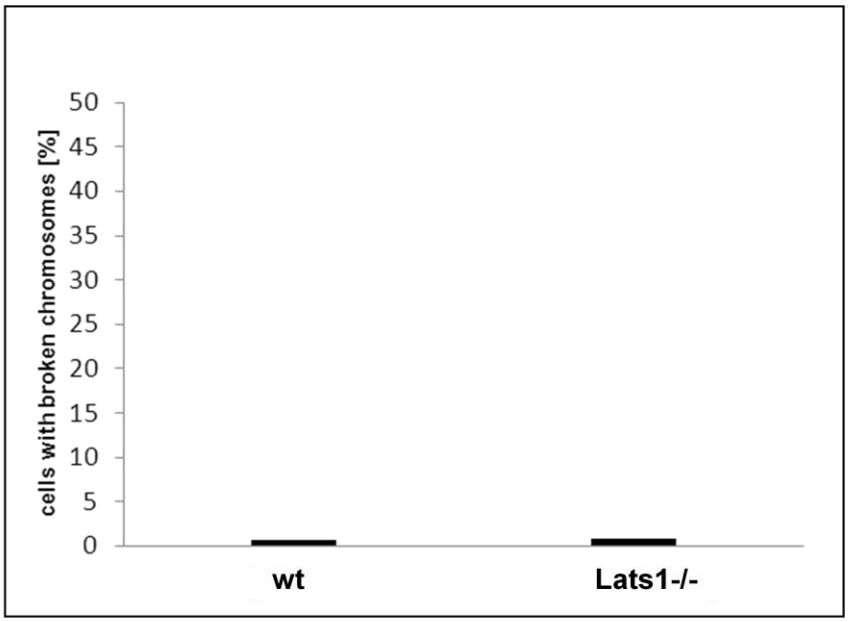


Figure 6.1 The Role of LATS1 in DNA damage signalling. In response to IR, LATS1 associates with CDKs and inhibits phosphorylation of S3291 located within C-terminus of BRCA2. BRCA2 stabilises RAD51 filament established on the stalled fork, which has reversed into 'chicken foot' structure. The stabilised filament protects nascent DNA strand on the regressed fork from Mre11-dependent degradation and subsequent breaks and radial chromosome structures.

Appendices

Appendix 1: Metaphase Spread



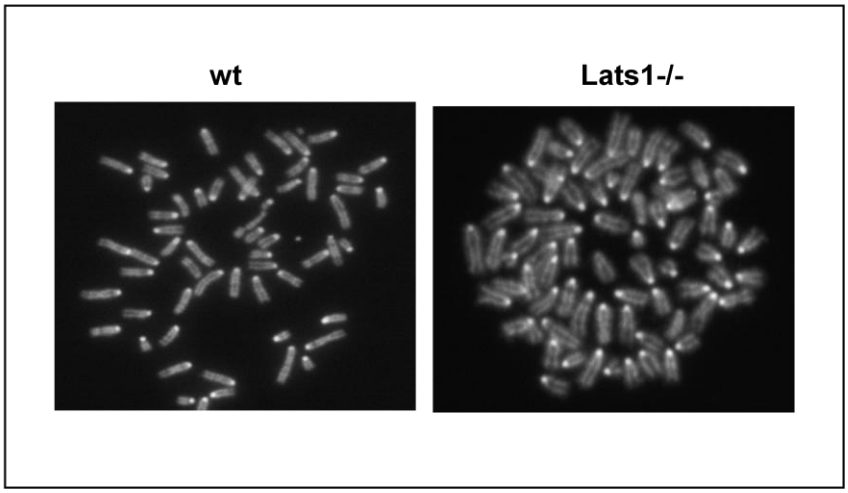


Figure S1. Cells Do Not Exhibit Genomic Instability in the Absence of LATS1. Metaphase spread analysis of MEFs. Both wt and Lats1-/- MEFs were cultured in 10 cm dishes and passaged 8 times prior to the collection. The cells were cultured to reach 80% confluence. The samples were first treated with 5 µM KaryoMAX Colcemid Solution for 16 hrs and then incubated in hypotonic buffer for 25 min in 37 °C. The samples were fixed in ice cold ethanol and spread over a glass slide. The chromosomes were stained with DAPI and observed using Nikon 90i microscope.

Appendix 2: Identification of Novel LATS1 Binding Partners

We undertook a proteomic screen to find novel binding partners that associate with LATS1 in response to IR. To identify the LATS1 co-immunoprecipitating proteins, the U2OS cells were transfected with a control plasmid or myc-tagged hLATS1 and exposed to 4 Gy IR. The lysates were prepared and incubated with a specific myc-tag antibody and the immunoprecipitates were eluted from beads with a pH gradient elution. Subsequently, the eluted proteins were separated by SDS-PAGE and visualised by staining with colloidal coomassie blue to reveal the LATS1 co-immunoprecipitating proteins. The protein bands that appear distinct to the myc-LATS1 were deemed as potential LATS1 binding proteins. Any further distinction in the pattern of banding when the cells are exposed to IR was noted and interpreted as potential DNA damage candidates. These gel bands were excised from the gel and subsequently analysed by mass spectrometry. The resulting peptides were identified using the automated peptide identification software, MASCOT (Matrix science, Boston, MA). The mass spectrometric identification of LATS1 binding partners was performed by Dr. Hamilton. The analysis of twenty three bands reveals three hits: p54(nrb), PSF and MATR3 with significant MOWSE scores of 577, 481 and 112 respectively. LATS1 interacted with all three proteins and the interaction was lost upon irradiation (Figure S2). The most significant interaction with LATS1 was attributed to p54 (nrb) as confirmed by MOWSE score 577. To validate the association, and to determine whether IR regulates the interaction we performed LATS1 IP and checked for association of p54 (nrb) by western blot. The U2OS cells were irradiated with 4 Gy and lysed at the indicated time points post IR. LATS1

interacted with p54 (nrb) in the non-irradiated samples and this interaction was maintained immediately after IR. The interaction of LATS1 and p54 (nrb) was lost 1 h post exposure to IR but recovered from 2 hrs after the treatment (Figure S3). Together, p54 (nrb), PSF and MATR3 form a complex which is recruited to the DNA damage site immediately after the DNA damage induction and is removed completely after 20 min post treatment (Salton, Lerenthal et al. 2010). The ablation of p54(nrb) leads to persistence of DNA damage, a decrease in the clonogenic survival and an increase in the chromosomal aberrations (Li, Kuhne et al. 2009). The p54(nrb)/PSF complex is involved in NHEJ and it interacts with Ku heterodimer to establish a functional pre-ligation complex with the DNA substrate (Bladen, Udayakumar et al. 2005). In addition to that, p54 (nrb) and PSF co-immunoprecipitate with RAD51D. Furthermore, PST binds to RAD51 and modulate its homologous-pairing and strand-exchange activity (Rajesh, Gruver et al. 2009; Morozumi, Takizawa et al. 2009). The significance of the interaction between LATS1 and p54(nrb) has not been yet identified. However, the time correlation between dissociation of CDKs and p54(nrb) from LATS1 suggests that hypothetically the interaction may be involved in the RAD51 filament stabilisation and may be interesting direction of future research.

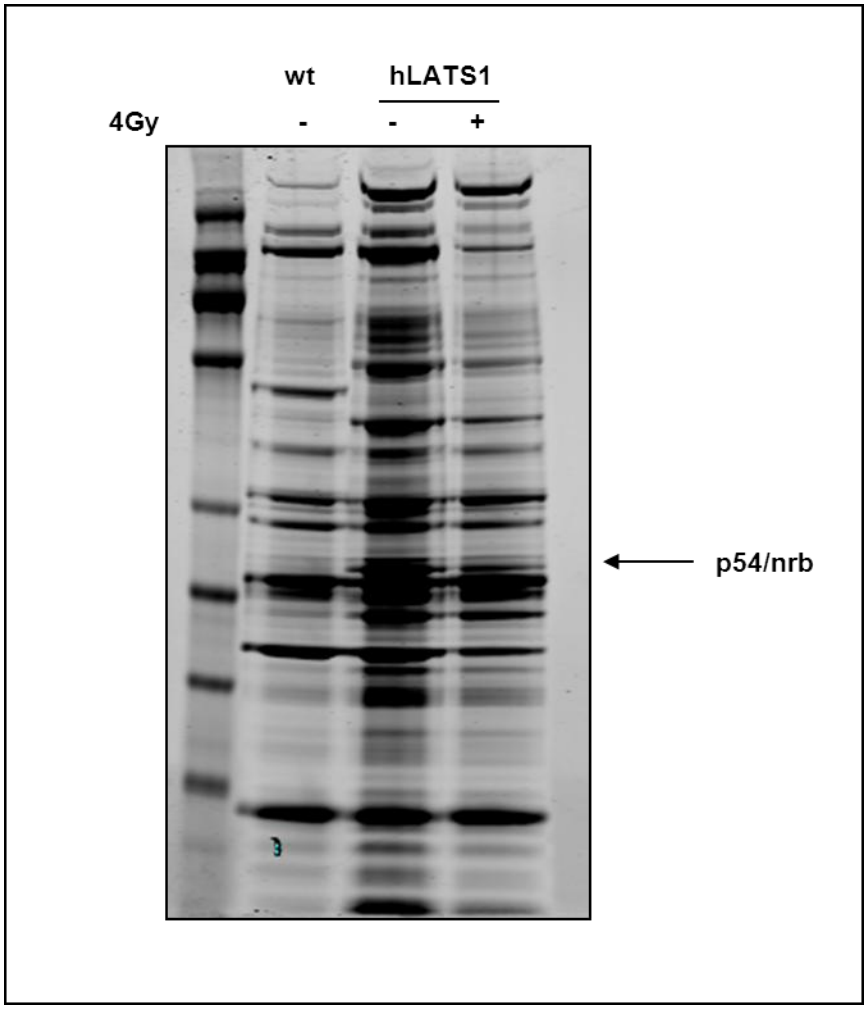


Figure S2. Proteomic Screen for LATS1 Binding Partners. HeLa cells were transfected with hLATS1 and lysed 24 hrs afterwards. Wt were not transfected with any plasmid or irradiated. hLATS1 HeLa were irradiated with 4 Gy and lysed 1 h post radiation treatment. The lysates were immunoprecipitated with LATS1 antibody conjugated to G Sepharose beads and eluted with a pH gradient. The samples were loaded onto a gel and electrophoresis was performed. The gel was stained with colloidal coomassie blue. The difference in banding pattern was observed and selected bands were excised and analysed using mass spectrometry.

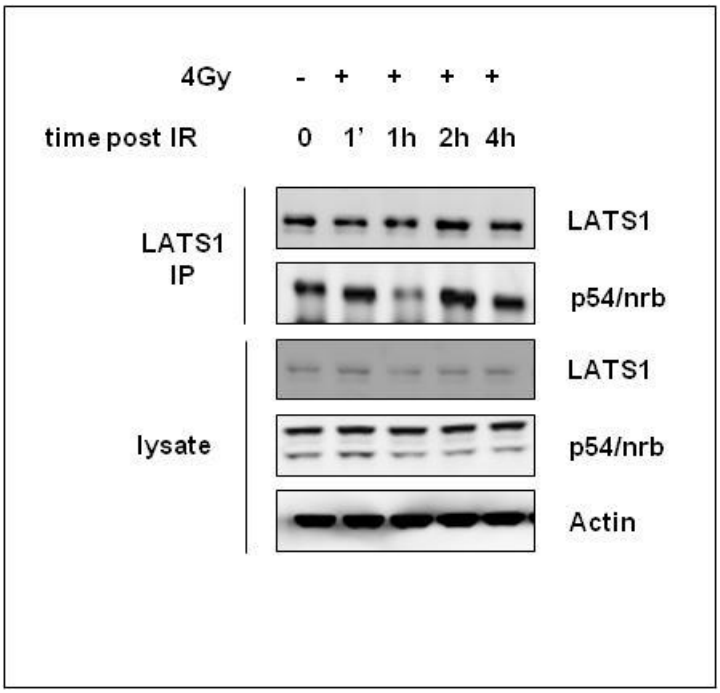


Figure S3. LATS1 Associates with P54 (nrb) in IR-Dependent Manner. The Western blot analysis of LATS1 IP and lysate. U2OS cells were irradiated with 4 Gy and lysed at the indicated time points post IR. The lysates were immunoprecipitated with the LATS1 antibody conjugated to G Sepharose beads. The samples were western blotted and probed with the indicated antibodies. The interaction was visualised using Odyssey scanner (Li-cor).

References

Agathanggelou, A., W. N. Cooper, et al. (2005). "Role of the Ras-association domain family 1 tumor suppressor gene in human cancers." Cancer Res **65**(9): 3497-3508.

Amano, T., N. Kaji, et al. (2002). "Mitosis-specific activation of LIM motif-containing protein kinase and roles of cofilin phosphorylation and dephosphorylation in mitosis." J Biol Chem **277**(24): 22093-22102.

Antony, E., E. J. Tomko, et al. (2009). "Srs2 disassembles Rad51 filaments by a protein-protein interaction triggering ATP turnover and dissociation of Rad51 from DNA." Mol Cell **35**(1):105-15.

Aplin, A. E., A. Howe, et al. (1998). "Signal transduction and signal modulation by cell adhesion receptors: the role of integrins, cadherins, immunoglobulin-cell adhesion molecules, and selectins." Pharmacol Rev **50**(2): 197-263.

Avruch, J., A. Khokhlatchev, et al. (2001). "Ras activation of the Raf kinase: tyrosine kinase recruitment of the MAP kinase cascade." Recent Prog Horm Res **56**: 127-155.

Aylon, Y., D. Michael, et al. (2006). "A positive feedback loop between the p53 and Lats2 tumor suppressors prevents tetraploidization." Genes Dev **20**(19):2687-700.

Aylon, Y., Y. Ofir-Rosenfeld, et al. (2010). "The Lats2 tumor suppressor augments p53-mediated apoptosis by promoting the nuclear proapoptotic function of ASPP1." Genes Dev **24**(21):2420-9.

Ayoub, N., E. Rajendra, et al. (2009). "The carboxyl terminus of Brca2 links the disassembly of Rad51 complexes to mitotic entry." Curr Biol **19**(13): 1075-1085.

Badouel, C., L. Gardano, et al. (2009). "The FERM-domain protein Expanded regulates Hippo pathway activity via direct interactions with the transcriptional activator Yorkie." Dev Cell **16**(3): 411-420.

Bakkenist, C. J. and M. B. Kastan (2003). "DNA damage activates ATM through intermolecular autophosphorylation and dimer dissociation." Nature **421**(6922): 499-506.

Ballif, B.A., J. Blenis (2001). “Molecular mechanisms mediating mammalian mitogen-activated protein kinase (MAPK) kinase (MEK)-MAPK cell survival signals.” Cell Growth Differ **12**(8):397-408.

Bartek, J., C. Lukas, et al. (2004). "Checking on DNA damage in S phase." Nat Rev Mol Cell Biol **5**(10): 792-804.

Basu, S., N. F. Totty, et al. (2003). "Akt phosphorylates the Yes-associated protein, YAP, to induce interaction with 14-3-3 and attenuation of p73-mediated apoptosis." Mol Cell **11**(1): 11-23.

Batty, D. P. and R. D. Wood (2000). "Damage recognition in nucleotide excision repair of DNA." Gene **241**(2): 193-204.

Baumgartner, R., I. Poernbacher, et al. (2010). "The WW domain protein Kibra acts upstream of Hippo in Drosophila." Dev Cell **18**(2): 309-316.

Bell, S. P. and B. Stillman (1992). "ATP-dependent recognition of eukaryotic origins of DNA replication by a multiprotein complex." Nature **357**(6374): 128-134.

Bennett, F. C. and K. F. Harvey (2006). "Fat cadherin modulates organ size in Drosophila via the Salvador/Warts/Hippo signaling pathway." Curr Biol **16**(21): 2101-2110.

Berkovich, E., R. J. Monnat, Jr., et al. (2007). "Roles of ATM and NBS1 in chromatin structure modulation and DNA double-strand break repair." Nat Cell Biol **9**(6): 683-690.

Bichsel, S. J., R. Tamaskovic, et al. (2004). "Mechanism of activation of NDR (nuclear Dbf2-related) protein kinase by the hMOB1 protein." J Biol Chem **279**(34): 35228-35235.

Bishop, J. M. (1991). "Molecular themes in oncogenesis." Cell **64**(2): 235-248.

Bladen, C. L., D. Udayakumar, et al. (2005). "Identification of the polypyrimidine tract binding protein-associated splicing factor.p54(nrb) complex as a candidate DNA double-strand break rejoining factor." J Biol Chem **280**(7): 5205-5210.

Blandino, G., Y. Shau, et al. (2009). “The Hippo tumor suppressor pathway: a brainstorming workshop.” Sci Signal **2**(95):mr6.

Block, W. D., Y. Yu, et al. (2004). "Autophosphorylation-dependent remodeling of the DNA-dependent protein kinase catalytic subunit regulates ligation of DNA ends." Nucleic Acids Res **32**(14): 4351-4357.

Bochkareva, E., S. Korolev, et al. (2002). "Structure of the RPA trimerization core and its role in the multistep DNA-binding mechanism of RPA." EMBO J **21**(7): 1855-1863.

Bonni, A., A. Brunet, et al. (1999). “Cell survival promoted by the Ras-MAPK signalling pathway by transcription-dependent and –independent mechanisms,” Science **286**(5443):1358-62.

Born, T. L., J. A. Frost, et al. (1994). "c-Myc cooperates with activated Ras to induce the cdc2 promoter." Mol Cell Biol **14**(9): 5710-5718.

Bothos, J., R. L. Tuttle, et al. (2005). "Human LATS1 is a mitotic exit network kinase." Cancer Res **65**(15): 6568-6575.

Braun, K., G. Holzl, et al. (1998). "Investigation of the cell cycle regulation of cdk3-associated kinase activity and the role of cdk3 in proliferation and transformation." Oncogene **17**(17): 2259-2269.

Bryant, P. J., B. Huettner, et al. (1988). "Mutations at the fat locus interfere with cell proliferation control and epithelial morphogenesis in Drosophila." Dev Biol **129**(2): 541-554.

Budzowska, M. and R. Kanaar (2009). "Mechanisms of dealing with DNA damage-induced replication problems." Cell Biochem Biophys **53**(1): 17-31.

Bugreev, D. V., O. M. Mazina, et al. (2006). "Rad54 protein promotes branch migration of Holliday junctions." Nature **442**(7102): 590-593.

Bugreev, D. V., M. J. Rossi, et al. (2011). "Cooperation of RAD51 and RAD54 in regression of a model replication fork." Nucleic Acids Res **39**(6): 2153-2164.

Bugreev, D. V, X. Yu, et al. (2007). “Novel pro- and anti- recombination activities of the Bloom’s syndrome helicase.” Genes Dev **21**(23):3085-94.

Burma, S., B. P. Chen, et al. (2001). "ATM phosphorylates histone H2AX in response to DNA double-strand breaks." J Biol Chem **276**(45): 42462-42467.

Burtelow, M. A., P. M. Roos-Mattjus, et al. (2001). "Reconstitution and molecular analysis of the hRad9-hHus1-hRad1 (9-1-1) DNA damage responsive checkpoint complex." J Biol Chem **276**(28): 25903-25909.

Busino, L., M. Donzelli, et al. (2003). "Degradation of Cdc25A by beta-TrCP during S phase and in response to DNA damage." Nature **426**(6962): 87-91.

Carnero, A. and G. J. Hannon (1998). "The INK4 family of CDK inhibitors." Curr Top Microbiol Immunol **227**: 43-55.

Carreira, A., J. Hilario, et al. (2009). "The BRC repeats of BRCA2 modulate the DNA-binding selectivity of RAD51." Cell **136**(6): 1032-1043.

Chan, E. H., M. Nousiainen, et al. (2005). "The Ste20-like kinase Mst2 activates the human large tumor suppressor kinase Lats1." Oncogene **24**(12): 2076-2086.

Chappell, C., L. A. Hanakahi, et al. (2002). "Involvement of human polynucleotide kinase in double-strand break repair by non-homologous end joining." EMBO J **21**(11): 2827-2832.

Chastain, P. D., 2nd, T. P. Heffernan, et al. (2006). "Checkpoint regulation of replication dynamics in UV-irradiated human cells." Cell Cycle **5**(18): 2160-2167.

Chen, L., P.G. Loh, et al. (2010). “Structural and functional insights into the TEAD-YAP complex in the Hippo signalling pathway.” Protein Cell **1**(12):1073-83.

Chen, X.B, R. Melchionna, et al. (2001). “Human Mus81-associated endonuclease cleaves Holliday junctions in vitro.” Mol Cell **8**(5):1117-27.

Chen, L., C. J. Nievera, et al. (2008). "Cell cycle-dependent complex formation of BRCA1.CtIP.MRN is important for DNA double-strand break repair." J Biol Chem **283**(12): 7713-7720.

Cheng, W. H., C. von Kobbe, et al. (2004). "Linkage between Werner syndrome protein and the Mre11 complex via Nbs1." J Biol Chem **279**(20): 21169-21176.

Chini, C. C. and J. Chen (2003). "Human claspin is required for replication checkpoint control." J Biol Chem **278**(32): 30057-30062.

Cho, E., Y. Feng, et al. (2006). "Delineation of a Fat tumor suppressor pathway." Nat Genet **38**(10): 1142-1150.

Chow, A., Y. Hao, et al. (2010). "Molecular characterization of human homologs of yeast MOB1." Int J Cancer **126**(9): 2079-2089.

Chowdhury, D., M. C. Keogh, et al. (2005). "gamma-H2AX dephosphorylation by protein phosphatase 2A facilitates DNA double-strand break repair." Mol Cell **20**(5): 801-809.

Ciccia, A., A. Constantinou, et al. (2003). "Identification and characterization of the human mus81-eme1 endonuclease." J Biol Chem **278**(27): 25172-25178.

Clark, H. F., D. Brentrup, et al. (1995). "Dachsous encodes a member of the cadherin superfamily that controls imaginal disc morphogenesis in Drosophila." Genes Dev **9**(12): 1530-1542.

Comings, D. E. (1973). "A general theory of carcinogenesis." Proc Natl Acad Sci U S A **70**(12): 3324-3328.

Cooper, J. A. and B. Howell (1993). "The when and how of Src regulation." Cell **73**(6): 1051-1054.

Creasy, C. L. and J. Chernoff (1995). "Cloning and characterization of a human protein kinase with homology to Ste20." J Biol Chem **270**(37): 21695-21700.

Creasy, C. L. and J. Chernoff (1995). "Cloning and characterization of a member of the MST subfamily of Ste20-like kinases." Gene **167**(1-2): 303-306.

Dahm, K. (2007). "Functions and regulation of human artemis in double strand break repair." J Cell Biochem **100**(6): 1346-1351.

Daksis, J. I., R. Y. Lu, et al. (1994). "Myc induces cyclin D1 expression in the absence of de novo protein synthesis and links mitogen-stimulated signal transduction to the cell cycle." Oncogene **9**(12): 3635-3645.

Davies, O.R., L. Pellegrini (2007). "Interaction with the BRCA2 C terminus protects RAD51-DNA filaments from disassembly by BRC repeats." Nat Struct Mol Biol **14**(6):475-83.

de Jager, M., J. van Noort, et al. (2001). "Human Rad50/Mre11 is a flexible complex that can tether DNA ends." Mol Cell **8**(5): 1129-1135.

Deckbar, D., P. A. Jeggo, et al. (2011). "Understanding the limitations of radiation-induced cell cycle checkpoints." Crit Rev Biochem Mol Biol **46**(4): 271-283.

DeFazio, L. G., R. M. Stansel, et al. (2002). "Synapsis of DNA ends by DNA-dependent protein kinase." EMBO J **21**(12): 3192-3200.

Denner, L. (1999). "Caspases in apoptotic death." Exp Opin Invest Drugs **8**(1):37-50.

Doe, C. L., J. S. Ahn, et al. (2002). "Mus81-Eme1 and Rqh1 involvement in processing stalled and collapsed replication forks." J Biol Chem **277**(36): 32753-32759.

Dong, J., G. Feldmann, et al. (2007). "Elucidation of a universal size-control mechanism in Drosophila and mammals." Cell **130**(6): 1120-1133.

Donnellan, R. and R. Chetty (1998). "Cyclin D1 and human neoplasia." Mol Pathol **51**(1): 1-7.

Donovan, S., J. Harwood, et al. (1997). "Cdc6p-dependent loading of Mcm proteins onto pre-replicative chromatin in budding yeast." Proc Natl Acad Sci U S A **94**(11): 5611-5616.

Downward, J. (2003). "Targeting RAS signalling pathways in cancer therapy." Nat Rev Cancer **3**(1): 11-22.

el-Deiry, W. S., T. Tokino, et al. (1993). "WAF1, a potential mediator of p53 tumor suppression." Cell **75**(4): 817-825.

Esashi, F., N. Christ, et al. (2005). "CDK-dependent phosphorylation of BRCA2 as a regulatory mechanism for recombinational repair." Nature **434**(7033): 598-604.

Esashi, F., V. E. Galkin, et al. (2007). "Stabilization of RAD51 nucleoprotein filaments by the C-terminal region of BRCA2." Nat Struct Mol Biol **14**(6): 468-474.

Evans, T., E. T. Rosenthal, et al. (1983). "Cyclin: a protein specified by maternal mRNA in sea urchin eggs that is destroyed at each cleavage division." Cell **33**(2): 389-396.

Falck, J., N. Mailand, et al. (2001). "The ATM-Chk2-Cdc25A checkpoint pathway guards against radioresistant DNA synthesis." Nature **410**(6830): 842-847.

Falck, J., J. H. Petrini, et al. (2002). "The DNA damage-dependent intra-S phase checkpoint is regulated by parallel pathways." Nat Genet **30**(3): 290-294.

Fekairi, S., S. Scaglione, et al. (2009). "Human SLX4 is a Holliday junction resolvase subunit that binds multiple DNA repai/recombination endonucleases." Cell **138**(1)78-89.

Feng, Y. and K. D. Irvine (2009). "Processing and phosphorylation of the Fat receptor." Proc Natl Acad Sci U S A **106**(29): 11989-11994.

Fero, M. L., E. Randel, et al. (1998). "The murine gene p27Kip1 is haplo-insufficient for tumour suppression." Nature **396**(6707): 177-180.

Fung, T. K. and R. Y. Poon (2005). "A roller coaster ride with the mitotic cyclins." Semin Cell Dev Biol **16**(3): 335-342.

Gaillard, P.H., E. Noguchi, et al. (2003). "The endogenous Mus81-Eme1 complex resolves Holliday junctions by a nick and counternick mechanism." Mol Cell **12**(3):747-59.

Galkin, V. E., F. Esashi, et al. (2005). "BRCA2 BRC motifs bind RAD51-DNA filaments." Proc Natl Acad Sci U S A **102**(24): 8537-8542.

Gartel, A. L., X. Ye, et al. (2001). "Myc represses the p21(WAF1/CIP1) promoter and interacts with Sp1/Sp3." Proc Natl Acad Sci U S A **98**(8): 4510-4515.

Garth Hamilton, K. s. Y., Simon Scrace and Eric O'Neill (December 15, 2009). "ATM Regulates a RASSF1A-Dependent DNA Damage Response." Current Biology **19**: 1-6.

Genevet, A., M. C. Wehr, et al. (2010). "Kibra is a regulator of the Salvador/Warts/Hippo signaling network." Dev Cell **18**(2): 300-308.

Giancotti, F. G. and E. Ruoslahti (1999). "Integrin signaling." Science **285**(5430): 1028-1032.

Gilbert, D. M. (2001). "Making sense of eukaryotic DNA replication origins." Science **294**(5540): 96-100.

Girard, F., U. Strausfeld, et al. (1991). "Cyclin A is required for the onset of DNA replication in mammalian fibroblasts." Cell **67**(6): 1169-1179.

Glantschnig, H., G. A. Rodan, et al. (2002). "Mapping of MST1 kinase sites of phosphorylation. Activation and autophosphorylation." J Biol Chem **277**(45): 42987-42996.

Goulev, Y., J. D. Fauny, et al. (2008). "SCALLOPED interacts with YORKIE, the nuclear effector of the hippo tumor-suppressor pathway in Drosophila." Curr Biol **18**(6): 435-441.

Grzeschik, N. A., L. M. Parsons, et al. (2010). "Lgl, aPKC, and Crumbs regulate the Salvador/Warts/Hippo pathway through two distinct mechanisms." Curr Biol **20**(7): 573-581.

Gu, J., H. Lu, et al. (2007). "Single-stranded DNA ligation and XLF-stimulated incompatible DNA end ligation by the XRCC4-DNA ligase IV complex: influence of terminal DNA sequence." Nucleic Acids Res **35**(17): 5755-5762.

Halder, G. and R. L. Johnson (2011). "Hippo signaling: growth control and beyond." Development **138**(1): 9-22.

Hamaratoglu, F., M. Willecke, et al. (2006). "The tumour-suppressor genes NF2/Merlin and Expanded act through Hippo signalling to regulate cell proliferation and apoptosis." Nat Cell Biol **8**(1): 27-36.

Hamilton, G., K. S. Yee, et al. (2009). "ATM regulates a RASSF1A-dependent DNA damage response." Curr Biol **19**(23): 2020-2025.

Hanada, K., M. Budzowska, et al. (2007). "The structure-specific endonuclease Mus81 contributes to replication restart by generating double-strand DNA breaks." Nat Struct Mol Biol **14**(11): 1096-1104.

Hanahan, D. and R. A. Weinberg (2000). "The hallmarks of cancer." Cell **100**(1): 57-70.

Hanson, K. D., M. Shichiri, et al. (1994). "Effects of c-myc expression on cell cycle progression." Mol Cell Biol **14**(9): 5748-5755.

Hao, Y., A. Chun, et al. (2008). "Tumor suppressor LATS1 is a negative regulator of oncogene YAP." J Biol Chem **283**(9): 5496-5509.

Harbour, J. W. and D. C. Dean (2000). "The Rb/E2F pathway: expanding roles and emerging paradigms." Genes Dev **14**(19): 2393-2409.

Harper, J. W., S. J. Elledge, et al. (1995). "Inhibition of cyclin-dependent kinases by p21." Mol Biol Cell **6**(4): 387-400.

Hartwell, L. H. and T. A. Weinert (1989). "Checkpoints: controls that ensure the order of cell cycle events." Science **246**(4930): 629-634.

Harvey, K. F., C. M. Pfleger, et al. (2003). "The Drosophila Mst ortholog, hippo, restricts growth and cell proliferation and promotes apoptosis." Cell **114**(4): 457-467.

Hashimoto, Y., A. R. Chaudhuri, et al. (2010). "Rad51 protects nascent DNA from Mre11-dependent degradation and promotes continuous DNA synthesis." Nat Struct Mol Biol **17**(11): 1305-1311.

Heldin, C. H. and B. Westermark (1999). "Mechanism of action and in vivo role of platelet-derived growth factor." Physiol Rev **79**(4): 1283-1316.

Heller, R. C. and K. J. Marians (2006). "Replisome assembly and the direct restart of stalled replication forks." Nat Rev Mol Cell Biol **7**(12): 932-943.

Henry-Mowatt, J., D. Jackson, et al. (2003). "XRCC3 and Rad51 modulate replication fork progression on damaged vertebrate chromosomes." Mol Cell **11**(4): 1109-1117.

Heyer, W. D., X. Li, et al. (2006). "Rad54: the Swiss Army knife of homologous recombination?" Nucleic Acids Res **34**(15): 4115-4125.

Hirota, T., T. Morisaki, et al. (2000). "Zyxin, a regulator of actin filament assembly, targets the mitotic apparatus by interacting with h-warts/LATS1 tumor suppressor." J Cell Biol **149**(5): 1073-1086.

Hisaoka, M., A. Tanaka, et al. (2002). "Molecular alterations of h-warts/LATS1 tumor suppressor in human soft tissue sarcoma." Lab Invest **82**(10): 1427-1435.

Hoang, A. T., K. J. Cohen, et al. (1994). "Participation of cyclin A in Myc-induced apoptosis." Proc Natl Acad Sci U S A **91**(15): 6875-6879.

Hofmann, F. and D. M. Livingston (1996). "Differential effects of cdk2 and cdk3 on the control of pRb and E2F function during G1 exit." Genes Dev **10**(7): 851-861.

Hong, J. H. and M. B. Yaffe (2006). "TAZ: a beta-catenin-like molecule that regulates mesenchymal stem cell differentiation." Cell Cycle **5**(2): 176-179.

Hopfner, K. P., L. Craig, et al. (2002). "The Rad50 zinc-hook is a structure joining Mre11 complexes in DNA recombination and repair." Nature **418**(6897): 562-566.

Hori, T., A. Takaori-Kondo, et al. (2000). "Molecular cloning of a novel human protein kinase, kpm, that is homologous to warts/lats, a Drosophila tumor suppressor." Oncogene **19**(27): 3101-3109.

Hu, Y., S. Raynard, et al. (2007). "RECQL5/Recql5 helicase regulates homologous recombination and suppresses tumour formation viadisruption of Rad51 presynaptic filaments." Genes Dev **21**(23):3073-84.

Huang, J., S. Wu, et al. (2005). "The Hippo signaling pathway coordinately regulates cell proliferation and apoptosis by inactivating Yorkie, the Drosophila Homolog of YAP." Cell **122**(3): 421-434.

Hubscher, U., G. Maga, et al. (2002). "Eukaryotic DNA polymerases." Annu Rev Biochem **71**: 133-163.

Huertas, P. and S. P. Jackson (2009). "Human CtIP mediates cell cycle control of DNA end resection and double strand break repair." J Biol Chem **284**(14): 9558-9565.

Huse, M. and J. Kuriyan (2002). "The conformational plasticity of protein kinases." Cell **109**(3): 275-282.

Iida, S., T. Hirota, et al. (2004). "Tumor suppressor WARTS ensures genomic integrity by regulating both mitotic progression and G1 tetraploidy checkpoint function." Oncogene **23**(31): 5266-5274.

Inamdar, K. V., J. J. Pouliot, et al. (2002). "Conversion of phosphoglycolate to phosphate termini on 3' overhangs of DNA double strand breaks by the human tyrosyl-DNA phosphodiesterase hTdp1." J Biol Chem **277**(30): 27162-27168.

Inoue, K., F. Zindy, et al. (2001). "Dmp1 is haplo-insufficient for tumor suppression and modifies the frequencies of Arf and p53 mutations in Myc-induced lymphomas." Genes Dev **15**(22):2934-9.

Jackson, S. P. (2002). "Sensing and repairing DNA double-strand breaks." Carcinogenesis **23**(5):687-96

Jansen-Durr, P., A. Meichle, et al. (1993). "Differential modulation of cyclin gene expression by MYC." Proc Natl Acad Sci U S A **90**(8): 3685-3689.

Jares, P., A. Donaldson, et al. (2000). "The Cdc7/Dbf4 protein kinase: target of the S phase checkpoint?" EMBO Rep **1**(4): 319-322.

Jeffrey, P. D., A. A. Russo, et al. (1995). "Mechanism of CDK activation revealed by the structure of a cyclinA-CDK2 complex." Nature **376**(6538): 313-320.

Jin, J., T. Shirogane, et al. (2003). "SCFbeta-TRCP links Chk1 signaling to degradation of the Cdc25A protein phosphatase." Genes Dev **17**(24): 3062-3074.

Jin, Y. H., R. Ayyagari, et al. (2003). "Okazaki fragment maturation in yeast. II. Cooperation between the polymerase and 3'-5'-exonuclease activities of Pol delta in the creation of a ligatable nick." J Biol Chem **278**(3): 1626-1633.

Johnson, L. N., M. E. Noble, et al. (1996). "Active and inactive protein kinases: structural basis for regulation." Cell **85**(2): 149-158.

Justice, R. W., O. Zilian, et al. (1995). "The Drosophila tumor suppressor gene warts encodes a homolog of human myotonic dystrophy kinase and is required for the control of cell shape and proliferation." Genes Dev **9**(5): 534-546.

Kanai, F., P. A. Marignani, et al. (2000). "TAZ: a novel transcriptional co-activator regulated by interactions with 14-3-3 and PDZ domain proteins." EMBO J **19**(24): 6778-6791.

Karow, J. K., L. Wu, et al. (2000). "RecQ family helicases: roles in cancer and aging." Curr Opin Genet Dev **10**(1):32-8.

Kastan, M. B. (2008). "DNA damage responses: mechanisms and roles in human disease: 2007 G.H.A. Clowes Memorial Award Lecture." Mol Cancer Res **6**(4): 517-524.

Kastan, M. B. and J. Bartek (2004). "Cell-cycle checkpoints and cancer." Nature **432**(7015): 316-323.

Ke, H., J. Pei, et al. (2004). "Putative tumor suppressor Lats2 induces apoptosis through downregulation of Bcl-2 and Bcl-x(L)." Exp Cell Res **298**(2):329-38.

Kerkhoff, E., U. R. Rapp (1998). “Cell cycle targets of Ras/Raf signalling.” Oncogene **17**(11):1457-62.

Kim, J. E., K. Minter-Dykhouse, et al. (2006). "Signaling networks controlled by the MRN complex and MDC1 during early DNA damage responses." Mol Carcinog **45**(6): 403-408.

Kim, S., H. G. Dallmann, et al. (1996). "Coupling of a replicative polymerase and helicase: a tau-DnaB interaction mediates rapid replication fork movement." Cell **84**(4): 643-650.

Kim, S. M. and J. A. Huberman (2001). "Regulation of replication timing in fission yeast." EMBO J **20**(21): 6115-6126.

Kim, S. T., B. Xu, et al. (2002). "Involvement of the cohesin protein, Smc1, in Atm-dependent and independent responses to DNA damage." Genes Dev **16**(5): 560-570.

Knudson, A. G., Jr. (1971). "Mutation and cancer: statistical study of retinoblastoma." Proc Natl Acad Sci U S A **68**(4): 820-823.

Kolibaba, K. S. and B. J. Druker (1997). "Protein tyrosine kinases and cancer." Biochim Biophys Acta **1333**(3): F217-248.

Kukimoto, I., H. Igaki, et al. (1999). "Human CDC45 protein binds to minichromosome maintenance 7 protein and the p70 subunit of DNA polymerase alpha." Eur J Biochem **265**(3): 936-943.

Kumagai, A. and W. G. Dunphy (2000). "Claspin, a novel protein required for the activation of Chk1 during a DNA replication checkpoint response in Xenopus egg extracts." Mol Cell **6**(4): 839-849.

Kuninaka, S., S. I. Iida, et al. (2007). "Serine protease Omi/HtrA2 targets WARTS kinase to control cell proliferation." Oncogene **26**(17): 2395-2406.

Kuninaka, S., M. Nomura, et al. (2005). "The tumor suppressor WARTS activates the Omi / HtrA2-dependent pathway of cell death." Oncogene **24**(34): 5287-5298.

Kunkel, T. A., Y. I. Pavlov, et al. (2003). "Functions of human DNA polymerases eta, kappa and iota suggested by their properties, including fidelity with undamaged DNA templates." DNA Repair (Amst) **2**(2): 135-149.

Labib, K. and J. F. Diffley (2001). "Is the MCM2-7 complex the eukaryotic DNA replication fork helicase?" Curr Opin Genet Dev **11**(1): 64-70.

Lai, Z. C., X. Wei, et al. (2005). "Control of cell proliferation and apoptosis by mob as tumor suppressor, mats." Cell **120**(5): 675-685.

Lambert, S. and A. M. Carr (2005). "Checkpoint responses to replication fork barriers." Biochimie **87**(7): 591-602.

Lambert, S., B. Froget, et al. (2007). "Arrested replication fork processing: interplay between checkpoints and recombination." DNA Repair (Amst) **6**(7): 1042-1061.

Lavin, M. F. and S. Kozlov (2007). "ATM activation and DNA damage response." Cell Cycle **6**(8): 931-942.

Lee, J. H., T. S. Kim, et al. (2008). "A crucial role of WW45 in developing epithelial tissues in the mouse." EMBO J **27**(8): 1231-1242.

Lee, J. K., Y. S. Seo, et al. (2003). "The Cdc23 (Mcm10) protein is required for the phosphorylation of minichromosome maintenance complex by the Dfp1-Hsk1 kinase." Proc Natl Acad Sci U S A **100**(5): 2334-2339.

Lee, J. W., L. Blanco, et al. (2004). "Implication of DNA polymerase lambda in alignment-based gap filling for nonhomologous DNA end joining in human nuclear extracts." J Biol Chem **279**(1): 805-811.

Lee, S., L. Cavallo, et al. (1997). "Human p53 binds Holliday junctions strongly and facilitates their cleavage." J Biol Chem **272**(11): 7532-7539.

Lehmann, A. R. and R. P. Fuchs (2006). "Gaps and forks in DNA replication: Rediscovering old models." DNA Repair (Amst) **5**(12): 1495-1498.

Lei, M., Y. Kawasaki, et al. (1997). "Mcm2 is a target of regulation by Cdc7-Dbf4 during the initiation of DNA synthesis." Genes Dev **11**(24): 3365-3374.

Lei, Q. Y., H. Zhang, et al. (2008). "TAZ promotes cell proliferation and epithelial-mesenchymal transition and is inhibited by the hippo pathway." Mol Cell Biol **28**(7): 2426-2436.

Leone, G., J. DeGregori, et al. (1997). "Myc and Ras collaborate in inducing accumulation of active cyclin E/Cdk2 and E2F." Nature **387**(6636):932.

Levin, D. S., W. Bai, et al. (1997). "An interaction between DNA ligase I and proliferating cell nuclear antigen: implications for Okazaki fragment synthesis and joining." Proc Natl Acad Sci U S A **94**(24): 12863-12868.

Levy, D., Y. Adamovich, et al. (2007). "The Yes-associated protein 1 stabilizes p73 by preventing Itch-mediated ubiquitination of p73." Cell Death Differ **14**(4):743-51.

Lew, D. J. and S. Kornbluth (1996). "Regulatory roles of cyclin dependent kinase phosphorylation in cell cycle control." Curr Opin Cell Biol **8**(6): 795-804.

Li, S., W. W. Kuhne, et al. (2009). "Involvement of p54(nrb), a PSF partner protein, in DNA double-strand break repair and radioresistance." Nucleic Acids Res **37**(20): 6746-6753.

Li, Y., J. Pei, et al. (2003). "Lats2, a putative tumor suppressor, inhibits G1/S transition." Oncogene **22**(28): 4398-4405.

Liao, S., T. Toczylowski, et al. (2008). "Identification of the Xenopus DNA2 protein as a major nuclease for the 5' -> 3' strand-specific processing of DNA ends." Nucleic Acids Res **36**(19):6091-100.

Ling, C., Y. Zheng, et al. (2010). "The apical transmembrane protein Crumbs functions as a tumor suppressor that regulates Hippo signaling by binding to Expanded." Proc Natl Acad Sci U S A **107**(23): 10532-10537.

Lisby, M., J. H. Barlow, et al. (2004). "Choreography of the DNA damage response: spatiotemporal relationships among checkpoint and repair proteins." Cell **118**(6): 699-713.

Liu, J., T. Doty, et al. (2010). “Human BRCA2 protein promotes RAD51 filament formation on RPA-covered single-stranded DNA.” Nat Struct Mol Biol **17**(10):1260-2.

Lomonosov, M., S. Anand, et al. (2003). "Stabilization of stalled DNA replication forks by the BRCA2 breast cancer susceptibility protein." Genes Dev **17**(24): 3017-3022.

Lopes, M., C. Cotta-Ramusino, et al. (2001). “The DNA replication checkpoint response stabilizes stalled replication forks.” Nature **412**(6846):557-61.

Lou, Z., C. C. Chini, et al. (2003). "Mediator of DNA damage checkpoint protein 1 regulates BRCA1 localization and phosphorylation in DNA damage checkpoint control." J Biol Chem **278**(16): 13599-13602.

Lukas, C., F. Melander, et al. (2004). "Mdc1 couples DNA double-strand break recognition by Nbs1 with its H2AX-dependent chromatin retention." EMBO J **23**(13): 2674-2683.

Lukas, J., C. Lukas, et al. (2004). "Mammalian cell cycle checkpoints: signalling pathways and their organization in space and time." DNA Repair (Amst) **3**(8-9): 997-1007.

Machwe, A., L. Xiao, et al. (2006). "The Werner and Bloom syndrome proteins catalyze regression of a model replication fork." Biochemistry **45**(47): 13939-13946.

Magnaghi-Jaulin, L., R. Groisman, et al. (1998). "Retinoblastoma protein represses transcription by recruiting a histone deacetylase." Nature **391**(6667): 601-605.

Mahajan, K. N., L. Gangi-Peterson, et al. (1999). "Association of terminal deoxynucleotidyl transferase with Ku." Proc Natl Acad Sci U S A **96**(24): 13926-13931.

Mahajan, K. N., S. A. Nick McElhinny, et al. (2002). "Association of DNA polymerase mu (pol mu) with Ku and ligase IV: role for pol mu in end-joining double-strand break repair." Mol Cell Biol **22**(14): 5194-5202.

Masuda, T., S. Mimura, et al. (2003). "CDK- and Cdc45-dependent priming of the MCM complex on chromatin during S-phase in Xenopus egg extracts: possible activation of MCM helicase by association with Cdc45." Genes Cells **8**(2): 145-161.

Matallanas, D., D. Romano, et al. (2007). "RASSF1A elicits apoptosis through an MST2 pathway directing proapoptotic transcription by the p73 tumor suppressor protein." Mol Cell **27**(6): 962-975.

Matallanas, D., D. Romano, et al. (2008). "A Hippo in the ointment: MST signalling beyond the fly." Cell Cycle **7**(7):879-84.

Matallanas, D., D. Romano, et al. (2011). "Mutant K-Ras activation of the proapoptotic MST2 pathway is antagonized by wild-type K-Ras." Mol Cell **44**(6):893-906.

Matsuoka, S., B. A. Ballif, et al. (2007). "ATM and ATR substrate analysis reveals extensive protein networks responsive to DNA damage." Science **316**(5828): 1160-1166.

Mauro, M., M.A., Rego, et al. "p21 promotes error-free replication-coupled DNA double-strand break repair." Nucleic Acids Res.

Mazloum, N. and W. K. Holloman (2009). "Brh2 promotes a template-switching reaction enabling recombinational bypass of lesions during DNA synthesis." Mol Cell **36**(4): 620-630.

McIlwraith, M. J., A. Vaisman, et al. (2005). "Human DNA polymerase eta promotes DNA synthesis from strand invasion intermediates of homologous recombination." Mol Cell **20**(5): 783-792.

Merrick, C. J., D. Jackson, et al. (2004). "Visualization of altered replication dynamics after DNA damage in human cells." J Biol Chem **279**(19): 20067-20075.

Michel, B., H. Boubakri, et al. (2007). "Recombination proteins and rescue of arrested replication forks." DNA Repair (Amst) **6**(7): 967-980.

Mickelsen, S., C. Snyder, et al. (1999). "Modulation of terminal deoxynucleotidyltransferase activity by the DNA-dependent protein kinase." J Immunol **163**(2): 834-843.

Mimitou, E. P. and L. S. Symington (2009). "DNA end resection: many nucleases make light work." DNA Repair (Amst) **8**(9): 983-995.

Mimura, S., T. Masuda, et al. (2000). "Central role for cdc45 in establishing an initiation complex of DNA replication in Xenopus egg extracts." Genes Cells **5**(6): 439-452.

Mimura, S. and H. Takisawa (1998). "Xenopus Cdc45-dependent loading of DNA polymerase alpha onto chromatin under the control of S-phase Cdk." EMBO J **17**(19): 5699-5707.

Mirkin, E. V. and S. M. Mirkin (2007). "Replication fork stalling at natural impediments." Microbiol Mol Biol Rev **71**(1): 13-35.

Mohaghegh, P., J. K. Karow, et al. (2001). "The Bloom's and Werner's syndrome proteins are DNA structure-specific helicases." Nucleic Acids Res **29**(13): 2843-2849.

Moroy, T. and C. Geisen (2004). "Cyclin E." Int J Biochem Cell Biol **36**(8): 1424-1439.

Morozumi, Y., Y. Takizawa, et al. (2009). "Human PSF binds to RAD51 and modulates its homologous-pairing and strand-exchange activities." Nucleic Acids Res **37**(13): 4296-4307.

Mossi, R. and U. Hubscher (1998). "Clamping down on clamps and clamp loaders--the eukaryotic replication factor C." Eur J Biochem **254**(2): 209-216.

Nick McElhinny, S. A., C. M. Snowden, et al. (2000). "Ku recruits the XRCC4-ligase IV complex to DNA ends." Mol Cell Biol **20**(9): 2996-3003.

Nimonkar, A. V., A. Z. Ozsoy, et al. (2008). "Human exonuclease 1 BLM helicase interacts to resect DNA and initiate DNA repair." Proc Natl Acad Sci USA **105**(44):16906-11.

Nishiyama, Y., T. Hirota, et al. (1999). "A human homolog of Drosophila warts tumor suppressor, h-warts, localized to mitotic apparatus and specifically phosphorylated during mitosis." FEBS letters **459**(2): 159-165.

Nolen, B., S. Taylor, et al. (2004). "Regulation of protein kinases; controlling activity through activation segment conformation." Mol Cell **15**(5): 661-675.

Nolo, R., C. M. Morrison, et al. (2006). "The bantam microRNA is a target of the hippo tumor-suppressor pathway." Curr Biol **16**(19): 1895-1904.

Nordling, C. O. (1953). "A new theory on cancer-inducing mechanism." Br J Cancer **7**(1): 68-72.

O'Neill, E. and W. Kolch (2005). "Taming the Hippo: Raf-1 controls apoptosis by suppressing MST2/Hippo." Cell Cycle **4**(3): 365-367.

O'Neill, E., L. Rushworth, et al. (2004). "Role of the kinase MST2 in suppression of apoptosis by the proto-oncogene product Raf-1." Science **306**(5705): 2267-2270.

Oh, H. and K. D. Irvine (2009). "In vivo analysis of Yorkie phosphorylation sites." Oncogene **28**(17): 1916-1927.

Ohtsubo, M., A. M. Theodoras, et al. (1995). "Human cyclin E, a nuclear protein essential for the G1-to-S phase transition." Mol Cell Biol **15**(5): 2612-2624.

Ota, M. and H. Sasaki (2008). "Mammalian Tead proteins regulate cell proliferation and contact inhibition as transcriptional mediators of Hippo signaling." Development **135**(24): 4059-4069.

Pages, V. and R. P. Fuchs (2003). "Uncoupling of leading- and lagging-strand DNA replication during lesion bypass in vivo." Science **300**(5623): 1300-1303.

Painter, R. B. and B. R. Young (1980). "Radiosensitivity in ataxia-telangiectasia: a new explanation." Proc Natl Acad Sci U S A **77**(12): 7315-7317.

Pantalacci, S., N. Tapon, et al. (2003). "The Salvador partner Hippo promotes apoptosis and cell-cycle exit in Drosophila." Nat Cell Biol **5**(10): 921-927.

Paques, F. and J. E. Haber (1999). "Multiple pathways of recombination induced by double-strand breaks in Saccharomyces cerevisiae." Microbiol Mol Biol Rev **63**(2): 349-404.

Patel, K. J., V. P. Yu, et al. (1998). "Involvement of Brca2 in DNA repair." Mol Cell **1**(3): 347-357.

Pearce, L. R., D. Komander, et al. (2010). "The nuts and bolts of AGC protein kinases." Nat Rev Mol Cell Biol **11**(1): 9-22.

Pearson, G., F. Robinson, et al. (2001). "Mitogen-Activated Protein (MAP) Kinase Pathways: Regulation and Physiological Functions." Endocr Rev **22**(2):153-83.

Petermann, E., M. L. Orta, et al. (2010). "Hydroxyurea-stalled replication forks become progressively inactivated and require two different RAD51-mediated pathways for restart and repair." Mol Cell **37**(4): 492-502.

Philipp, A., A. Schneider, et al. (1994). "Repression of cyclin D1: a novel function of MYC." Mol Cell Biol **14**(6): 4032-4043.

Pierce, A. J., R. D. Johnson, et al. (1999). "XRCC3 promotes homology-directed repair of DNA damage in mammalian cells." Genes Dev **13**(20): 2633-2638.

Pines, J. (1991). "Cyclins: wheels within wheels." Cell Growth Differ **2**(6): 305-310.

Pines, J. and T. Hunter (1991). "Cyclin-dependent kinases: a new cell cycle motif?" Trends Cell Biol **1**(5): 117-121.

Polesello, C., S. Huelsmann, et al. (2006). "The Drosophila RASSF homolog antagonizes the hippo pathway." Curr Biol **16**(24): 2459-2465.

Postow, L., N. J. Crisona, et al. (2001). "Topological challenges to DNA replication: conformations at the fork." Proc Natl Acad Sci U S A **98**(15): 8219-8226.

Povirk, L. F., T. Zhou, et al. (2007). "Processing of 3'-phosphoglycolate-terminated DNA double strand breaks by Artemis nuclease." J Biol Chem **282**(6): 3547-3558.

Powell, S. N., L. A. Kachnic, (2003). “Roles of Brca1 and Brca2 in homologous recombination, DNA replication fidelity and the cellular response to ionizing radiation.” Oncogene **22**(37):5784-91.

Prasanth, K. V., S. G. Prasanth, et al. (2005). "Regulating gene expression through RNA nuclear retention." Cell **123**(2): 249-263.

Rajesh, C., A. M. Gruver, et al. (2009). "The interaction profile of homologous recombination repair proteins RAD51C, RAD51D and XRCC2 as determined by proteomic analysis." Proteomics **9**(16): 4071-4086.

Rass, U., S.A. Compton, et al. (2010). “Mechanism of Holliday junction resolution by the human GEN1 protein.” Genes Dev **24**(14):1559-69.

Raynard, S., W. Bussen, et al. (2006). "A double Holliday junction dissolvasome comprising BLM, topoisomerase IIIalpha, and BLAP75." J Biol Chem **281**(20): 13861-13864.

Remus, D., E. L. Beall, et al. (2004). "DNA topology, not DNA sequence, is a critical determinant for Drosophila ORC-DNA binding." EMBO J **23**(4): 897-907.

Reynisdottir, I., K. Polyak, et al. (1995). "Kip/Cip and Ink4 Cdk inhibitors cooperate to induce cell cycle arrest in response to TGF-beta." Genes Dev **9**(15): 1831-1845.

Roberts, J. M., A. Koff, et al. (1994). "Cyclins, Cdks, and cyclin kinase inhibitors." Cold Spring Harb Symp Quant Biol **59**: 31-38.

Robinson, B. S., J. Huang, et al. (2010). "Crumbs regulates Salvador/Warts/Hippo signaling in Drosophila via the FERM-domain protein Expanded." Curr Biol **20**(7): 582-590.

Rodrigues, G. A. and M. Park (1994). "Oncogenic activation of tyrosine kinases." Curr Opin Genet Dev **4**(1): 15-24.

Rogakou, E. P., D. R. Pilch, et al. (1998). "DNA double-stranded breaks induce histone H2AX phosphorylation on serine 139." J Biol Chem **273**(10): 5858-5868.

Romano, D., D. Matallanas, et al. (2010). "Proapoptotic kinase MST2 coordinates signaling crosstalk between RASSF1A, Raf-1, and Akt." Cancer Res **70**(3): 1195-1203.

Rothkamm, K., I. Kruger, et al. (2003). "Pathways of DNA double-strand break repair during the mammalian cell cycle." Mol Cell Biol **23**(16):5706-15.

Rubinfeld, B., B. Souza, et al. (1993). "Association of the APC gene product with beta-catenin." Science **262**(5140): 1731-1734.

Rudolph, B., R. Saffrich, et al. (1996). "Activation of cyclin-dependent kinases by Myc mediates induction of cyclin A, but not apoptosis." EMBO J **15**(12):3065-76.

Saintigny, Y., F. Delacote, et al. (2001). "Characterization of homologous recombination induced by replication inhibition in mammalian cells." EMBO J **20**(14): 3861-3870.

Salton, M., Y. Lerenthal, et al. (2010). "Involvement of Matrin 3 and SFPQ/NONO in the DNA damage response." Cell Cycle **9**(8): 1568-1576.

San Filippo, J., P. Sung, et al. (2008). "Mechanism of eukaryotic homologous recombination." Annu Rev Biochem **77**: 229-257.

Santocanale, C., K. Sharma, et al. (1999). "Activation of dormant origins of DNA replication in budding yeast." Genes Dev **13**(18): 2360-2364.

Sartori, A. A., C. Lukas, et al. (2007). "Human CtIP promotes DNA end resection." Nature **450**(7169): 509-514.

Schafer, K. A. (1998). "The cell cycle: a review." Vet Pathol **35**(6): 461-478.

Scheel, H. and K. Hofmann (2003). "A novel interaction motif, SARAH, connects three classes of tumor suppressor." Curr Biol **13**(23): R899-900.

Schlacher, K., N. Christ, et al. (2011). "Double-strand break repair-independent role for BRCA2 in blocking stalled replication fork degradation by MRE11." Cell **145**(4): 529-542.

Schulze, W. X., L. Deng, et al. (2005). "Phosphotyrosine interactome of the ErbB-receptor kinase family." Mol Syst Biol **1**: 2005 0008.

Scully, R. and D. M. Livingston (2000). "In search of the tumour-suppressor functions of BRCA1 and BRCA2." Nature **408**(6811): 429-432.

Segurado, M., A. de Luis, et al. (2003). "Genome-wide distribution of DNA replication origins at A+T-rich islands in Schizosaccharomyces pombe." EMBO Rep **4**(11): 1048-1053.

Seiler, J. A., C. Conti, et al. (2007). "The intra-S-phase checkpoint affects both DNA replication initiation and elongation: single-cell and -DNA fiber analyses." Mol Cell Biol **27**(16): 5806-5818.

Seong, C., S. Colavito, et al. (2009). "Regulation of Rad51 recombinase presynaptic filament assembly via interactions with the Rad52 mediator and the Srs2 anti-recombinase." J Biol Chem **284**(36): 24363-24371.

Sharpless, N. E. and R. A. DePinho (1999). "The INK4A/ARF locus and its two gene products." Curr Opin Genet Dev **9**(1): 22-30.

Shen, Y. and E. White (2001). "p53-dependent apoptosis pathways." Adv Cancer Res **82**: 55-84.

Sherr, C. J. (1994). "G1 phase progression: cycling on cue." Cell **79**(4): 551-555.

Sherr, C. J. (1996). "Cancer cell cycles." Science **274**(5293): 1672-1677.

Sherr, C. J. (2001). "The INK4a/ARF network in tumour suppression." Nat Rev Mol Cell Biol **2**(10): 731-737.

Sherr, C. J. and J. M. Roberts (1995). "Inhibitors of mammalian G1 cyclin-dependent kinases." Genes Dev **9**(10): 1149-1163.

Shimada, K., P. Pasero, et al. (2002). "ORC and the intra-S-phase checkpoint: a threshold regulates Rad53p activation in S phase." Genes Dev **16**(24): 3236-3252.

Shivji, M. K., O. R. Davies, et al. (2006). "A region of human BRCA2 containing multiple BRC repeats promotes RAD51-mediated strand exchange." Nucleic Acids Res **34**(14): 4000-4011.

Shivji, M. K., S. R. Mukund, et al. (2009). "The BRC repeats of human BRCA2 differentially regulate RAD51 binding on single- versus double-stranded DNA to stimulate strand exchange." Proc Natl Acad Sci U S A **106**(32): 13254-13259.

Silva, E., Y. Tsatskis, et al. (2006). "The tumor-suppressor gene fat controls tissue growth upstream of expanded in the hippo signaling pathway." Curr Biol **16**(21): 2081-2089.

Simpson, L. and R. Parsons (2001). "PTEN: life as a tumor suppressor." Exp Cell Res **264**(1): 29-41.

Sirbu, B. M., F. B. Couch, et al. (2011). "Analysis of protein dynamics at active, stalled, and collapsed replication forks." Genes Dev **25**(12): 1320-1327.

Sobhian, B., G. Shao, et al. (2007). "RAP80 targets BRCA1 to specific ubiquitin structures at DNA damage sites." Science **316**(5828):1198-202.

Sogo, J.M., M. Lopes, et al. (2002). "Fork reversal and ssDNA accumulation at stalled replication forks owing to checkpoint defects." Science **297**(5581):599-602.

Solinger, J. A., K. Kiianitsa, et al. (2002). "Rad54, a Swi2/Snf2-like recombinational repair protein, disassembles Rad51:dsDNA filaments." Mol Cell **10**(5): 1175-1188.

Sommers, J. A., N. Rawtani, et al. (2009). "FANCJ uses its motor ATPase to destabilize protein-DNA complexes, unwind triplexes, and inhibit RAD51 strand exchange." J Biol Chem **284**(12):7505-17.

Song, H., K. K. Mak, et al. (2010). "Mammalian Mst1 and Mst2 kinases play essential roles in organ size control and tumor suppression." Proc Natl Acad Sci U S A **107**(4): 1431-1436.

Sonoda, E., M. S. Sasaki, et al. (1998). "Rad51-deficient vertebrate cells accumulate chromosomal breaks prior to cell death." EMBO J **17**(2):598-608.

Sopko, R., E. Silva, et al. (2009). "Phosphorylation of the tumor suppressor fat is regulated by its ligand Dachsous and the kinase discs overgrown." Curr Biol **19**(13): 1112-1117.

Sorensen, C. S., R. G. Syljuasen, et al. (2003). "Chk1 regulates the S phase checkpoint by coupling the physiological turnover and ionizing radiation-induced accelerated proteolysis of Cdc25A." Cancer Cell **3**(3): 247-258.

Sorensen, C. S., R. G. Syljuasen, et al. (2004). "ATR, Claspin and the Rad9-Rad1-Hus1 complex regulate Chk1 and Cdc25A in the absence of DNA damage." Cell Cycle **3**(7): 941-945.

Srinivasula, S. M., S. Gupta, et al. (2003). "Inhibitor of apoptosis proteins are substrates for the mitochondrial serine protease Omi/HtrA2." J Biol Chem **278**(34): 31469-31472.

St John, M. A., W. Tao, et al. (1999). "Mice deficient of Lats1 develop soft-tissue sarcomas, ovarian tumours and pituitary dysfunction." Nat Genet **21**(2): 182-186.

Steigerwald, K., G. K. Behbehani, et al. (2005). "The APC tumor suppressor promotes transcription-independent apoptosis in vitro." Mol Cancer Res **3**(2): 78-89.

Stocker, H. (2011). "Growth control: Myc and Yorkie get connected." Curr Biol **21**(1): R37-39.

Straub, T., P. Grue, et al. (1998). "The RNA-splicing factor PSF/p54 controls DNA-topoisomerase I activity by a direct interaction." J Biol Chem **273**(41): 26261-26264.

Stucki, M., J. A. Clapperton, et al. (2005). "MDC1 directly binds phosphorylated histone H2AX to regulate cellular responses to DNA double-strand breaks." Cell **123**(7): 1213-1226.

Su, Y., J. A. Meador, et al. (2010). "Analysis of ionizing radiation-induced DNA damage and repair in three-dimensional human skin model system." Exp Dermatol **19**(8): e16-22.

Sudol, M. (1994). "Yes-associated protein (YAP65) is a proline-rich phosphoprotein that binds to the SH3 domain of the Yes proto-oncogene product." Oncogene **9**(8): 2145-2152.

Suzuki, Y., K. Takahashi-Niki, et al. (2004). "Mitochondrial protease Omi/HtrA2 enhances caspase activation through multiple pathways." Cell Death Differ **11**(2): 208-216.

Takahashi, Y., Y. Miyoshi, et al. (2005). "Down-regulation of LATS1 and LATS2 mRNA expression by promoter hypermethylation and its association with biologically aggressive phenotype in human breast cancers." Clin Cancer Res **11**(4): 1380-1385.

Takisawa, H., S. Mimura, et al. (2000). "Eukaryotic DNA replication: from pre-replication complex to initiation complex." Curr Opin Cell Biol **12**(6): 690-696.

Tal, A., R. Arbel-Goren, et al. (2009). "Cancer-associated mutations in BRC domains of BRCA2 affect homologous recombination induced by Rad51." J Mol Biol **393**(5): 1007-1012.

Tan, Y., H. Ruan, et al. (1999). “p90(RSK) blocks bad-mediated cell death via a protein kinase C-dependent pathway.” J Biol Chem **274**(49):34859-67.

Tao, W., S. Zhang, et al. (1999). "Human homologue of the Drosophila melanogaster lats tumour suppressor modulates CDC2 activity." Nat Genet **21**(2): 177-181.

Tao, W., S. Zhang, et al. (1999). "Human homologue of the Drosophila melanogaster lats tumour suppressor modulates CDC2 activity." Nature genetics **21**(2): 177-181.

Tapon, N., K. F. Harvey, et al. (2002). "salvador Promotes both cell cycle exit and apoptosis in Drosophila and is mutated in human cancer cell lines." Cell **110**(4): 467-478.

Tercero, J.A., J.F. Diffley (2001). "Regulation of DNA replication fork progression through damaged DNA by the Mec1/Rad53 checkpoint." Nature **412**(6846):553-7.

Tercero, J. A., K. Labib, et al. (2000). "DNA synthesis at individual replication forks requires the essential initiation factor Cdc45p." EMBO J **19**(9): 2082-2093.

Thompson, B. J. and S. M. Cohen (2006). "The Hippo pathway regulates the bantam microRNA to control cell proliferation and apoptosis in Drosophila." Cell **126**(4): 767-774.

Tsai, C. J., S. A. Kim, et al. (2007). "Cernunnos/XLF promotes the ligation of mismatched and noncohesive DNA ends." Proc Natl Acad Sci U S A **104**(19): 7851-7856.

Tsatsanis, C. and D. A. Spandidos (2000). "The role of oncogenic kinases in human cancer (Review)." Int J Mol Med **5**(6): 583-590.

Tschop, K., A. R. Conery, et al. (2011). "A kinase shRNA screen links LATS2 and the pRB tumor suppressor." Genes Dev **25**(8): 814-830.

Turenchalk, G. S., M. A. St John, et al. (1999). "The role of lats in cell cycle regulation and tumorigenesis." Biochim Biophys Acta **1424**(2-3): M9-M16.

Udan, R. S., M. Kango-Singh, et al. (2003). "Hippo promotes proliferation arrest and apoptosis in the Salvador/Warts pathway." Nat Cell Biol **5**(10): 914-920.

Uematsu, N., E. Weterings, et al. (2007). "Autophosphorylation of DNA-PKCS regulates its dynamics at DNA double-strand breaks." J Cell Biol **177**(2): 219-229.

Unsal-Kacmaz, K., P. D. Chastain, et al. (2007). "The human Tim/Tipin complex coordinates an Intra-S checkpoint response to UV that slows replication fork displacement." Mol Cell Biol **27**(8): 3131-3142.

Valerie, K. and L. F. Povirk (2003). "Regulation and mechanisms of mammalian double-strand break repair." Oncogene **22**(37): 5792-5812.

van den Heuvel, S. and E. Harlow (1993). "Distinct roles for cyclin-dependent kinases in cell cycle control." Science **262**(5142): 2050-2054.

Van Hatten, R. A., A. V. Tutter, et al. (2002). "The Xenopus Xmus101 protein is required for the recruitment of Cdc45 to origins of DNA replication." J Cell Biol **159**(4): 541-547.

Vandel, L., E. Nicolas, et al. (2001). "Transcriptional repression by the retinoblastoma protein through the recruitment of a histone methyltransferase." Mol Cell Biol **21**(19): 6484-6494.

Vashee, S., C. Cvetic, et al. (2003). "Sequence-independent DNA binding and replication initiation by the human origin recognition complex." Genes Dev **17**(15): 1894-1908.

Vichalkovski, A., E. Gresko, et al. (2008). "NDR kinase is activated by RASSF1A/MST1 in response to Fas receptor stimulation and promotes apoptosis." Curr Biol **18**(23):1889-95.

Visser, S. and X. Yang (2010). "LATS tumor suppressor: a new governor of cellular homeostasis." Cell Cycle **9**(19): 3892-3903.

Vujcic, M., C. A. Miller, et al. (1999). "Activation of silent replication origins at autonomously replicating sequence elements near the HML locus in budding yeast." Mol Cell Biol **19**(9): 6098-6109.

Walker, J. R., R. A. Corpina, et al. (2001). "Structure of the Ku heterodimer bound to DNA and its implications for double-strand break repair." Nature **412**(6847): 607-614.

Walter, J. and J. Newport (2000). "Initiation of eukaryotic DNA replication: origin unwinding and sequential chromatin association of Cdc45, RPA, and DNA polymerase alpha." Mol Cell **5**(4): 617-627.

Walter, J. C. (2000). "Evidence for sequential action of cdc7 and cdk2 protein kinases during initiation of DNA replication in Xenopus egg extracts." J Biol Chem **275**(50): 39773-39778.

Wang, R., G. He, et al. (2007). "Regulation of Cdc25C by ERK-MAP kinases during the G2/M transition." Cell **128**(6):1119-32.

Wang, B., S. Matsuoka, et al. (2007). "Abraxas and RAP80 from a BRCA1 protein complex required for the DNA damage response." Science **23**(16):5706-15.

Wang, W., M. Seki, et al. (2000). "Possible association of BLM in decreasing DNA double strand breaks during DNA replication." EMBO J **19**(13):3428-35.

Ward, I. M. and J. Chen (2001). "Histone H2AX is phosphorylated in an ATR-dependent manner in response to replicational stress." J Biol Chem **276**(51): 47759-47762.

Ward, J. F. (1988). "DNA damage produced by ionizing radiation in mammalian cells: identities, mechanisms of formation, and reparability." Prog Nucleic Acid Res Mol Biol **35**: 95-125.

Wei, X., T. Shimizu, et al. (2007). "Mob as tumor suppressor is activated by Hippo kinase for growth inhibition in Drosophila." EMBO J **26**(7): 1772-1781.

Weinberg, R. A. (1995). "The retinoblastoma protein and cell cycle control." Cell **81**(3): 323-330.

West, S. C. (2003). "Molecular views of recombination proteins and their control." Nat Rev Mol Cell Biol **4**(6): 435-445.

Weterings, E. and D. J. Chen (2007). "DNA-dependent protein kinase in nonhomologous end joining: a lock with multiple keys?" J Cell Biol **179**(2): 183-186.

Weterings, E. and D. C. van Gent (2004). "The mechanism of non-homologous end-joining: a synopsis of synapsis." DNA Repair (Amst) **3**(11): 1425-1435.

Weterings, E., N. S. Verkaik, et al. (2003). "The role of DNA dependent protein kinase in synapsis of DNA ends." Nucleic Acids Res **31**(24): 7238-7246.

Whitby, M. C., F. Osman, et al. (2003). "Cleavage of model replication forks by fission yeast Mus81-Eme1 and budding yeast Mus81-Mms4." J Biol Chem **278**(9): 6928-6935.

Willecke, M., F. Hamaratoglu, et al. (2006). "The fat cadherin acts through the hippo tumor-suppressor pathway to regulate tissue size." Curr Biol **16**(21): 2090-2100.

Williams, G. J., S. P. Lees-Miller, et al. (2010). "Mre11-Rad50-Nbs1 conformations and the control of sensing, signaling, and effector responses at DNA double-strand breaks." DNA Repair (Amst) **9**(12): 1299-1306.

Wohlschlegel, J. A., S. K. Dhar, et al. (2002). "Xenopus Mcm10 binds to origins of DNA replication after Mcm2-7 and stimulates origin binding of Cdc45." Mol Cell **9**(2): 233-240.

Wong, A. K., R. Pero, et al. (1997). "RAD51 interacts with the evolutionarily conserved BRC motifs in the human breast cancer susceptibility gene brca2." J Biol Chem **272**(51): 31941-31944.

Wu, S., J. Huang, et al. (2003). "hippo encodes a Ste-20 family protein kinase that restricts cell proliferation and promotes apoptosis in conjunction with salvador and warts." Cell **114**(4): 445-456.

Wyman, C. and R. Kanaar (2006). "DNA double-strand break repair: all's well that ends well." Annu Rev Genet **40**: 363-383.

Xia, H., H. Qi, et al. (2002). "LATS1 tumor suppressor regulates G2/M transition and apoptosis." Oncogene **21**(8): 1233-1241.

Xu, B., S. Kim, et al. (2001). "Involvement of Brca1 in S-phase and G(2)-phase checkpoints after ionizing irradiation." Mol Cell Biol **21**(10): 3445-3450.

Xu, L. and K. J. Marians (2002). "A dynamic RecA filament permits DNA polymerase-catalyzed extension of the invading strand in recombination intermediates." J Biol Chem **277**(16): 14321-14328.

Xu, T., W. Wang, et al. (1995). "Identifying tumor suppressors in genetic mosaics: the Drosophila lats gene encodes a putative protein kinase." Development **121**(4): 1053-1063.

Yabuta, N., T. Fujii, et al. (2000). "Structure, expression, and chromosome mapping of LATS2, a mammalian homologue of the Drosophila tumor suppressor gene lats/warts." Genomics **63**(2): 263-270.

Yan, H., Z. Dobbie, et al. (2002). "Small changes in expression affect predisposition to tumorigenesis." Nat Genet **30**(1):25-6.

Yang, Q. H., R. Church-Hajduk, et al. (2003). "Omi/HtrA2 catalytic cleavage of inhibitor of apoptosis (IAP) irreversibly inactivates IAPs and facilitates caspase activity in apoptosis." Genes Dev **17**(12): 1487-1496.

Yang, W. (2003). "Damage repair DNA polymerases Y." Curr Opin Struct Biol **13**(1): 23-30.

Yang, X., D. M. Li, et al. (2001). "Human homologue of Drosophila lats, LATS1, negatively regulate growth by inducing G(2)/M arrest or apoptosis." Oncogene **20**(45): 6516-6523.

Yang, X., K. Yu, et al. (2004). "LATS1 tumour suppressor affects cytokinesis by inhibiting LIMK1." Nat Cell Biol **6**(7): 609-617.

Yarbro, J. W. (1992). "Mechanism of action of hydroxyurea." Semin Oncol **19**(3 Suppl 9): 1-10.

Yata, K., F. Esashi (2009). "Dual role of CDKs in DNA repair: to be, or not to be." DNA Repair **8**(1):6-18.

Yazdi, P. T., Y. Wang, et al. (2002). "SMC1 is a downstream effector in the ATM/NBS1 branch of the human S-phase checkpoint." Genes Dev **16**(5): 571-582.

Yoo, S., A. Kimzey, et al. (1999). "Photocross-linking of an oriented DNA repair complex. Ku bound at a single DNA end." J Biol Chem **274**(28): 20034-20039.

Young, B. R. and R. B. Painter (1989). "Radioresistant DNA synthesis and human genetic diseases." Hum Genet **82**(2): 113-117.

Yu, J. and L. Zhang (2008). "PUMA, a potent killer with or without p53." Oncogene **27 Suppl 1**: S71-83.

Yu, J., Y. Zheng, et al. (2010). "Kibra functions as a tumor suppressor protein that regulates Hippo signaling in conjunction with Merlin and Expanded." Dev Cell **18**(2): 288-299.

Yu, V. P., M. Koehler, et al. (2000). "Gross chromosomal rearrangements and genetic exchange between nonhomologous chromosomes following BRCA2 inactivation." Genes Dev **14**(11): 1400-1406.

Yu, X., S. Fu, et al. (2006). "BRCA1 ubiquitinates its phosphorylation-dependent binding partner CtIP." Genes Dev **20**(13): 1721-1726.

Yu, X., L. C. Wu, et al. (1998). "The C-terminal (BRCT) domains of BRCA1 interact in vivo with CtIP, a protein implicated in the CtBP pathway of transcriptional repression." J Biol Chem **273**(39): 25388-25392.

Yuan, S., X. Yu, et al. (2011). "The holo-apoptosome: activation of procaspase-9 and interactions with caspase-3." Structure **19**(8):1084-96.

Zarich, N., J. L. Oliva, et al. (2006). "Grb2 is a negative modulator of the intrinsic Ras-GEF activity of hSos1." Mol Biol Cell **17**(8): 3591-3597.

Zhang, Z. and G. G. Carmichael (2001). "The fate of dsRNA in the nucleus: a p54(nrb)-containing complex mediates the nuclear retention of promiscuously A-to-I edited RNAs." Cell **106**(4): 465-475.

Zhao, B., X. Wei, et al. (2007). "Inactivation of YAP oncoprotein by the Hippo pathway is involved in cell contact inhibition and tissue growth control." Genes Dev **21**(21): 2747-2761.

Zhu, Z., W. H. Chung, et al. (2008). "Sgs1 helicase and two nucleases Dna2 and Exo1 resect DNA double-strand break ends." Cell **134**(6):981-94.

Zou, L. and S. J. Elledge (2003). "Sensing DNA damage through ATRIP recognition of RPA-ssDNA complexes." Science **300**(5625): 1542-1548.

Zou, H., Y. Li, et al. (1999). "An APAF-1 cytochrome c multimeric complex is a functional apoptosome that activates procaspase-9." J Biol Chem **274**(17):11549-56

Zou, L., D. Liu, et al. (2003). "Replication protein A-mediated recruitment and activation of Rad17 complexes." Proc Natl Acad Sci U S A **100**(24): 13827-13832.

Zou, L. and B. Stillman (1998). "Formation of a preinitiation complex by S-phase cyclin CDK-dependent loading of Cdc45p onto chromatin." Science **280**(5363): 593-596.